October 2021

A NOVEL INTERVENTION TO PREVENT POST-TRAUMATIC OSTEOARTHRITIS FOLLOWING KNEE JOINT INJURY

Gerardo E. Narez
University of Massachusetts Amherst

A NOVEL INTERVENTION TO PREVENT POST-TRAUMATIC OSTEOARTHRITIS FOLLOWING KNEE JOINT INJURY

A Dissertation Presented

by

GERARDO E. NAREZ

Submitted to the Graduate School of the
University of Massachusetts Amherst in partial fulfillment
of the requirements for the degree of

DOCTOR OF PHILOSOPHY

September 2021

Department of Biomedical Engineering

A NOVEL INTERVENTION TO PREVENT POST-TRAUMATIC OSTEOARTHRITIS FOLLOWING KNEE JOINT INJURY

A Dissertation Presented

by

GERARDO E. NAREZ

Approved as to style and content by:

_____
Tammy L. Haut Donahue, Chair

_____
Katherine Boyer, Member

_____
Shelly Peyton, Member

_____
Seth Donahue, Member

_____
Thai Thayumanavan, Department Head
Biomedical Engineering Department

DEDICATION

Para mi madre, Sofia, mi hermana, Yesenia, y el resto de mi familia. Gracias por todo el apoyo y amor incondicional que me han dado toda mi vida. No podria haber logrado todo lo que e hecho sin ustedes. Gracias.

To my mother, Sofia, my sister, Yesenia, and the rest of my family. Thank you for all of the support and unconditional love you have given me throughout my life. I could not have accomplished everything I have done without you. Thank you.

ACKNOWLEDGMENTS

I would like to thank my advisor, Dr. Tammy L. Haut Donahue for her outstanding mentorship she has given me throughout my tenure as a graduate student. I took a huge risk moving across the country with you to continue my education and achieve my goals, but it has been an invaluable experience. Thank you for everything you have done to help me grow as a researcher, mentor, and person.

I would also like to thank my committee members Dr. Seth Donahue, Dr. Katherine Boyer, and Dr. Shelly Peyton, for their insightful feedback and continuous support both academically and professionally. This work could not have been possible without our collaborators at Michigan State University, Dr. Roger C. Haut, Dr. Feng Wei, Dr. Loic Dejardin, and Cliff Beckett.

Special recognition goes to my lab mates, both at Colorado State and at UMass Amherst, particularly Dr. Kristine M. Fischenich, Dr. Hannah M. Pauly, Dr. Brett Steinemen, Dr. Benjamin Wheatly, Gabriel Brown, Ryan Ek and Ashley Herrick. Being a graduate student and working in the lab would not have been as enjoyable without all of you being there. I would also like to thank the valuable friendships I have made outside of the lab: James A. Garlant, Luca H. Fuller, Cole J. Ferreira, Tara B. Wigmosta, and Jessi R. Vlcek. You all helped make my time as a graduate student that much more memorable and exciting.

Finally, I would like to thank the friends who have been my side long before I ever considered graduate school. John Weng, Jennifer Kan, Tania Serrano, Francisco Serrano, Cynthia Lopez, Angelica Marquez, and Marisa Marquez. You have all been there for me through my highs and lows. I am excited to continue growing our friendships as the next chapter in my life begins.

ABSTRACT

A NOVEL INTERVENTION TO PREVENT POST-TRAUMATIC OSTEOARTHRITIS FOLLOWING KNEE JOINT INJURY

SEPTEMBER 2021

GERARDO E. NAREZ, B.S., UC SAN DIEGO

Ph.D., UNIVERSITY OF MASSACHUSETTS AMHERST

Directed by: Professor Tammy L. Haut Donahue

The knee joint is the most commonly injured body part in the human body. Injuries as a result of participation in sports, or other recreational activities, often leads to damage to the anterior cruciate ligament (ACL) and meniscus. Injury to these tissues are strongly associated with subsequent knee post-traumatic osteoarthritis (PTOA), which is considered a serious disease because it greatly impacts a patient's quality of life and significantly increases their risk of premature death. To return stability to the joint, the current clinical treatment is to perform reconstruction of the torn ACL and a meniscal debridement, or meniscectomy, when needed. However, long term studies have shown that surgical intervention does not prevent the onset or progression of PTOA. It is believed that reconstruction surgery fails to address the occult damage to the soft tissues within the knee joint at the cellular level. Recently, a single dose of the amphipathic and nonionic surfactant Poloxamer 188 (P188) has been shown to be an effective inhibitor of acute cell death and inhibit pathways associated with inflammation in articular cartilage in both *in-vitro* and *in-vivo* studies.

This project strives to test if combined surgical and P188 treatment following injury to the ACL will help prevent PTOA in an *in-vivo* closed-joint traumatic injury model. It is hypothesized that combined treatment will mitigate or delay the progression of the disease joint by returning normal knee kinematics and restoring the integrity of damaged cell membranes in the soft tissues. Thus, the aims of the proposed project are to:

1) Determine the efficacy of a single and multiple temporal administrations of P188 in inhibiting cell death following traumatic impact in meniscal tissue.
2) Assess morphological, functional and histological changes in the meniscus
3) Evaluate chronic changes in subchondral cortical and trabecular bone of femurs and tibias
4) Determine the presence of biomarkers associated with PTOA in the synovial fluid

Finding solutions to prevent the onset of PTOA, in conjunction with ACL reconstructive surgery, would provide a novel treatment to improve the quality of life for millions of people and decrease their risk of premature death.

TABLE OF CONTENTS

LIST OF TABLES

LIST OF FIGURES

CHAPTER 1

INTRODUCTION

Knee Anatomy

The knee is the most complex joint in the human body that is composed of various hard and soft tissues. The four bones, hard tissue, found within the join include the femur, patella, tibia and fibula. Subchondral bone is the layer of bone found directly beneath the articular cartilage, separated by a zone of calcified cartilage, and extends to the growth plate of the femur and tibia.[55] (Figure 1) This region consists of both nonporous cortical bone and spongy trabecular bone. Bone is an adaptive tissue that remodels itself and responds to mechanical stimulus from every day use. During this process, osteoclasts first resorb bone and osteoblasts then go through a phase of bone formation.[159] In normal physiological conditions, the amount of bone removed during the resorption phase is balanced by the bone formation phase, such that bone mass is

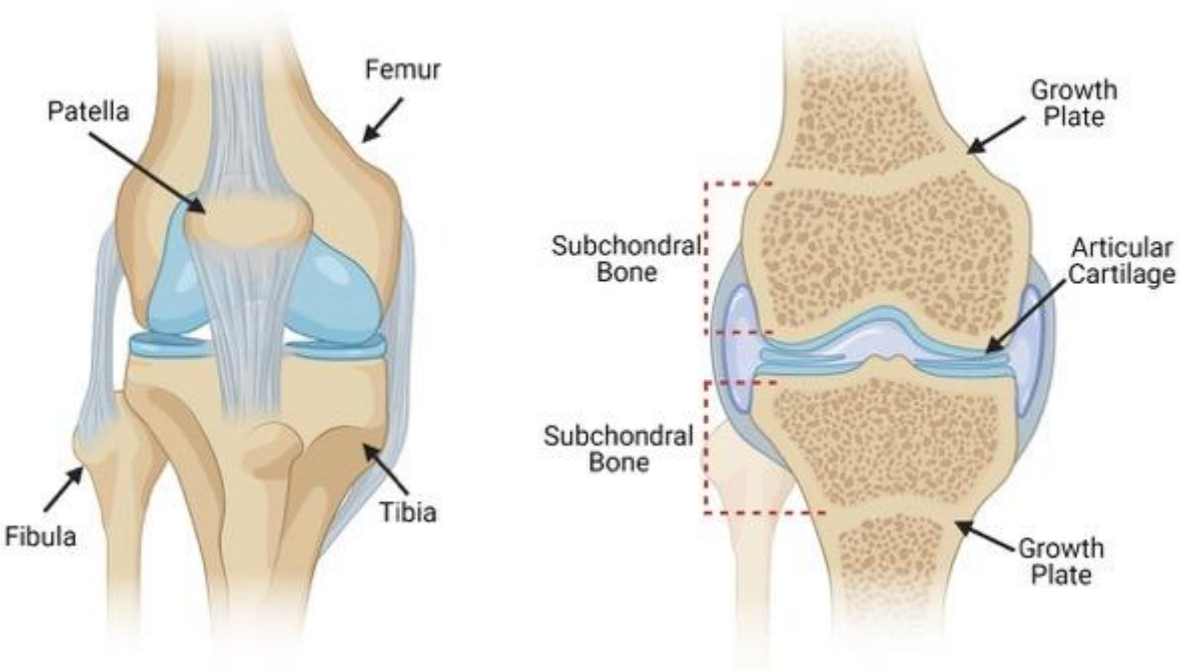

Figure 1. Anatomy of the main bones found in the knee joint and the area defined as subchondral bone.

maintained although the shape and architecture of bone is modified in response to repair micro-damage to the bone during mechanical loading.[55,159]

The main soft tissues within the joint include the anterior cruciate ligament (ACL), posterior cruciate ligament (PCL), medial collateral ligament (MCL), lateral collateral ligament (LCL), the patellar tendon, two menisci, articular cartilage, and the synovium. (Figure 2) The four ligaments connect the femur to the tibia and aid in preventing anterior, posterior and translation movements between the two bones. The ACL and PCL are located in the center of the joint, or the intercondylar fossa. The ACL primarily functions to prevent excessive anterior movement of the tibia relative to the femur during normal knee motion.[21] It is composed of two functional bundles; the anteromedial bundle which becomes taught at 90 degrees if flexion and the posteromedial bundle which becomes tight during full knee flexion.[4,34] The PCL primarily functions to prevent posterior translation of the tibia relative to the femur.[3] Both the ACL and PCL also aid in preventing internal and external rotation.[3,21] The MCL and PCL connect the

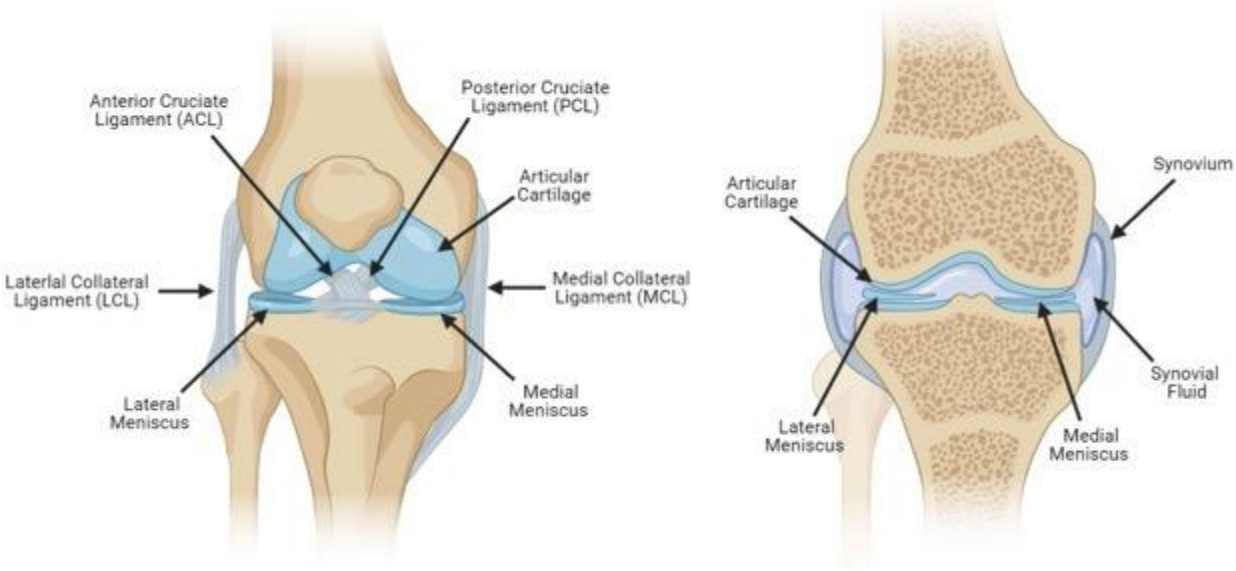

Figure 2. Anatomy of the main soft tissues found in the knee joint.

tibia to the femur on the medial and lateral side of the knee joint, respectively and aid in preventing valgus and varus rotation.[84,167] The four ligaments are primarily composed of collagen bundles that give them their mechanical structure to stabilize the joint.

Articular cartilage covers the ends of long bones and its primary function is to act as a smooth, lubricated lining between joint surfaces to facilitate load transmission. Chondrocytes are the main type of cell found within articular cartilage and they are responsible for creating the dense extracellular matrix (ECM); which is composed of water, collagen, proteoglycans and other non-collagenous proteins.[18] Through negative electrostatic repulsions forces, proteoglycan molecules help retain water within the ECM. This feature ultimately gives articular cartilage its biphasic properties, which give the tissue its unique response to tensile, compressive and shear forces.[111,113]

The menisci are two crescent shaped, fibro-cartilaginous structures that provide congruency between the tibial plateau and the femoral condyles.[52] Similar to articular cartilage, the fibrochondrocytes found in the menisci produce an ECM, primarily composed of collagen and proteoglycans, which retains water and gives the tissue its biphasic mechanical properties.[111] The primary function of these tissues are to increase congruency, maintain stability, and distribute compressive loads into hoop stresses, which also allows them to protect the underlying articular cartilage.[163]

The synovium, or synovial membrane, is the soft connective tissue layer that lines the inside of the joint capsule. It is composed of two layers – the outer layer (subintima) and the inner layer (intima). The subintima contains blood vessels, which allows it to nourish and maintain knee homeostasis by removing metabolites and other products of matrix degradation.[89,143] The cells found within the intima are called synoviocytes and are

highly metabolically active. The synovium is where the synovial fluid is produced, which a viscous fluid that lubricates and nourishes the tissues found within the joint capsule.[143]

Due to the enclosed knee capsule surrounded by the synovium, most of the soft tissues found within the joint are avascular, giving these tissues limited ability to heal and repair themselves. Therefore, both macroscopic damage and biochemical alteration of these tissues can have adverse effects on their integrity and can trigger other pathways for further tissue degeneration.

Knee Injuries and Post-traumatic Osteoarthritis

The knee joint is the most commonly injured joint in the human body. Acute joint trauma to the joint is a result from excessive joint forces, which are caused by participation in sports, jump landings, or other recreational activities, and often lead to damage and tearing of the ACL and meniscus.[62,98,119] Injury to these soft tissues are highly associated with the onset and progression of post-traumatic osteoarthritis (PTOA), a secondary form of osteoarthritis (OA).[38,39,44] PTOA is more commonly documented in a younger, more active population and it accounts for 12% of all patients exhibiting OA in the US with a financial burden of $2-3.06 billion dollars annually.[17] It is important to note that although the mechanisms that lead to the onset of each disease are different, they both have the similar end stage result.

PTOA is known to negatively impact the meniscus, articular cartilage, subchondral bone and synovium of the knee due to the damage and inflammatory response due to the initial trauma and subsequent changes in load distribution.[54] (Figure 3) In both the meniscus and articular cartilage, the disease is known to cause a fibrillation and damage to the surface, decrease in the mechanical properties, and a deterioration of

the solid matrix.[103] Previous studies have shown that in a process known as mechanotransduction, a cells response to mechanical stimulus, chondrocytes in the articular cartilage respond to the changes in loading pattern and begin to go through a process of ossification.[33,56] This ultimately leads to an increase in the advancement of the tidemark and eventual thinning and loss of the tissue, accelerating osteoarthritic changes in the joint. These changes are more commonly observed in the medial compartment of the joint compared to the lateral compartment.

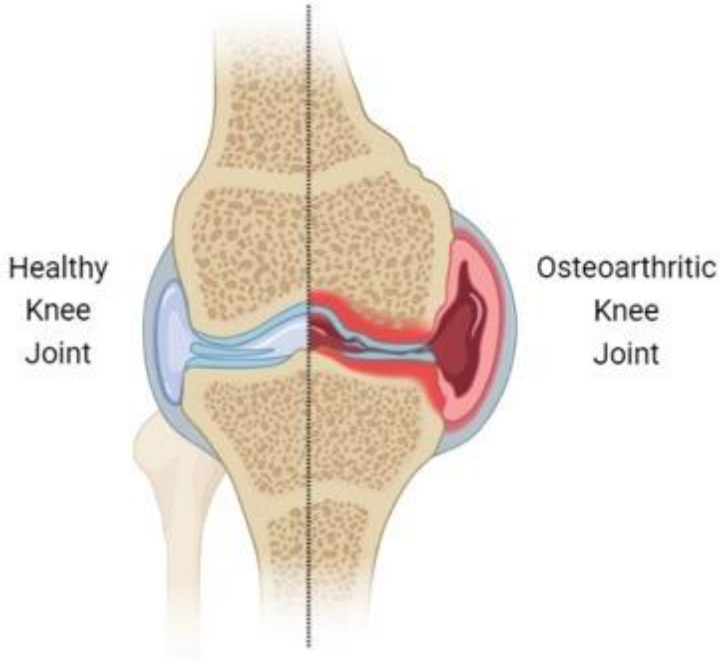

Figure 3. A healthy knee joint compared to an osteoarthritic knee joint.

As previously mentioned, bone is an adaptive tissue that goes through stages of remodeling and modeling as a response to mechanical loading, therefore changes in loading pattern as a result of alterations to bone contour during articulation can cause changes in bone architecture and mineral content. In subchondral bone, PTOA/OA is associated with the formation of osteophytes (bone spurs), a decrease in bone mineral density, and an increase in cortical bone thickness. Osteophyte formation is thought to be caused by alterations in joint mechanics and are commonly the first trademark sign of

PTOA observed in the knee joint. PTOA is known to disrupt the normal remodeling and modeling stages of bone, which can cause rates of bone resorption being high and rates of bone formation being low, leading to hypomineralized bone. These changes in bone mineralization affect the overall size and shape of subchondral bone that can also lead to a change in joint loading and further progress the disease.

A healthy synovium produces soluble mediators including, cytokines, chemokines, eicosanoids, and free radicals, to maintain homeostasis of the joint.[143] Following trauma to the joint, the synovium goes through an inflammatory response to protect the joint from further injury, eliminate the stimulus, and promote repair of the affected tissues. Inflammation of the synovium that occurs as a result of PTOA is referred to as synovitis. Synovitis causes the synovium to overproduce and release soluble mediators that promote solid matrix degradation in soft tissues through a positive feedback loop that increases cartilage damages and impairing repair, resulting in a vicious cycle.[89,139,145,147] Some of the pro-inflammatory mediators strongly associated with OA include, but are not limited to; interleukins (IL-1β, IL-6, IL-8 and IL-15), monocyte chemoattractant protein (MCP-1), tumor necrosis factor (TNF-α), macrophage inflammatory protein (MIP-1γ), and interferon (IFNγ).[146] These mediators, produced by the synoviocytes, interact and communicate with the other tissues in the knee joint, causing further degradation and increasing the severity of OA.

As of 2016, the Food and Drug Association (FDA) has classified OA/PTOA as a severe disease because it greatly increases a patient's likelihood of living with other co-morbidities, decreases life expectancy, and ultimately reduces the patient's quality of life.[121] Currently, there are no known effective treatments for OA, with the only FDA

approved treatment involves using non-steroidal anti-inflammatory drugs (NSAIDs). However, NSAIDs can have adverse side effects and even lethal in patients who suffer of cardiac problems, which is one of the co-morbidities strongly associated with OA.[121] Therefore, there is a need for better treatment options to delay or prevent the onset of OA/PTOA.

Current Treatments

The most common treatment to repair damage or a tear in the ACL or meniscus involves surgical intervention to both tissues. The goals of the surgery are to return normal kinematics to the joint and delay or prevent the onset of PTOA. Each year in the US, between 100,000 and 400,000 patients undergo ACL surgeries, with total costs on the order of $2 billion US dollars.[32,58,166]

In an ACL reconstruction surgery, the torn and damaged tissue is removed and it is replaced with a tendon graft harvested from the medial hamstring, the middle third of the patellar tendon, or allograft tissue. After choosing the appropriate graft for the patient, the surgeon performs a diagnostic arthroscopy to determine if any damage occurred to the menisci and the articular cartilage. If damage to the meniscus is observed, a meniscal debridement is performed to remove any portions of damaged or torn meniscus. This procedure is often referred to a meniscectomy. Following debridement of the meniscus, a small incision is made into the knee joint and tunnels are drilled into both the intercondylar fossa of the femur and tibial plateau along the point of insertion of the native ACL. The graft is then fed through the tibial bone tunnel and then through the femoral bone tunnel and it is anchored at the bone ends using a Nitinol pin. Prior to fixing the graft to the tibia, it is often rotated to mimic the 90 degree rotation in the collagen

bundles of the native ACL. Once the graft is anchored, the knee capsule is sterilized and closed. The amount of tension placed on the reconstructed ACL varies between surgeon and the graft used to recreate the reconstructed tissue and has a direct effect on rehabilitation following surgery.[100,106,112]

ACL reconstruction has been shown to be effective in restoring the sagittal plane stability to the knee,[106,112] however multiple studies have reported that surgical intervention does not appear to significantly decrease the risk of developing PTOA in the joint.[51,94,131] Some studies have shown that regardless if patients undergo surgical intervention or not, 78-83% will develop PTOA 10-14 years post-surgery, and the prevalence of the disease increases if ACL tear occurs in combination with an injury to the meniscus.[46,131] A previous study reports that patients with damage to the ACL have a 7-fold increase in needing a total knee replacement due to end stage OA, but that likelihood increases to 15-fold if there is damage to the meniscus.[80]

Although the exact mechanisms that lead to PTOA following surgical intervention are not well understood, it is hypothesized that occult damage at the matrix cellular level that is not addressed during reconstruction surgery plays a key role in the onset and progression of the disease. Pharmaceutical intervention that mitigates the progression of damage at the cellular following traumatic impact may be able to help mitigate further damage to the joint than surgery alone, which could help prevent the onset and progression of the disease.

Poloxamer 188 (P188)

Poloxamer 188 (P188) is an amphipathic, non-ionic surfactant that has been approved by the US FDA as safe for oral or intravenous administration and is excreted in the kidneys un-metabolized. P188 is a tri-block copolymer with an average molecular weight of 8,400 Da and is made of two poly(exythylene) (POE) tails and a poly(oxypropylene) (POP) body. The two POE chains are hydrophilic and the POP body is hydrophobic, mimicking the composition of the lipid bilayer found in cells. This composition allows the surfactant to insert itself and reseal cell membranes that have been damaged by electric shock, thermal damage, physical stress or chemical agents and is able to return normal cell membrane surface pressures.[65,85,124,148] (Figure 4)

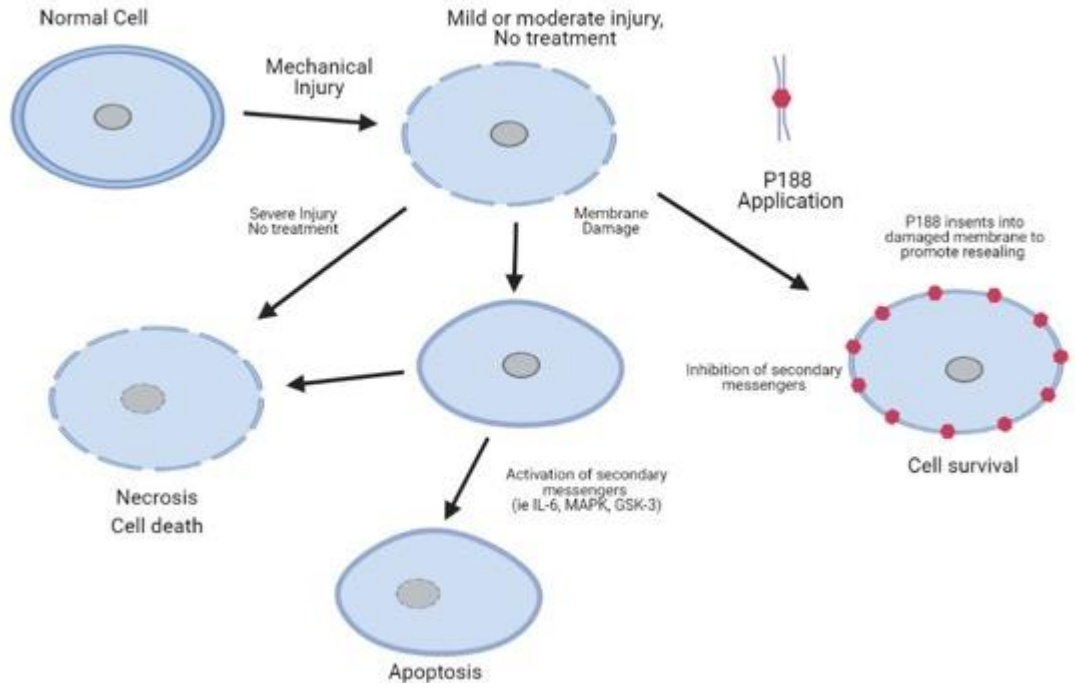

Figure 4. Life cycle of cells following traumatic mechanical injury. P188 is able to facilitate cell membrane resealing, inhibits pathways of secondary messengers, and prevents cell death.

Multiple *in-vitro* studies have reported that a single 8mg/mL dose of P188 administered immediately following traumatic impact to cartilage explants was able to

significantly reduce cell death.[8,9,53,118,130] Interestingly, the surfactant was shown to limit the area of cell death to that local to the site of initial trauma[53], signifying that it could potentially be affecting the mediators chondrocytes were expressing and releasing into the ECM.[9,148] Upon further investigation, it was found that P188 was able to inhibit the IL-6, mitogen-activated protein kinase, and GSK-3 pathways, all of which are strongly associated with an inflammatory response in cartilage. (Figure 1-4) Thus, *in-vitro* studies found that P188 is able to reseal compromised cell membranes which resulted in higher levels of cell viability, but by doing so, it could also control the tissues inflammatory response, making it a promising therapeutic agent in PTOA.

Similarly, the efficacy of the surfactant in *in-vivo* models has also found promising results.[29,74,138] Two studies found that a single dose of P188 injected directly into the knee capsule immediately following traumatic injury to the closed joint in rabbits was able to reduce cell death in articular cartilage, when compared to the non-treated group.[74,138] The results from these studies were not as promising as those from *in-vivo* studies, which lead the authors to suggest that by timing multiple administrations of the surfactant to cell necrosis, which happens immediately following impact, and cell apoptosis, programmed cell death that occurs hours or days after impact, could improve the efficacy of the surfactant. One *in-vivo* study found that the surfactant was able to significantly reduce proteoglycan (GAG) loss when compared to the impact only group.[29] This suggests that the surfactant is also able to prevent degenerative changes of the ECM *in-vivo*, thus further supporting the use of P188 as a potential treatment following traumatic impact to the knee joint. However, it remains unclear if multiple temporal

administrations of the surfactant would improve its efficacy and if it is able to prevent cell death in other soft tissues in the knee, besides the articular cartilage.

Animal Models to Study PTOA

Due to the complex and dynamic nature of OA and PTOA, it is difficult to study the etiological and progressive aspects of these diseases in humans, as only end-stage tissue is readily available. Therefore, translational animal models are powerful tools that enable a more detailed investigation into the origins and progression of these diseases. Induction of PTOA in animal models, with lapine or rabbit models being more widely used, often involves mechanical disturbances to various tissues, induced through open joint surgery, impact models, or some combination.[12,22,47,48,99,127,162,168]

The most common technique to destabilize the knee to induce PTOA involves surgically transecting the ACL[12,22,162] and/or a partial or full medial meniscectomy.[48] (Figure 5) Although surgical transection models induce changes to the tissues in the knee

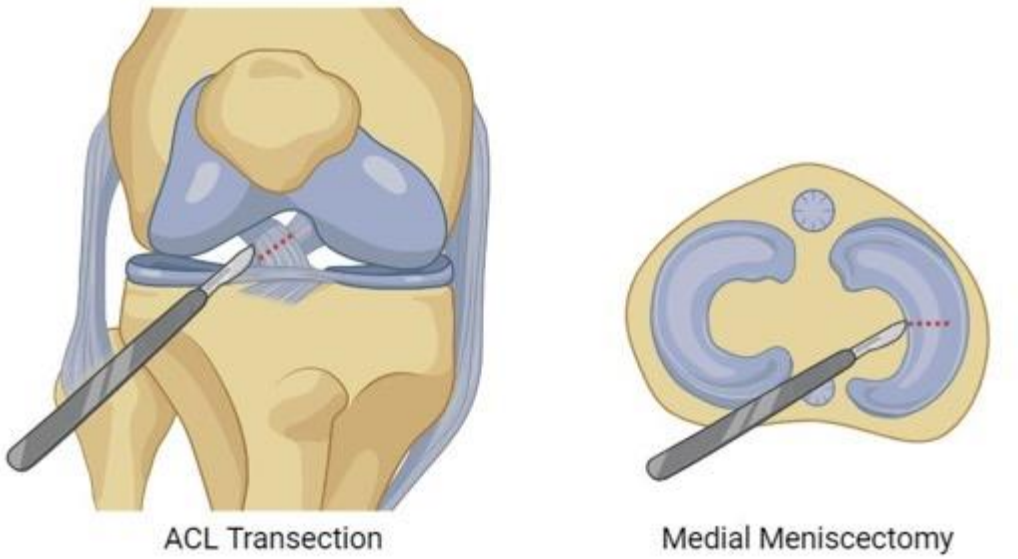

Figure 5. Representative images of surgical methods used to destabilize the knee joint to induce PTOA in animal model studies.

joint that are consistent with PTOA, the observed changes are often times not consistent with those observed in the clinical setting following a traumatic impact to the knee joint.[108,153,154] These models fail to address occult damage to other structures including; cartilage, meniscus, and subchondral bone, which could skew pathological findings. It is also likely that these models influence synovial swelling, up-regulation of inflammation, and pain, all of which could affect study findings.[134]

Recent advances in animal models have developed models to deliver an injurious impact to the closed or open joint to cause the destabilization of the knee.[47,48,127] These models are able to cause damage to both the ACL and meniscus as well as other tissues the knee, making them more clinically relevant to study the onset and progression of PTOA. Previous studies have directly compared the closed-joint impact model to the ACLT model and found that the impact model showed changes in articular cartilage, meniscus, and subchondral bone that were more representative of PTOA.[48,127] It has been suggested that to better study the disease, closed-joint impact models should be used over transection models. Currently, there are a number of studies that investigate the onset and progression of PTOA using a closed-joint impact model, however, no closed-joint impact model study has reconstructed the ACL following failure due to impact and assessed the soft tissues in the knee for the onset and progression of the disease.

Multiple studies using animal models primarily focus on the degenerative changes in one tissue over the others, with most studies focusing on the articular cartilage. The pathology of PTOA should be considered as a whole joint disease, in which disturbances and responses from various tissues elicit and propagate degenerative responses in the surrounding tissues. Therefore, future studies investigating the progression of the disease

should evaluate degenerative changes in numerous tissues to better encapsulate the progression of the disease. This approach could shed light into the onset of the disease and provide better insight into methodologies that may aid in preventing the disease.

Research Aims

There exists a clear need for other treatments to prevent or delay the onset of PTOA following ACL reconstruction surgery, one that may address the occult damage at the cellular level from the initial impact. The goal of the study is to determine if combined targeted treatment of ACL reconstruction surgery and administration of P188 in a closed-joint impact model will limit, delay, or mitigate the development of PTOA in the affected joint. In order to address this goal, the following specific aims are proposed:

Aim 1: Determine the efficacy of a single and multiple temporal administrations of P188 in inhibiting cell death following traumatic impact in meniscal tissue.

No studies have documented the efficacy of P188 in meniscal tissue in preventing cell death following a traumatic impact and/or the efficacy of multiple temporal administrations of the surfactant. Meniscal explants will be harvested from Flemish Giant rabbits and be subjected to a traumatic impact known to cause cell death. Following impact, meniscal explants will be randomly assigned to one of six treatment groups to test the efficacy of P188 in meniscal tissue and if temporal administrations of the surfactant to coincide with cell apoptosis further improve cell viability. Meniscal tissue will be subjected to cyclic loading at 10% strain for one hour, five days a week in order to encourage the loading environment the tissue is accustomed to. After two weeks, cell viability, proteoglycan content, and cell apoptosis will be assessed using assays and histology.

Aim 2: Assess morphological, functional, and histological changes in the meniscus.

Using a novel closed-joint and surgical reconstruction model to cause ACL failure, both the lateral and medial menisci will be assessed for changes associated with PTOA. Morphological grading will be used to determine if P188 treatment is able to prevent significant macroscopic degeneration of the tissue. Mechanical testing via indentation-relaxation in a water bath will be used determine the instantaneous and equilibrium modulus of the tissue to assess the functional properties of the tissue. Finally, Safranin-O/Fast Green stain will be used to determine any changes in GAG staining intensity and coverage of the tissue.

Aim 3: Evaluate chronic changes in subchondral cortical and trabecular bone of femurs and tibias.

Using a novel closed-joint and surgical reconstruction model to cause ACL failure, subchondral bone of both femurs and tibias will be assessed for changes associated with PTOA using micro-computed tomography. After determining the regions of interest that coincide with mechanical testing of the articular cartilage, both cortical and trabecular bone will be assessed for changes in bone quality and architecture. Parameters of interest in cortical bone include bone mineral density, porosity, and thickness. Parameters of interest in trabecular bone include bone mineral density, bone volume fraction, trabecular strut number, trabecular strut thickness, and trabecular strut separation. Both bones will also be analyzed for osteophyte formation outside the normal joint margin.

Aim 4: Determining the presence of biomarkers associated with PTOA in the synovial fluid

Using a novel closed-joint and surgical reconstruction model to cause ACL failure, synovial fluid will be assessed to determine the presence of inflammatory mediators associated with PTOA using mass spectrometry. Following euthanasia, the synovial fluid from the intact knee joint will be harvested and frozen for later analysis. Once thawed, samples will have albumin removed using a MultiSpecies Albumin depletion column. Samples will then be prepared for mass spec by overnight trypsin digestion and be cleaned using desalting columns. The proteome of the synovial fluid will then be analyzed using quantitative tandem mass targeting mass spectrometry. Samples from treatment groups will be normalized to their respective control to account for variation in protein expression in each animal.

CHAPTER 2

A SINGLE DOSE OF P188 PREVENTS CELL DEATH IN MENISCAL EXPLANTS FOLLOWING IMPACT INJURY[1]

INTRODUCTION

Menisci are fibro-cartilaginous structures that aid in joint stability, load distribution and act to protect the underlying articular cartilage from large pressures in the knee joint. Traumatic injuries to the knee joint often lead to damaged menisci[62,98,119]. It has been long established that injuries to soft tissues of the knee can induce post-traumatic osteoarthritis (PTOA)[38,40,79,107], although the exact mechanisms to the onset of the disease remains unknown. Previous studies have shown that damage to the menisci can lead to early degeneration of the underlying cartilage[31,71,102], and a 15-fold increase in the likelihood of a patient developing end stage osteoarthritis and undergoing total knee replacement[80], whereby highlighting the importance of these structures within the knee joint. Current clinical treatment for meniscal injuries focuses on macroscopic acute tissue damage by removing the damaged portions, but it neglects any occult microscopic damage that may prove crucial in the development of PTOA. Pharmaceutical intervention that mitigates the progression of occult damage on the cellular level following a traumatic impact may be able to help mitigate further damage to the menisci and avert the progression of PTOA.

---

[1]Reprinted from the Journal of the Mechanical Behavior of Biomedical Materials, Vol. 17, Narez GE, Wei F, Dejardin L, Haut RC, Haut Donahue TL, "A single dose of P188 prevents cell death in meniscal explants following impact injury", Pages 104406, Copyright (2021), with permission from Elsevier.

Poloxamer 188 (P188) is an amphipathic, non-ionic surfactant that has been shown to prevent cell death in neurons[86] and cartilage[8,9,53,74,118,130,138]. P188 is a tri-block polymer consisting of hydrophilic ends and a hydrophobic body, thus allowing itself to insert within the lipid bilayer of cell membranes to restore their integrity after physical stress. Previous *in-vitro* studies have demonstrated the ability of a single 8mg/mL dose of P188, administered immediately following impact, in preserving cell viability in articular cartilage[8,9,53,118,130]. Similarly, two animal impact models report that P188 significantly reduces the amount of cell death in articular cartilage, when compared to untreated groups[74,138]. Multiple studies suggest that timing additional P188 administrations to coincide with cell apoptosis would potentially improve the efficacy of the surfactant[8,74,118,130,138]. To the best of the authors' knowledge, only one study has evaluated the efficacy of the surfactant on meniscal tissue. In a closed-joint animal impact model, Coatney et al. report that at six weeks post injection, a single intraarticular injection of P188 significantly helped to preserve the proteoglycan content of the meniscus when compared to menisci from an untreated impact group[29]. Although the study did not report data on cell viability, the results show that P188 is a viable option in preserving the integrity of other soft tissues in the knee joint. It is not clear if the P188 injection directly affected meniscal changes or if it was indirectly through effects on other tissues in the knee joint. Thus, to better understand the actions of P188 on meniscal tissue directly, it is necessary to run isolated *in vitro* studies with isolated meniscal tissue to determine the direct effects of P188 on meniscus in the absence of other joint tissues. The current literature suggests that multiple administrations of P188 post-impact, that coincide with cell necrosis and apoptosis time points, may be necessary to maintain

meniscal cell membrane integrity following the acute injury, and potentially slowly or halting the progression of PTOA.

The objective of the current study therefore is to characterize the effects of single and multiple temporal administrations of P188 to meniscal explants after being subjected to a traumatic impact. The administration time points of immediate (time 0)[41], 4 days[30] and 7 days[53] post-impact were chosen to coincide with previously reported high levels of cell necrosis and apoptosis. It was hypothesized that P188 would reduce cell death, thereby maintaining the biochemical integrity of the tissue similar to that of an unimpacted control group. This would be the first *in-vitro* study to assess the efficacy of P188 on cell viability and tissue biochemistry in meniscal tissue.

METHODS

Sample collection and treatments

Hind limbs from ten mature Flemish Giant rabbits (5.97 ± 0.54 kg) were obtained following euthanasia. The study was approved by the Institutional Animal Care and Use Committee (IACUC) at Colorado State University. All animals were housed in individual cages prior to euthanasia. A biopsy punch was used to excise 2 mm diameter meniscal explants from both the lateral and medial menisci. Explants were then cut to 1 mm in height by cutting off tissue from the superficial layer using a specialized cutting tool (Figure 6). In order to obtain 1 mm tall explants it was necessary to take biopsy punches only from the outer region of the meniscus where the tissue is thick enough. The inner, avascular zone is too thin to obtain samples from this region. Due to differences in size and thickness, four explants were not always able to be harvested from each meniscus.

While the superficial layer has been shown to be mechanically sensitive[23], this surface was removed to create uniform cylindrical explants with the flat distal surface.

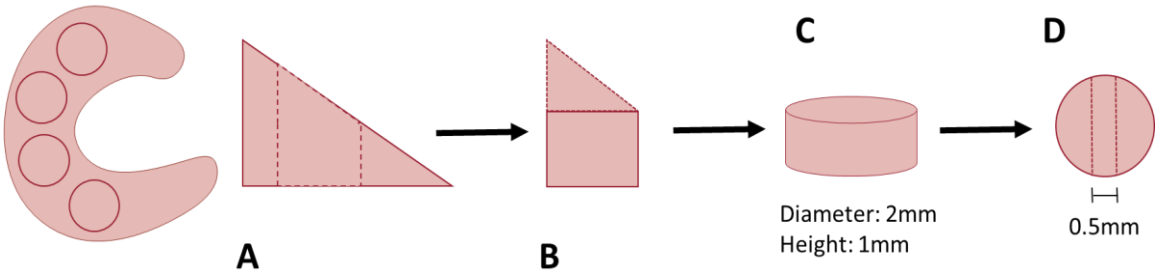

Figure 6. Explant harvest workflow. (A) Meniscus is harvested from Flemish Giant hind limbs (top and side view of meniscus body) (B) biopsy punch is used to collect 2mm explant plugs from the meniscus (C) explants are cut to 1mm in height (D) a 0.5mm section is collected per explant and used for

Explants were equilibrated for 24 hours in culture media (88% Dulbecco's Modified Eagle Medium: F12, 10% fetal bovine serum, 2% penicillin/streptomycin) in a humidity-controlled incubator (37°C, 5% CO_2, 95% humidity). Culture media was replaced every two days during the experimental protocol.

Explants were randomly assigned to one of six treatment groups, i.e. unimpacted no P188 (UNIMP), unimpacted P188 day 0 (UNIMP188), impacted no P188 (IMP), impacted P188 day 0 (IMP188), impacted P188 days 0 & 4 (IMP188-4), and impacted P188 days 0 & 7 (IMP188-7) with day 0 denoting immediately following impact (Table 1). At least one explant from each animal was randomly assigned to one of the six treatment groups. Explants in the impacted groups were exposed to an injurious impact known to produce significant levels of cell death [82]. Using a hydraulic testing system (MTS Corp, Eden Prairie, MN), explants were pre-loaded to 100mN and then subjected to a 50% impact strain using a ramp stroke in 1 second. 50% strain impact resulted in approximately 7 MPa of pressure on the explants. 7 MPa of pressure has been shown to be representative of a 30% meniscectomy as indicated by Zielinska et al,[41]. Thus this

level of loading has direct clinical significance. Immediately following impact, explants were placed in their respective media and compressed in unconfined sinusoidal compression using a custom-built bioreactor[59,104] to 10% strain in 1 second for one hour per day, five days per week over a 2-week period. This level of daily loading was necessary for two reasons. First, it has previously been shown that unloaded meniscal explants in culture will start to show degenerative changes[42], and secondly, previous studies have suggested that compressive loading and unloading helped to facilitate uptake of P188 from culture media into the explant[43].

Table 1. List of the six treatment groups explants were randomly assigned to and the sample size per group. Day 0 represents the day explants received the injurious impact.

Treatment	Sample Size
Unimpacted, No P188 (UNIMP)	22
Unimpacted, P188 Day 0 (UNIMP188)	20
Impacted, No P188 (IMP)	21
Impacted, P188 Day 0 (IMP188)	20
Impacted, P188 Day 0 & 4 (IMP188-4)	20
Impacted, P188 Day 0 & 7 (IMP188-7)	18

Cell Viability

At 14 days post-impact explants were removed from the culture media and a single 0.5mm thick rectangular cross section was collected from the middle of each sample (Figure 2-1). Sections of menisci were immediately incubated in 2mM Calcein AM and 8mM ethidium homodimer-1 (Life Technologies, Grand Island, NY) in phosphate-buffered saline (PBS) and incubated for 25 minutes (37°C, 5% CO_2, 95% humidity). Images were captured for both live (green fluorescence) and dead (red

fluorescence) cells using a fluorescence microscope (Leica Microsystems Inc., Buffalo Grove, IL) at 4x magnification. ImageJ (National Institutes of Health, Bethesda, Maryland) was used to count live and dead cells, where the percentage of cell viability was defined as the amount of live cells divided by the total sum of dead and live cells. Data for each treatment group were averaged and normalized to the unimpacted, no P188 group (UNIMP).

Proteoglycan Staining

Meniscal explants were fixed in 10% formalin. Explants were then immersed in 30% sucrose solution for cryoprotection, embedded in Optimal Cutting Temperature Compound (OCT) (Sakura Finetek, Torrance, CA) and flash frozen using liquid nitrogen. The explants were cryosectioned to 6μm and stained for glycosaminoglycan (GAG) using hematoxylin, Safranin-O, and Fast Green (FCF) staining. Slides were imaged using an Olympus BH2 Microscope (Olympus, Center Valley, PA) and Micro-Publisher 5.0 RTV camera (QImaging, Surrey, BC, Canada). Staining intensity was graded similar to previous studies with no Safranin-O staining represented by a score of 0, slight staining = 1, moderate staining = 2, and strong staining = 3 (Figure 7)[29,49,126]. Reported intensity grades were averaged from four separate blinded graders.

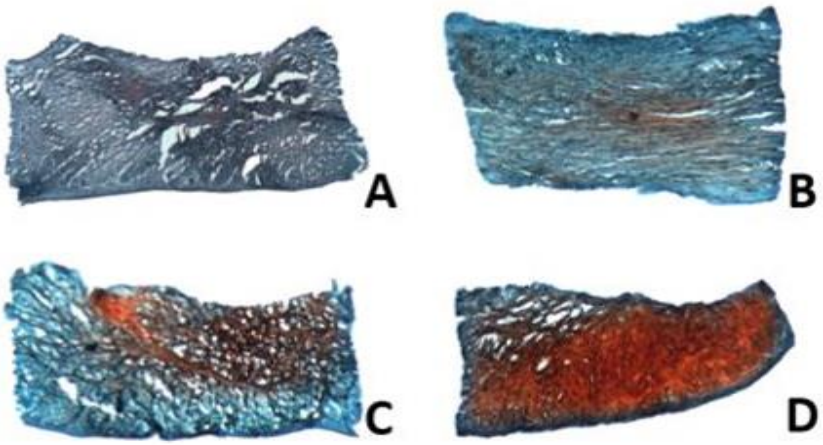

Figure 7 Safranin-O and fast green staining intensity grading. (A) No stain = 0, (B) slight staining = 1, (C) moderate staining = 2, (D) strong staining = 3.

GAG staining was analyzed using ImageJ. Briefly, total area of the section was calculated using the 'Analyze Particles' tool and summing particles. The area stained red, or the area associated with GAG coverage, was separated from the image using the "Colour Deconvolution" tool[137]. The percent area of GAG stain coverage was calculated as the total area of GAG stain coverage divided by the total area of the section multiplied by 100 (Figure 8)[29,49].

Cell Apoptosis

Cell apoptosis was assessed using the DeadEnd Fluorometric TUNEL Kit (Promega Corporation, Madison, WI). Briefly, tissue sections were washed to remove excess OCT and fixed in 4% paraformaldehyde. Tissues were then treated with 20µg/ml proteinase K in PBS for 3 minutes and then rinsed in PBS. Sections were incubated in an incubation buffer that included fluorescein-12-dUTP for one hour (37°C. 5% CO_2, 95%

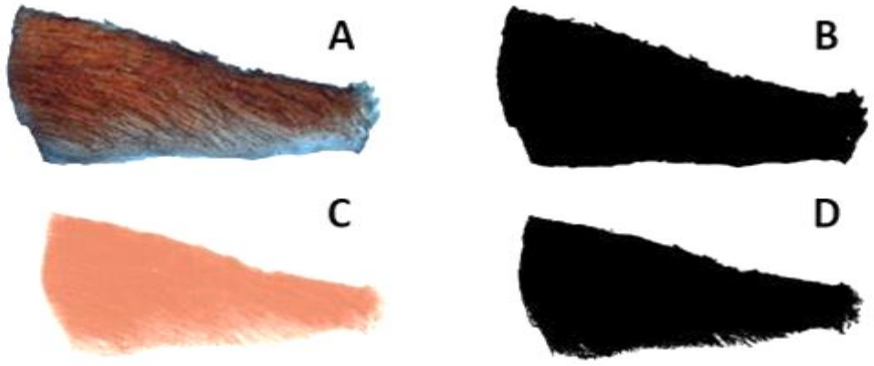

Figure 8. Representative images showing the image analysis for calculating GAG area coverage using ImageJ: (A) stitched and trimmed image of explant was imported, (B) threshold and analyze particles of tissue section was used to determine overall area of cross section, (C) colour deconvolution tool was used to isolate area stained for GAG from imported image, (D) analyze particles was used on the colour deconvolution image to determine area of GAG coverage.

humidity). Tissues were then stained in a 1µg/ml solution of propidium iodide in PBS. Images were captured for TUNEL positive apoptotic (green fluorescence) and total (red fluorescence) cells using a fluorescence microscope at 4x magnification. ImageJ was used to count TUNEL positive and total cells, where the percentage of apoptotic cells was defined as the number of TUNEL positive cells divided by the number of total cells. Data for each treatment group were averaged.

Statistics

Statistical data analysis was performed using Minitab (Minitab18, State College, PA). Statistical significance was assessed for cell viability using a one-way analysis of variance (ANOVA) with Tukey's post-hoc test after normalization to the UNIMP treatment group. Comparisons for GAG intensity, GAG coverage, and cell apoptosis were made using a one-way ANOVA with Tukey's post-hoc test. Differences corresponding to a p-value of less than 0.05 were considered to be statistically

significant. A post hoc power analysis powered the study at 89%. To reduce animal to animal variability, data was normalized to unimpacted groups. Additionally, to ensure independence between the samples and measured outcomes, multiple linear regression was used with animal, limb, hemijoint, and region as explanatory variables using R (R Core Team, 2019).

RESULTS

A single impact of 50% strain significantly decreased ($p < 0.05$) the amount of viable cells in the impacted menisci compared to the unimpacted explants (Figure 9). This decrease in cell viability was reversed when impacted explants were treated with P188. No significant differences were documented between the UNIMP explants and the impacted explants that received single or multiple administrations of P188 after impact. A significant difference was documented between the IMP explants and the UNIMP188 ($p < 0.05$), IMP188 ($p = 0.002$), IMP188-4 ($p = 0.033$), and the IMP188-7 ($p = 0.015$)

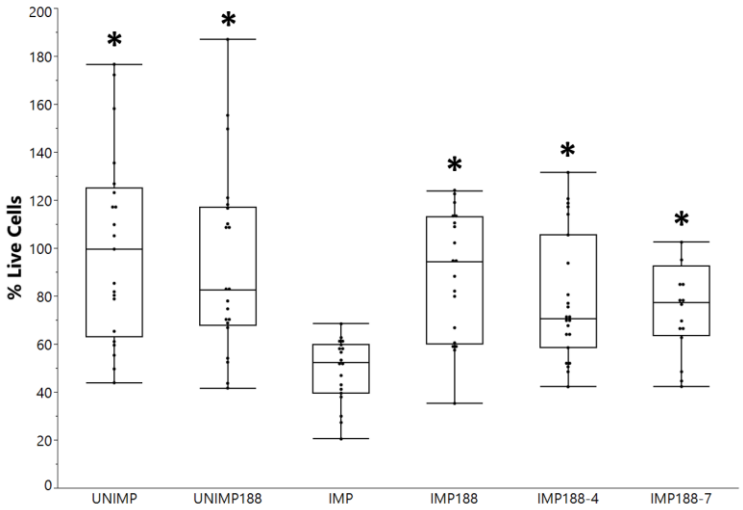

Figure 9. Results for meniscal cell viability per treatment group, normalized to the UNIMP group. * denotes significant difference ($p < 0.05$) from the IMP treatment group.

explants. P188 did not affect cell viability when administered to the unimpacted explants. No depth dependent differences in cell viability were noted in any treatment groups.

Histologically, there were no documented significant differences in GAG intensity (Figure 10) or GAG coverage (Figure 11) between any of the treatment groups.

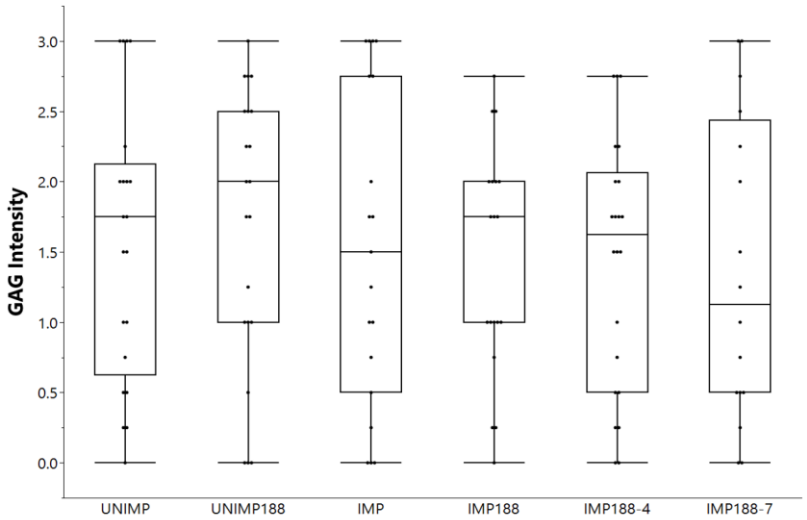

Figure 10. Results for GAG staining intensity in meniscal explants per treatment group.

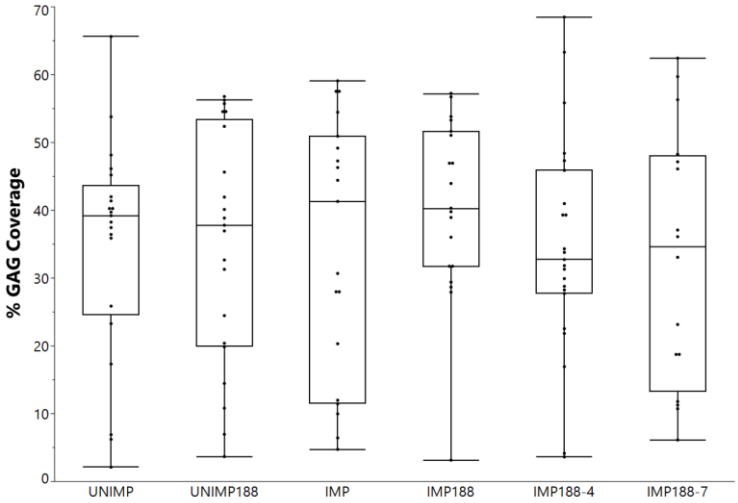

Figure 11. Results for percent GAG coverage in meniscal explants per treatment group.

Similarly, there were no documented significant differences in cell apoptosis levels between any of the treatment groups (Figure 12) for these samples at day 14.

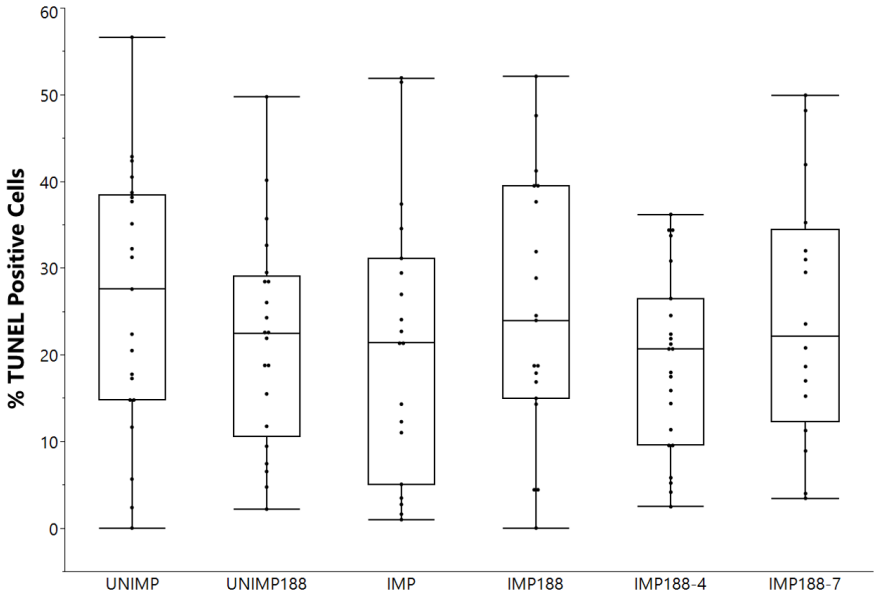

Figure 12. Results for percentage of apoptotic cells per treatment group.

DISCUSSION

To the best of the authors' knowledge, this is the first study to show data on the efficacy of P188 on cell viability for traumatized meniscal tissue, as well as the efficacy of multiple administrations of the surfactant. In the current study an impact of 50% strain produced significant cell death over the 14-day period. Similar to previous studies in articular cartilage[53,74,118,130,138], the current study documented that a single administration of P188 immediately following impact was effective in reducing cell death 14-days later. Some previous studies in articular cartilage suggest that giving the impacted tissues multiple administrations of the surfactant may result in a more effective treatment in preventing cell death and maintaining tissue integrity[53,74,118]. It has been reported that by

sealing the cell membrane, P188 is able to counteract signaling pathways involved in the inflammatory response following impact, thus preventing cell death in articular cartilage[9,118]. The results of the current study were consistent with these studies in articular cartilage showing that P188 was able to prevent cell death in impacted knee joints. However, no significant differences between single or multiple administrations of the surfactant were documented in the current study. This may suggest that at least for meniscal tissue, a single administration of P188 immediately following impact may be all that is necessary to prevent meniscal cell death. Sealing the cell membrane with P188 in meniscal cells may inhibit the release of mediators in the tissue following impact. Taken together, the findings of the current study suggest that a single dose of P188 immediately following impact may be all that is necessary to inhibit cell death in menisci. This inhibition of cell death following an impact load demonstrates that meniscal tissue is mechanically sensitive, which is consistent with previous studies.[23-25, 36,42,44]

The findings on cell viability and cell apoptosis levels could suggest that necrosis from the physical stress of impact was likely the predominant cause of cell death in these menisci. However, no significant differences in apoptosis is not surprising given that apoptosis likely peaked earlier than day 14. Cells that undergo apoptosis-like cell death exhibit some of the signs associated with cells undergoing apoptosis, but they do not necessarily require caspase activity[88]. In articular cartilage, Garrido et al. reported that 7 days after impact there was an increase in the rate of apoptosis, suggesting that immediate administration of P188 only delayed the onset of apoptosis rather than blocking it[53]. The current study documented no significant differences in the levels of apoptosis between the six different treatment groups, albeit only evaluated at 14 days. It

should be noted that approximately 20-25% of cells are undergoing apoptosis in all groups. It is hypothesized that this is potentially due to the explants being in cell culture versus *in vivo* conditions.

No significant changes in GAG content were documented between any of the treatment groups. Only one previous long-term study has assessed the efficacy of P188 in preserving GAG content in menisci. In a 6-week *in vivo*, post-traumatic injury animal model, Coatney et al. reported that a single intra-articular injection of P188 prevented significant GAG loss when compared to that of an impacted, untreated group[29]. It is unknown if the effect on GAG loss was direct or indirectly the result of injected P188. Fibrochondrocytes play a key role in meniscal function by producing the extracellular matrix that is responsible in maintaining the mechanical integrity of the tissue[1,36,114]. Previous studies have shown that musculoskeletal tissues subjected to a traumatic load release catabolic mediators, which contribute to the breakdown of the tissue matrix[63,64,69,122,149]. Furthermore, previous studies in lapine menisci have documented the decrease in GAG following an injurious impact over 8 and 12 week time points[49]. While there was a decrease in GAG coverage in the impacted limbs, compared to unimpacted controls, and P188 was able to keep GAG coverage levels the same as unimpacted controls, these changes were not significant. This may suggest that a 14-day post-traumatic injury time point, as used in the current study, is perhaps too early to observe a significant difference in the long-term efficacy of P188 in preserving GAG content in menisci. It should also be noted that this study did remove the superficial zone and take samples from the outer region of the menisci in order to get a flat sample. Hence, these

results are primarily for the deep zone, which is where more glycosaminoglycans are present, compared to the superficial zone which is more interwoven collagen[38].

Only a few studies have documented the mechanosensitivity of meniscal tissue to impact loading. Kisiday et al., found that mechanical overloading resulted in significant increases in cell death in meniscal explants[82]. Hufeland et al., found a single injurious impact induced cell damage and release of GAG and reduced nitric oxide production and transcription of matrix-degrading enzymes 3 days post impact. Thus, this study contributes to the base knowledge of how meniscal tissue responds to injurious impact loads. Previous studies documented the behavior of meniscal tissue under normal loading conditions (10% strain) as well as conditions simulating partial meniscectomy (20% strain)[59,104]. These studies found proteoglycan breakdown, increases in cytokine-inducible nitric oxide synthase and interleukin-1 gene expression and increase in nitric oxide release to the surrounding media to occur at higher levels of strain. Studies have also shown that meniscal fibrochondrocytes are responsive to changes in shear stress[44]. These previous studies, along with the current study, demonstrate that the menisci are mechanically sensitive tissues. Thus, as the current study suggests, injurious impact loads likely ruptures cell membranes and the addition of P188 can maintain cell viability levels comparable to non-impacted meniscal tissue.

The findings of the current study suggest that a single dose of P188 immediately following injury reduces the amount of cell death in the meniscus. A limitation of the current study includes qualitatively assessing changes in proteoglycan content. Future studies should also include quantitatively measuring the amount of GAGs in each sample to aid in determining if the treatment was successful in preventing changes in the

biochemical composition of the tissue. Similarly, changing the end point to later than the 14-day period may show that there were changes in the qualitative changes (coverage and intensity scoring) of proteoglycans between the six different treatment groups. Exploring longer time points following impact may also help determine when P188 is no longer a viable option in preventing significant levels of cell death in tissues of the knee. Cell necrosis levels have been shown to significantly increase 24 hours post-impact[24,90], thus finding the ideal window to administer P188 will provide insight into the practicality of using the surfactant in a clinical setting.

CONCLUSIONS

A single, early dose of P188 was sufficient to inhibit cell death over 14 days in this *in vitro* study. This result may have direct implications in the potential administration of this surfactant in the clinical setting following anterior cruciate ligament rupture in order to save joint tissues from long term disease such as PTOA. Future studies, particularly *in-vivo* animal studies, will be needed to certainly recommend the use of P188. By addressing changes at the cellular level, pharmacological intervention paired with surgical intervention may prove to prevent or delay the onset and progression of the disease.

CHAPTER 3

ASSESSING MORPHOLOGICAL, FUNCTIONAL, AND HISTOLOGICAL CHANGES IN THE MENISCUS[2]

INTRODUCTION

Menisci are crescent shaped tissues found within the knee joint that aid in joint stability, load distribution and act to protect the underlying articular cartilage from large pressures during everyday loading.[42,144] The mechanical properties of the tissue are largely contributed to the organization and composition of the solid matrix, which is mostly composed of collagen and proteoglycans (GAG).[2,25,78] The collagen fibers found in the tissue are circumferentially oriented, which allow the menisci to convert the compressive forces it experiences from the femoral condyles into hoop stresses.[5,129] Proteoglycans are negatively charged proteins primarily found in the inner 2/3 of the tissue and aid in distributing compressive forces by attracting and retaining water in the tissue.[2,78] Unfortunately, only the outer 1/3 of the tissue is vascularized, meaning damage and tears that occur within the inner 2/3 of the tissue are not able to heal properly.[28,109]

Traumatic injuries to the knee joint often lead to damage to the anterior cruciate ligament (ACL) and menisci10–12. It has been long established that injuries to these soft tissues of the knee can induce post-traumatic osteoarthritis (PTOA)13–16, although the exact mechanisms to the onset of the disease remains unknown. Due to both the ACL and

---

[2]Portions of this chapter are adapted from a publication in the Journal of Biomechanics, Vol. 126, Narez GE, Brown G, Herrick A, Ek R, Wei F, Dejardin L, Haut RC, Haut Donahue TL, "Assessment of Changes in the Meniscus and Subchondral Bone in a Novel Closed-Joint Impact and Surgical Reconstruction Lapine Model", Pages 110630, Copyright (2021), with permission from Elsevier.

meniscus being mostly avascular tissues, the most common treatment following damage include ACL reconstruction surgery and meniscal debridement for damage occurring in the avascular region of the meniscus. The goal of the surgery is to return normal knee kinematics and remove portions of the damaged tissue that could cause pain and discomfort to the patient. However, previous studies have shown that 78-83% of patients will develop PTOA 10-14 years post-injury, regardless of whether or not they receive surgical intervention following damage to the ACL and meniscus.[46,131] It is believed that because surgical intervention fails to address any of the occult damage at the cellular level, which may play a crucial role in the onset of PTOA. Thus, pharmaceutical intervention that mitigates the progression of occult damage on the cellular level following a traumatic impact may be able to help mitigate further damage to the soft tissues within the knee joint and avert the progression of PTOA.

Poloxamer 188 (P188) is a tri-block copolymer that has been shown to be an effective inhibitor of cell death in articular cartilage and meniscal tissue following traumatic impact.[8,9,53,117,118,130] Both *in-vivo* and *in-vitro* studies using articular cartilage from the knee and ankle have found that a single 8mg/mL dose of the surfactant administered immediately following impact was able to significantly reduce cell death, compared to untreated samples.[8,9,53,74,118,130,138] One study assessed the efficacy and multiple administrations of the surfactant in meniscal tissue and found that a single dose immediately following impact was all that was necessary to significantly reduce cell death in the tissue.[117] Not only was P188 effective in preventing cell death, but by resealing compromised cell membranes following impact, P188 has also been shown to interfere with pathways associated with cell death and inflammation.[9,148] All of these

findings suggest that P188 treatment may be able to address the occult damage following impact at the cellular level and merits further investigation in the *in-vivo* setting.

The goal of the study was to assess if combined surgical and P188 treatment would be able to prevent or delay the onset of PTOA in meniscal tissue at three-time points (1, 3, and 6 months) compared to surgical treatment alone in an *in-vivo* lapine model that combined both closed-joint traumatic impact and surgical reconstruction. It was hypothesized that, compared to surgical intervention alone, combined treatment would be more effective in preventing degenerative changes associated with PTOA in the meniscus.

METHODS

Animal Model

This study was approved by the Institutional Animal Care and Use Committee at Michigan State University. Ninety skeletally mature Flemish Giant rabbits (6.34 ± 0.75 kg) aged 7 - 9 months were used for this study. Animals were a mix of male (n = 41) and female (n = 49). Animals were anesthetized (2% isoflurane and oxygen) and subjected to an impact of the right tibiofemoral joint until ACL failure and meniscal tissue damage. As previously described, the right knee of each rabbit was shaved and placed in a custom rigid fixture in a servo-hydraulic testing system (Instron Corp, Norwood, MA) while the rabbit was in a prone position (Figure 13).28,29 A 400 N preload was applied and a controlled impact pushed the tibia downward 3.5 mm at a rate of 0.5 Hz.30 The left knee served as a contralateral control.

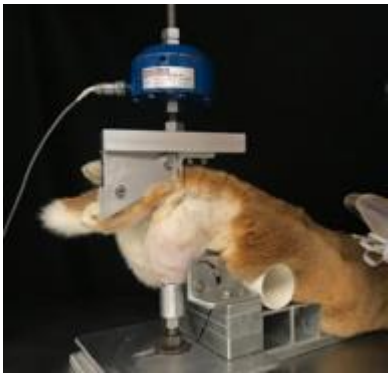

Figure 13. Injurious impact of rabbit knee set-up. In prone position (belly down) the rabbit's hind paw is supported directly below the actuator of an Instron and the knee is supported to prevent lateral and medial motion.

Animals were then randomly assigned to one of four treatment groups; Group 1 received reconstruction surgery only and no P188 treatment (Recon.), Group 2 received reconstruction surgery and a single dose of P188 immediately following impact (P188 D0), Group 3 received reconstruction surgery and a dose of P188 immediately following impact and a second dose 24 hours after impact (P188 D1), and finally Group 4 received reconstruction surgery, a dose of P188 immediately following impact, a second dose 24 hours following impact, and a third dose seven days after impact (P188 D7). For P188 treatment groups, 1mL of P188 at a concentration of 8mg/mL was injected into the knee capsule at the respective time point. The knee joint was then flexed and extended to mix the P188 injection with the synovial fluid.

Reconstruction of the torn ACL was performed by a board-certified veterinary surgeon (LD) approximately 2 weeks post-impact. A medial parapatellar arthrotomy was performed to assess the condition of the ACL and meniscus. Meniscal injuries, if present, were recorded and were treated via a partial, in which only the damaged or torn regions were removed, or full meniscectomy, in which the entire damaged medial or lateral meniscus was removed. The joint capsule was then opened and the semitendinosus (ST)

tendon was exposed on the posterior aspect of the medial tibial plateau. To minimize the amount of damage to the surrounding musculature, the ST tendon was then transected at the musculotendinous junction while leaving the tibial attachment intact. A 2.7 mm diameter tibial bone tunnel and a 3.2 mm diameter femoral tunnel were drilled at the ACL footprint. The free end of the ST graft was fed under the medial collateral ligament and then passed through the tunnels in the tibia and femur using a suture loop. Tension was applied on the graft and a custom interference fit screw was placed in the femoral bone tunnel to stabilize the graft.30,31 An anterior drawer test was performed on the reconstructed knee to ensure the joint was stable post-reconstruction.32 Animals were then euthanized at one of three time points 1-, 3-, and 6-months after the traumatic injury. The number of samples in each treatment group at each time point can be found in Table 2. Following euthanasia, meniscal tissue was harvested for assessment of morphological, mechanical, and histological changes.

Table 2. Number of samples per treatment group at each time point.

Treatment Group	1 mo.	3 mo.	6 mo.
Reconstruction Only (Recon)	6	6	6
Reconstruction + P188 D0 (P188 D0)	8	8	8
Reconstruction + P188 D0 &1 (P188 D1)	8	8	8
Reconstruction + P188 D0, 1 &7 (P188 D1)	8	8	8

Mechanical Analysis

Indentation relaxation testing was conducted on the anterior, central and posterior regions of the menisci in a 1x PBS bath at room temperature using a servo-hydraulic testing system (MTS Corp, Eden Praire, MN) and a 9 N load cell (Futek, Irvine, CA). Following a 20mN pre-load, a 1.59-mm diameter steel indenter tip traveled to a depth of

0.25 mm and was held for 900 seconds to reach equilibrium. Similar to previous studies, Hertzian contact was assumed between an elastic half-space (meniscus) and a rigid sphere (indenter).28,29,33,34 A Poisson's ratio of 0.01 was assigned to the tissue.35 The elastic modulus and Poisson's ratio of the indenter were 210 GPa and 0.3 respectively. After testing, the tissue was fixed in 10% buffered formalin. A custom algorithm in MATLAB (Mathworks, Natick, MA) was used to calculate the instantaneous and equilibrium moduli from the data collected in the hydraulic testing system.

Histological Analysis

Tissue samples were immersed in a 30% sucrose solution for cryoprotection before being embedded in optimal cutting temperature (OCT) compound (Sakura, Finetek, Torrence, CA) and flash frozen in liquid nitrogen. The tissue samples were then sectioned to 6 μm and stained for glycosaminoglycan (GAG) content using hematoxylin, Safranin-O (Saf-O), and Fast Green (FG) staining. The slides were then imaged using a bright field microscope (Leica Microsystems Inc., Buffalo Grove, IL) and an Olympus DP25 camera (Olympus, Center Valley, PA). Staining intensity was graded similar to previous studies with no Saf-O staining represented by a score of 0, slight staining = 1, moderate staining = 2, and strong staining = 3 (Figure 14).33,36,37 Reported intensity grades were averaged from four separate blinded graders.

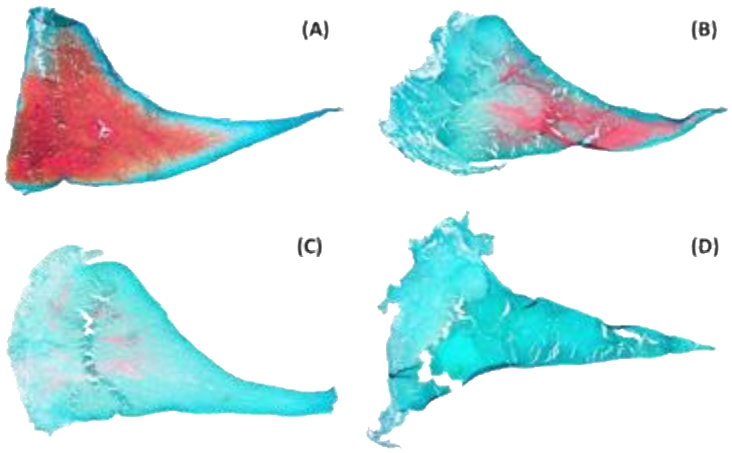

Figure 14. Histological scoring of meniscus. (A) Strong staining is assigned a score of 3, (B) moderate staining is assigned a score of 2, (C) slight staining is assigned a score of 2, and (D) no staining is assigned a score of 0.

GAG coverage was analyzed using ImageJ (NIH, Bethesda, MD) with the FIJI package.33,36 Briefly, total area of the section was calculated using the 'Analyze Particles' tool and summing particles. The area associated with GAG coverage (area stained red) was separated from the image using the 'Colour Deconvolution' tool. The percentage of GAG coverage was calculated as the total area of GAG coverage divided by the total area of the section multiplied by 100.

Statistics

To determine the influence of different treatments on the reconstructed limbs for the outcome measures (mechanical properties and GAG coverage), a mixed fixed effects model with repeated measures with Tukey's post-hoc was applied with animal, time, and treatments as fixed effects. For both meniscal GAG staining intensity and morphology grading, a Mann-Whitney post-hoc on assigned-ranks was applied. Due to the amount of damage to the menisci of reconstructed limbs, not all regions had a sufficient sample size to perform regional analyses, hence all analyses were performed on average compartment data for each animal. A difference with $p < 0.05$ was considered statistically significant.

RESULTS

Animal Model

The average peak impact load was 770 ± 137 N. During reconstructive surgery, the veterinarian surgeon (LD) documented that 50/90 experienced ACL rupture and 40/90 experienced a partial ACL tear. Half of the animals had documented damage to the medial meniscus; 39/90 animals had tears in the posterior region, 4/90 had bucket handle tears, one animal had a small tear, and one animal had a discoid shape meniscus. In contrast, only four animals had documented damage to the lateral meniscus; three had tears in the posterior region and one had a bucket handle tear. Due to the initial damage, medial meniscectomies were more commonly performed; 40 animals received a partial medial meniscectomy and six received a full meniscectomy. Only four meniscectomies were performed on the lateral meniscus, three partial and one full. It was observed that the animals bore more weight on the contralateral control limb for 1-3 days following impact and 5-10 days following surgery before returning to normal gait.

Morphological Analysis

Statistically significant increases in damage between treated (right) and contralateral control (left) limbs were observed in both menisci (Table 3). At 1-month, in

Table 3. Morphology grading for the meniscus. Values reported as Avg. ± Standard Deviation. * denotes statistical significant difference compared to control group at similar time point.

		Recon Ctrl	Recon	P188 D0 Ctrl	P188 D0	P188 D1 Ctrl	P188 D1	P188 D7 Ctrl	P188 D7
	1 mo.	0.45 ± 0.37	1.21 ± 0.74*	0.67 ± 0.51	0.78 ± 0.51	0.78 ± 0.99	1.15 ± 0.48	0.48 ± 0.60	1.32 ± 1.23
Lateral	3 mo.	0.57 ± 0.26	2.04 ± 1.34*	0.72 ± 0.42	1.79 ± 1.16*	0.60 ± 0.43	1.51 ± 0.85*	0.34 ± 0.21	1.40 ± 1.12*
	6 mo.	0.50 ± 0.27	2.2 ± 0.77*	0.56 ± 0.37	1.90 ± 0.74*	0.62 ± 0.49	1.93 ± 0.95*	0.33 ± 0.35	1.79 ± 1.02*
	1 mo.	0.53 ± 0.27	2.19 ± 1.63*	0.37 ± 0.36	1.17 ± 0.67	0.78 ± 0.58	2.77 ± 0.88*	1.18 ± 0.67	2.05 ± 1.17
Medial	3 mo.	0.60 ± 0.46	2.52 ± 1.2*	0.81 ± 0.83	2.32 ± 1.03*	0.45 ± 0.26	2.46 ± 0.79*	0.74 ± 0.51	2.52 ± 0.78*
	6 mo.	0.56 ± 0.19	2.49 ± 0.86*	0.75 ± 0.62	3.21 ± 0.69*	1.06 ± 0.78	2.06 ± 0.98	1.14 ± 1.26	2.36 ± 0.93

the lateral meniscus, P188 treated limbs saw a less significant increase in morphology grading, when compared to reconstruction surgery alone. However, P188 treatment did not seem to have the same effect at the later 3 and 6-month time points, as all treatment groups had a significant increase in damage, when compared to their respective control. In the medial meniscus, there was more severe damage found across all time-points in the treated limbs, regardless of treatment group.

Mechanical Analysis

Due to the excessive damage and degradation observed on the menisci of the reconstructed limbs, not all regions or tissue samples were able to be tested for changes in mechanical properties. Therefore, indentation results from the three regions (anterior, central, and posterior) of each menisci were averaged for each compartment and not all time points or treatment groups had similar sample sizes. Indentation-relaxation testing indicated that at the 1-month time point, all P188 treatments were effective in preventing a significant decrease in the instantaneous modulus of the lateral meniscus, compared to reconstruction only treatment. (Figure 15A.) At the later time points (3- and 6-months), multiple administrations of P188 were more effective in preventing further decreases in the modulus, compared to the Recon and P188 D0 groups. However, in the equilibrium

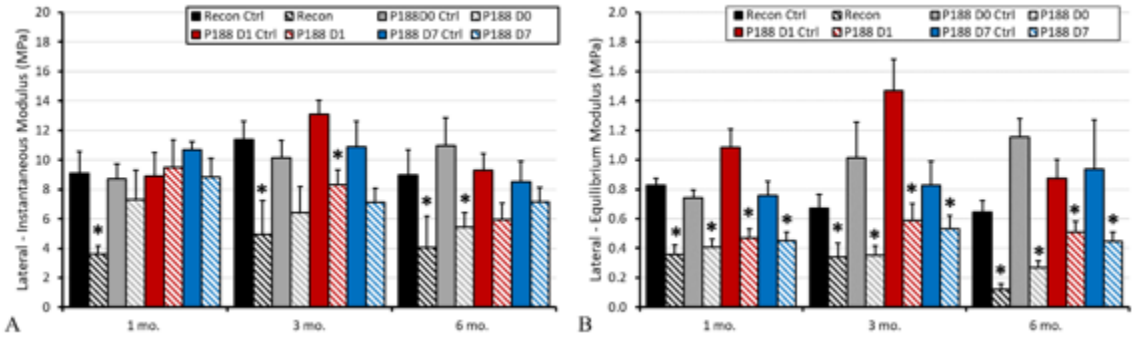

Figure 15. Lateral meniscus mechanical property results. (A) Results for the instantaneous modulus (B) results for the equilibrium modulus. All values reported as Avg. ± Standard Error. * denotes statistical significant difference compared to control group at similar time point.

modulus of the lateral meniscus, it was documented that no treatment group, at any time point, was able to prevent a decrease in the modulus compared to their respective control (Figure 15B).

In the medial meniscus, multiple doses of P188 (P188 D1 and P188 D7) were more consistent in preventing a significant decrease in the instantaneous modulus compared to control limbs, specifically at the later time 3- and 6-month time points. (Figure 16A). Similar results were observed in the equilibrium modulus of the tissue, where the multiple doses of P188 groups (P188D1 and P188 D7) were more effective in preventing a significant decrease in the modulus at the 3- and 6-month time points (Figure 16B).

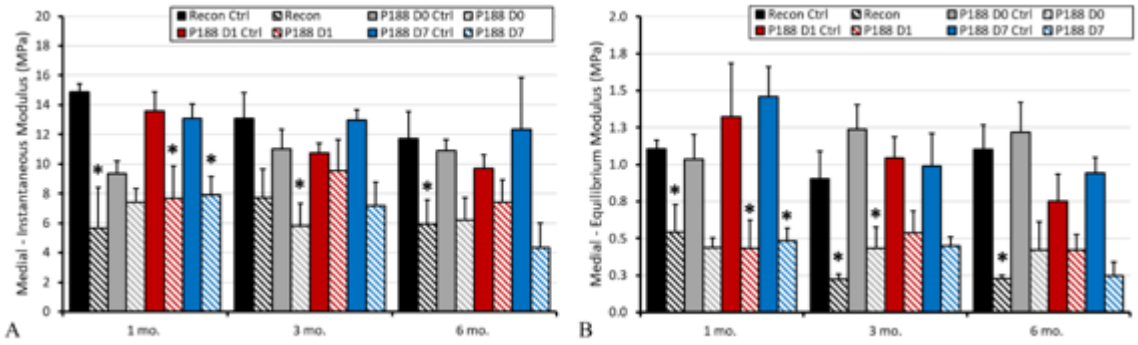

Figure 16. Medial meniscus mechanical property results. (A) Results for the instantaneous modulus (B) results for the equilibrium modulus. All values reported as Avg. ± Standard Error. * denotes statistical significant difference compared to control group at similar time point.

Histological Analysis

Qualitatively assessing GAG staining intensity of the lateral meniscus found that at 1-month, there were only significant decreases in the P188 D0 and P188 D1 groups, compared to controls. (Figure 17A) At the 6-month time point, the only documented decrease was found in the Recon only group. At 3- and 6-months, all P188 treatment groups were able to prevent significant decreases in staining intensity in the lateral

meniscus compared to controls. In the medial meniscus, the only significant difference found was a decrease in staining intensity in the P188 D1 group. (Figure 17B).

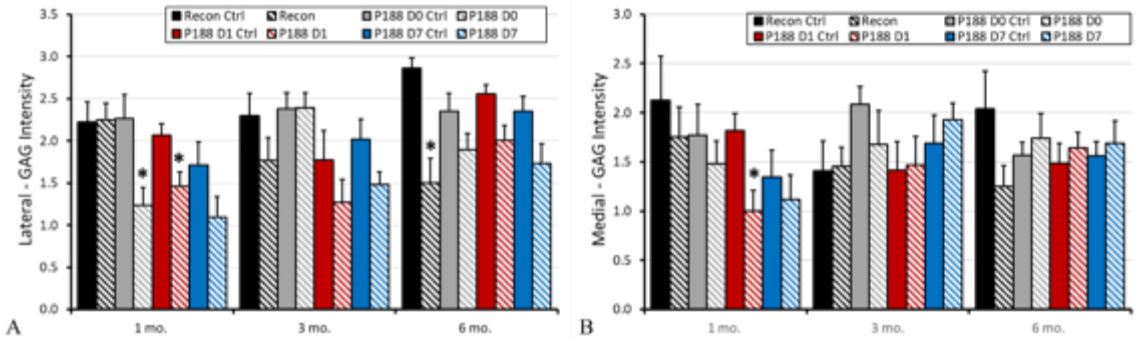

Figure 17. GAG intensity results for both menisci. (A) Results for the lateral meniscus (B) results for the medial meniscus. All values reported as Avg. ± Standard Error. * denotes statistical significant difference compared to control group at similar time point.

Quantitatively assessing GAG coverage of the lateral meniscus found that at the 1-month time points, all P188 treatment groups had a significant decrease in coverage compared to control groups. There was no significant decrease in the Recon group at this time point. However, at the 3-month time point, there was a significant decrease in the Recon group, but all P188 treatment groups were able to prevent a significant decrease compared to controls. (Figure 18A). In the medial meniscus, there was only a significant decrease in GAG coverage found in the 1-month Recon group. (Figure 18B).

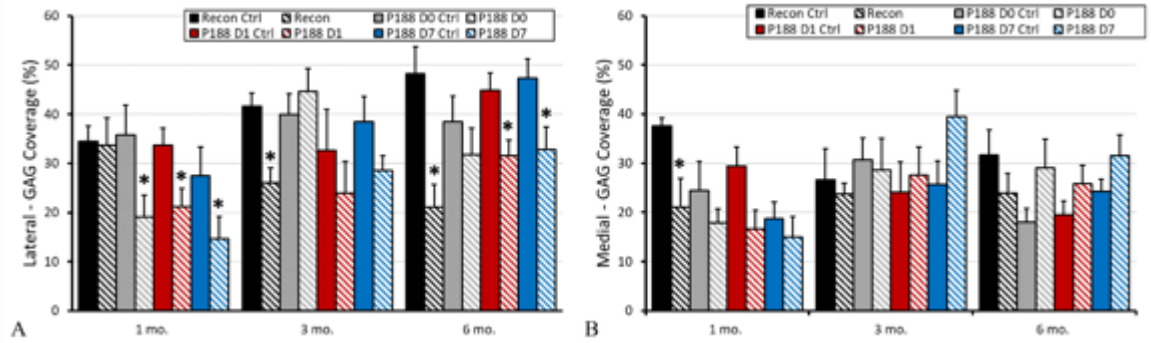

Figure 18. GAG coverage results for both menisci. (A) Results for the lateral meniscus (B) results for the medial meniscus. All values reported as Avg. ± Standard Error. * denotes statistical significant difference compared to control group at similar time point.

DISCUSSION

This animal model was successful in simulating acute knee joint damage by creating rupture or damage to the ACL and menisci. The observed damage to the menisci was more commonly found in the medial meniscus compared to the lateral meniscus, therefore medial meniscectomies were more commonly performed. These observations match observed clinical results in humans who have suffered traumatic injuries to the knee and received surgical intervention, further highlighting the clinical relevance of this model. Changes documented in the mechanical properties and GAG staining of the meniscus in the Recon group match signs of PTOA found in humans as well. Some of these changes were documented as early as 1-month following the traumatic impact. Although not always consistent, this study found that both single and multiple administrations of P188 were able to limit changes in mechanical properties and GAG staining associated with the disease, when compared to reconstruction treatment alone, especially at later time points.

Previous *in-vivo* lapine studies have utilized a similar closed-joint traumatic impact injury model to induce ACL failure and meniscal damage without surgical intervention to repair the ACL and treat damaged menisci. These previous studies reported significant changes in morphology grading, mechanical properties, and GAG staining of both menisci, but only at later time points (8 and 12 weeks).[48,49] In contrast, the earlier differences documented in the current study could be attributed to the partial or full meniscectomies performed during reconstruction surgery, since this surgical procedure has been documented to cause a change in loading patterns within the joint.[151,155,160] Compared to the previous studies with no reconstruction, at the 3-month

time point (12 weeks), it appears that surgical intervention was able to limit the amount of degradation in the mechanical properties and loss of proteoglycans in the meniscus. The effect of surgical intervention aiding in limiting the amount of degradation in the meniscus is further supported by the current study, since the amount of total degradation found at 6-months was not as severe as in the two previous studies, although the previous studies did not include such a long time point.

In the current study, morphological assessments of the meniscus before and after surgical intervention showed more damage to the medial meniscus than the lateral meniscus, with the severity of damage increasing over time, regardless of which treatment group animals were in. These changes could be attributed to the meniscectomy performed on the tissue during reconstruction surgery, as medial meniscectomies were more commonly performed and this procedure involves removing portions of the tissue, affecting its gross appearance. Morphological grading of the lateral meniscus at the 1-month time point suggested that P188 treatment was able to help limit degenerative changes in the tissue, since only the Recon group had an increase in tissue degeneration. A previous study by Bajaj et al., in which the mechanisms of P188 on cellular signaling were explored, documented that the surfactant was able to inhibit the Stat1 and Stat3 pathways, which are associated with the down regulation of collagen and ultimately impairs matrix formation.23,41 By preventing the down regulation of collagen, a single or multiple treatments of P188 may have been able to prevent further degradation of the solid matrix of the tissue, which in turn could aid in helping limit morphological degradation.

P188 treatment may have been effective in preventing damage to the lateral menisci at an early time point, but perhaps a shift in load distribution within the joints of the animals caused an increase in damage as noted in the morphology grading of the tissue, especially at later time points. At the 3- and 6-month time points, there were degenerative changes documented in the lateral meniscus of all treatment groups. These changes could be attributed to the meniscectomy performed on the medial meniscus. As previously mentioned, it has been reported that meniscectomies cause changes in joint loading, which could shift larger amounts of load onto the lateral meniscus and ultimately lead to the greater amount of damage observed.[151,155,160]

A single and multiple administrations of P188 were more consistent in maintaining the instantaneous modulus of the lateral meniscus comparable to that of the control limbs across all three time points. A similar trend was observed in the medial meniscus, but only at the later 3- and 6-month time points. Previous studies have proposed that, under compression, the instantaneous modulus of the tissue is related to the water content and permeability, and the equilibrium modulus is related to the solid matrix, primarily GAG content.[11,110,132,140,161] As previously mentioned, P188 treatment has been shown to inhibit pathways associated with the down regulation of collagen production, which could explain the lack of changes documented in the lateral meniscus across all time points and in the medial meniscus at later time points. Within the solid matrix, collagen helps prevent the secretion of water out of the tissue by creating drag forces, thus aiding in supporting large loads immediately following compression.[25]

Although P188 treatment seemed to have helped prevent changes in the instantaneous modulus of the tissue, the current study found no benefit of P188 treatment

in preventing changes in the equilibrium modulus. Both the lateral and medial meniscus experienced a decrease in the equilibrium modulus at 1-month, regardless of treatment group. At this time point, a decrease in the modulus of the P188 treated groups was accompanied by a decrease in both GAG coverage and staining intensity, which supports the understanding of the relationship between GAG content and the mechanical properties of the tissue at equilibrium. The observed decrease in modulus of the tissue in the Recon group could be associated with possible changes in collagen content within the solid matrix, which could explain the decreases in the equilibrium modulus, but lack of changes in GAG content. Interestingly, at later time points, a decrease in the equilibrium modulus was only consistently documented in both menisci of the Recon groups. These decreases were accompanied with decreases in GAG coverage and staining intensity.

In the P188 treated limbs, decreases of the equilibrium modulus were more commonly documented in the lateral meniscus, compared to the medial meniscus. Unlike at the 1-month time point, these changes were not accompanied with a decrease in GAG coverage or staining intensity. As it has been documented that either single or multiple treatments of P188 are able to prevent cell death following a traumatic impact in the meniscus, perhaps the mechanism by increasing cell viability the fibrochondrocytes in the meniscus were able to upregulate the production of proteoglycans over time.[117] A previous *in-vivo* study by Coatney et al. testing the efficacy of P188 in preventing proteoglycan loss in the meniscus using a constrained joint impact model reported that 6-weeks following treatment, a single dose of P188 was able to significantly prevent the loss of GAGs compared to the untreated impact group[29], matching the findings of the current study in the P188 treatment groups.

There were a number of limitations in the current study including reduced sample size of meniscal tissue for mechanical testing in the treated limbs. Due to the amount of damage documented in the tissues, particularly the medial meniscus, not all groups had a full sample size based on the total number of animals enrolled in the study. Future studies should anticipate severe damage to the meniscus as a result of the impact and should include a larger sample size. To test if P188 treatments were able to limit the down regulation of collagen within the tissue, future studies should conduct tensile testing as well as investigate collagen content through histological, biochemical, or other imaging analysis. Since the current study documented somewhat inconsistent longitudinal changes associated with PTOA between the three P188 treatment groups, future studies may want to include much later time points to assess the effect of the different treatments over a longer period of time.

CONCLUSIONS

This is the first study to assess changes in the menisci following combined P188 and surgical treatment. The current study suggests that P188 treatment and subsequent surgical intervention may be effective in limiting changes associated with PTOA in the meniscus, when compared to reconstruction only treatments. However, in order to fully prevent changes associated with the disease, alternative treatments that address the damage and tears from the initial impact may be necessary, such as a full meniscal replacement.

CHAPTER 4

EVALUATING CHRONIC CHANGES IN SUBCHONDRAL CORTICAL AND TRABECULAR BONE OF FEMURS AND TIBIAS[2]

INTRODUCTION

Subchondral bone plays a critical role within the knee joint by providing mechanical support and nutrition to the articular cartilage.[97] This region of bone consists of both nonporous cortical bone and spongy trabecular bone that undergo constant adaptation, through resorption and remodeling, in response to changes in the mechanical loading the knee experiences from every day activities.[20,101,159] Under normal physiological conditions, the amount of bone removed during the resorption phase is balanced by the amount of bone that is made during the formation phase. Through this process, bone mass is maintained, although the shape and architecture of bone is modified to repair micro-damage resulting from external loading.[56,159]

Traumatic injuries to the knee joint often lead to damage to the anterior cruciate ligament (ACL) and menisci[35,93,120] and are known to induce biological responses in the bone and soft tissues of the joint, which are strongly associated with the onset of post-traumatic osteoarthritis (PTOA).[44,62,98,119] Following a traumatic injury and ACL rupture, subchondral bone remodels resulting in changes to trabecular bone architecture, loss of mineral density, formation of osteophytes, and the advancement of the tidemark, which

---

[2]Portions of this chapter are adapted from a publication in the Journal of Biomechanics, Vol. 126, Narez GE, Brown G, Herrick A, Ek R, Wei F, Dejardin L, Haut RC, Haut Donahue TL, "Assessment of Changes in the Meniscus and Subchondral Bone in a Novel Closed-Joint Impact and Surgical Reconstruction Lapine Model", Pages 110630, Copyright (2021), with permission from Elsevier.

causes a decrease in articular cartilage thickness.[14,19,57,105,170] These changes are amplified with the onset and progression of the disease.

The most common treatment following injury to the ACL and meniscus includes ACL reconstructive surgery and meniscal debridement. The goal of treatment is to return normal kinematics to the joint and decrease pain by removing damaged and torn pieces of tissue. While the surgery alleviates pain and returns some normal knee kinematics, patients still develop PTOA 10-14 years post injury.[46,50,115,131] It is believed that occult damage at the cellular level that is caused by the initial impact, which is not addressed during surgical intervention, may play a crucial role in the onset of the disease. Thus, pharmaceutical intervention that addresses and mitigates cellular damage following traumatic impact may be able to prevent further damage to the tissues within the knee joint and avert the progression of PTOA following ACL reconstruction surgery.

In recent years, Poloxamer 188 (P188) has become a surfactant of interest as it has been shown that a single 8mg/mL dose is an effective inhibitor of cell death in articular cartilage and meniscal tissue following traumatic impact.[8,9,53,117,118,130] A previous study by Bajaj et al. reported that P188 treatment was able to inhibit pathways associated with cell death, inflammation, and matrix degradation in articular cartilage explants.[9] These findings suggest that P188 treatment may be able to arrest the occult damage following impact at the cellular level and merits further investigation in the *in-vivo* setting. To the author's knowledge, no previous studies have tested the efficacy of the surfactant on bone tissue following an injurious joint impact.

The goal of the study was to assess if combined surgical and intra-articular P188 treatment would be able to prevent or delay the longitudinal development of PTOA in

meniscal tissue compared to surgical treatment alone in an *in-vivo* lapine model that combined both closed-joint traumatic impact and surgical reconstruction. It was hypothesized that, compared to surgical treatment alone, combine treatment would be more effective in preventing degenerative changes associated with PTOA in the subchondral bone.

METHODS

Animal Model

This study was approved by the Institutional Animal Care and Use Committee at Michigan State University. Ninety skeletally mature Flemish Giant rabbits (6.34 ± 0.75 kg) aged 7 - 9 months were used for this study. Animals were a mix of male (n = 41) and female (n = 49). Animals were anesthetized (2% isoflurane and oxygen) and the right tibiofemoral joint was subjected to an impact resulting in ACL failure and meniscal tissue damage. As previously described, the right knee of each rabbit was shaved and placed in a custom rigid fixture in a servo-hydraulic testing system (Instron Corp, Norwood, MA) while the rabbit was in a prone position (Figure 13).28,29 A 400 N preload was applied and a controlled impact pushed the tibia downward 3.5 mm at a rate of 0.5 Hz.30 The left knee served as a contralateral control.

Animals were then randomly assigned to one of four treatment groups; Group 1 received reconstruction surgery only and no P188 treatment (Recon.), Group 2 received reconstruction surgery and a single dose of P188 immediately following impact (P188 D0), Group 3 received reconstruction surgery and a dose of P188 immediately following impact and 24 hours after impact (P188 D1), and finally Group 4 received reconstruction surgery and a dose of P188 immediately following impact, 24 hours, and seven days after

impact (P188 D7). For P188 treatment groups, 1mL of P188 at a concentration of 8mg/mL was injected into the knee capsule at the respective time point. The knee joint was then flexed and extended to mix the P188 injection with the synovial fluid.

Reconstruction of the torn ACL was performed by a board-certified veterinary surgeon (LD) approximately 2 weeks post-impact. A medial parapatellar arthrotomy was performed to assess the condition of the ACL and meniscus. Meniscal injuries, if present, were recorded and were treated via a partial, in which only the damaged or torn regions were removed, or full meniscectomy, in which the entire damaged medial or lateral meniscus was removed. The joint capsule was then opened and the semitendinosus (ST) tendon was exposed on the posterior aspect of the medial tibial plateau. To minimize the amount of damage to the surrounding musculature, the ST tendon was then transected at the musculotendinous junction while leaving the tibial attachment intact. A 2.7 mm diameter tibial bone tunnel and a 3.2 mm diameter femoral tunnel were drilled at the ACL footprint. The free end of the ST graft was fed under the medial collateral ligament and then passed through the tunnels in the tibia and femur using a suture loop. Tension was applied on the graft and a custom interference fit screw was placed in the femoral bone tunnel to stabilize the graft.30,31 An anterior drawer test was performed on the reconstructed knee to ensure the joint was stable post-reconstruction.32 Following mechanical testing on the articular cartilage of the femurs and tibias by the collaborating lab at Michigan State University, both bones were fixed in 10% neutral buffered formalin for further analysis. The number of animals included in each treatment group at euthanized at 1-, 3-, or 6-months following impact can be found in Table 2.

Micro - Computed Tomography (μCT)

The distal femur and proximal tibia from both the contralateral control (left) and treated (right) limbs from each animal were scanned in 10% neutral buffered formalin using a Bruker Skyscan 1276 (Bruker, Billerica, MA) μCT machine. Bones were scanned with a voxel size of 20 μm and a 1mm aluminum and copper filter. The x-ray tube parameters were a voltage of 100 kV, current of 125 μA, and exposure time of 473 ms. Images were collected every 0.4^{o} using a 360^{o} rotation around the sample.

Three-dimensional image reconstructions were performed using NRecon software (Bruker, Billerica, MA). All reconstructions were performed using a dynamic range of 0 to 0.030, universal beam hardening of 30%, Gaussian smoothing of 3, and a ring artifact correction of 4. Misalignment compensations varied between each reconstruction image set to ensure images were of the highest quality. Reconstructed images were then imported to DataViewer software (Bruker, Billerica, MA) to isolate the volume of interest (VOIs) for each type of bone being analyzed. Trabecular VOIs ranged from just below the cortical bone to growth plate. Cortical bone VOIs ranged from the joint margin to the trabecular bone.

CTAn software (Bruker, Billerica, MA) was used for all quantitative bone analysis. Similar to previous studies, four regions of interest (ROI) were chosen to coincide with areas of mechanical testing on the articular cartilage of the lateral and medial compartments.[13,48,128] (Figure 19).

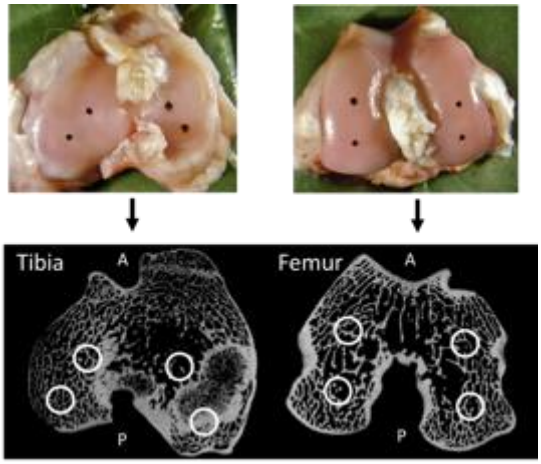

Figure 19. Representative images of mechanical testing locations on both tibias and femurs and the corresponding locations on the reconstructed images using CTAn Software.

Parameters of interest for subchondral bone include bone mineral density (Tb.BMD), bone volume/tissue volume (BV/TV), trabecular number (Tb.N), trabecular thickness (Tb.Th), and trabecular separation (Tb.Sp). Parameters of interest for cortical bone include bone mineral density (Co.BMD), porosity (Co.Po), and cortical thickness (Co.Th). Using CTAn software, osteophytes were identified by manually outlining new bone growth outside of the normal joint margins every 20 slides by a single operator and morphing the images together. Osteophytic bone volume was identified by reduced bone mineral density and as being outside the original joint margins (Figure 20).

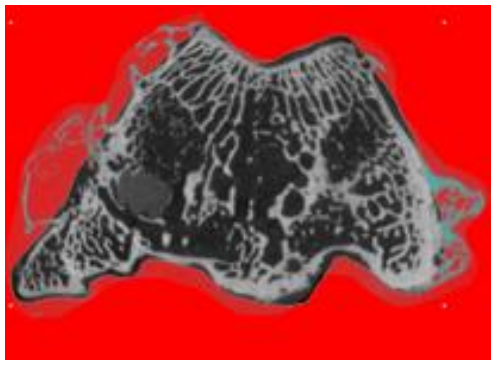

Figure 20. Representative image of a tibia with new osteophytic bone being outlined (bone in red area).

Statistics

To determine the influence of different treatments on the reconstructed limbs on the analyzed variables (subchondral bone morphometry, mineral composition, and osteophyte volume), a mixed fixed effects model with repeated measures with Tukey's post-hoc was applied with animal, time, and treatments as fixed effects. All comparisons made were between the treated limbs and contralateral control limbs for each treatment group, except for osteophyte volume, in which comparisons were made for the femurs and tibias between treatment groups at each time point due to no osteophyte volume being documented in control limbs. A difference with $p < 0.05$ was considered statistically significant.

RESULTS

Animal Model

The average peak impact load was 770 ± 137 N. During reconstructive surgery, the veterinarian surgeon (LD) documented that 50/90 experienced ACL rupture and 40/90 experienced a partial ACL tear. Half of the animals had documented damage to the medial meniscus; 39/90 animals had tears in the posterior region, 4/90 had bucket handle tears, one animal had a small tear, and one animal had a discoid shape meniscus. In contrast, only four animals had documented damage to the lateral meniscus; three had tears in the posterior region and one had a bucket handle tear. Due to the initial damage, medial meniscectomies were more commonly performed; 36 animals received a partial medial meniscectomy, six received a full meniscectomy, and four received a posterior horn release meniscectomy. Only four meniscectomies were performed on the lateral meniscus, three partial and one full. It was observed that the animals favored the

contralateral control limb for 1-3 days following impact and 5-10 days following surgery before returning to normal gait.

Trabecular Bone

When compared to contralateral control limbs, the lateral (Figure 21A) and medial (Figure 21B) condyles of the Recon group had an 11% and 16% decrease, respectively, in mineral density at 3-months. At 6-months, there was a 10% decrease in the medial condyle in the P188 D1 group (Figure 21B). At this time point, in the lateral compartments of tibias, there was a 12% decrease in mineral density in the Recon group and a 13% decrease in the P188 D7 group (Figure 21C). There were no significant decreases found in the medial plateau in any treatment group (Figure 21D).

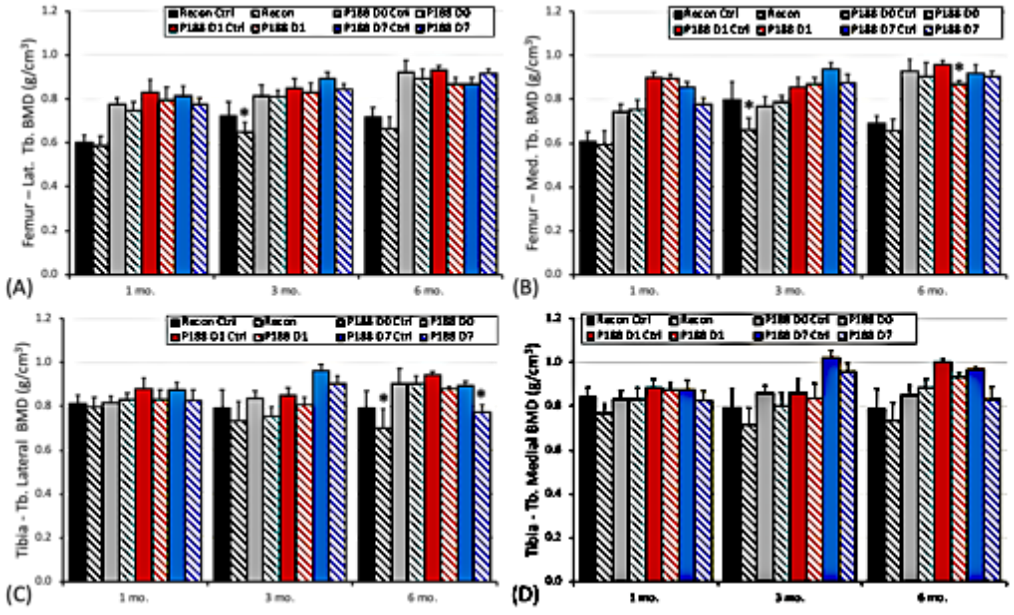

Figure 21. Bone mineral density (BMD) measurements for the trabecular bone of (A) lateral and (B) femoral condyles as well as the (C) lateral and (D) medial compartments of the tibia. Values reported as average ± standard error. * denotes significant difference between treated (right) limb to respective control (left) limbs.

Analyses of trabecular BV/TV documented no changes in the lateral condyle of the femurs in any treatment group (Figure 22A), but there was a 19% decrease in the

medial condyle in the P188 D7 group at 6-months (Figure 22B). In the tibias, there were documented decreases in BV/TV in the lateral compartment in the Recon group at 3- and 6-months (Figure 22C). At 3-months, there was a 36% decrease in the lateral compartment in the P188 D0 group (Figure 22C). There were no documented changes in the medial plateau in any treatment group (Figure 22D).

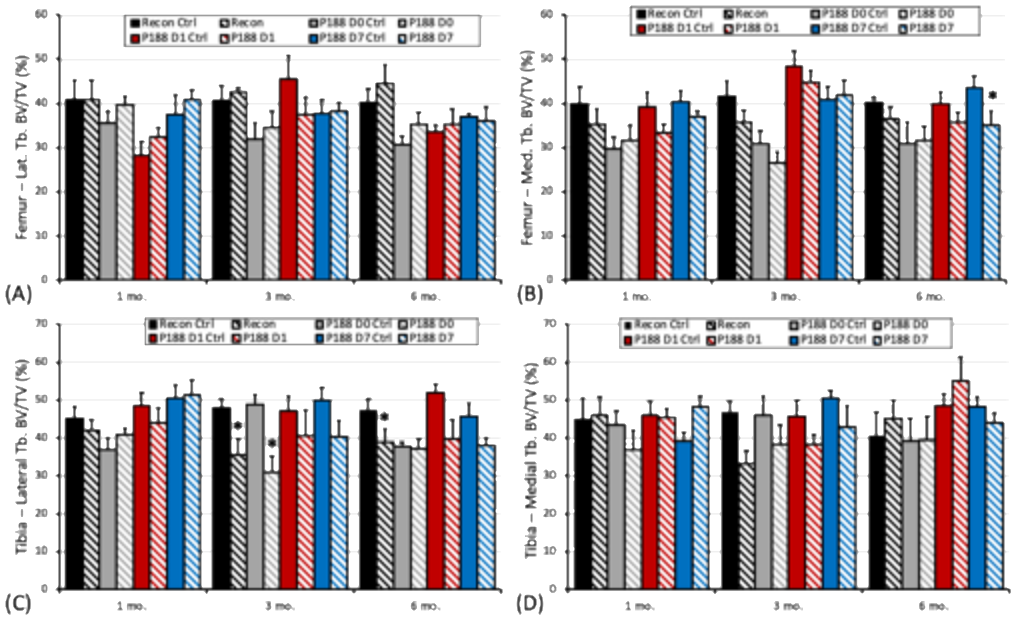

Figure 22. Bone volume tissue volume (BV/TV) measurements for the trabecular bone of (A) lateral and (B) femoral condyles as well as the (C) lateral and (D) medial compartments of the tibia. Values reported as average ± standard error. * denotes significant difference between treated (right) limb to respective control (left) limbs.

Bone morphometry analyses found more significant changes in the lateral condyles than the medial condyles of the femurs (Table 4). In the P188 D1 group, there was a 25% increase in Tb.N in the lateral condyles at 1-month and a 19% decrease in Tb.Th at 3-months. Both condyles in the P188 D0 group had an increase in Tb.Sp at 3-months.

Table 4. Measured trabecular bone parameters for each condyle of the femur. Values reported as average ± standard deviation. * denotes significant difference between treated (right) limb to respective control (left) limbs.

			Lateral			Medial		
			Tb.N (mm^{-1})	Tb.Th (mm)	Tb.Sp (mm^{-1})	Tb.N (mm^{-1})	Tb.Th (mm)	Tb.Sp (mm^{-1})
1 mo.	Recon	Control	1.70 ± 0.44	0.24 ± 0.03	0.41 ± 0.09	1.62 ± 0.40	0.24 ± 0.01	0.42 ± 0.08
		Treated	1.74 ± 0.46	0.24 ± 0.02	0.39 ± 0.14	1.44 ± 0.44	0.25 ± 0.04	0.47 ± 0.12
	P188 D0	Control	1.70 ± 0.36	0.21 ± 0.04	0.41 ± 0.09	1.44 ± 0.33	0.28 ± 0.19	0.46 ± 0.09
		Treated	1.86 ± 0.10	0.21 ± 0.04	0.34 ± 0.05	1.55 ± 0.3	0.22 ± 0.03	0.42 ± 0.06
	P188 D1	Control	1.55 ± 0.36	0.18 ± 0.02	0.45 ± 0.07	1.86 ± 0.54	0.20 ± 0.04	0.38 ± 0.14
		Treated	1.93 ± 0.22*	0.17 ± 0.02	0.35 ± 0.06	1.68 ± 0.14	0.18 ± 0.03	0.37 ± 0.10
	P188 D7	Control	2.02 ± 0.45	0.18 ± 0.03	0.37 ± 0.12	1.94 ± 0.27	0.21 ± 0.02	0.36 ± 0.06
		Treated	2.10 ± 0.34	0.20 ± 0.01	0.33 ± 0.08	1.96 ± 0.23	0.19 ± 0.01	0.37 ± 0.06
3 mo.	Recon	Control	1.77 ± 0.4	0.23 ± 0.04	0.42 ± 0.16	1.61 ± 0.44	0.27 ± 0.04	0.43 ± 0.12
		Treated	2.04 ± 0.27	0.22 ± 0.04	0.31 ± 0.06	1.71 ± 0.25	0.21 ± 0.03	0.36 ± 0.10
	P188 D0	Control	1.53 ± 0.35	0.21 ± 0.05	0.41 ± 0.06	1.55 ± 0.34	0.21 ± 0.04	0.43 ± 0.06
		Treated	1.52 ± 0.36	0.22 ± 0.04	0.43 ± 0.09*	1.30 ± 0.33	0.20 ± 0.02	0.55 ± 0.16*
	P188 D1	Control	1.83 ± 0.16	0.25 ± 0.05	0.37 ± 0.07	2.04 ± 0.23	0.24 ± 0.02	0.35 ± 0.07
		Treated	1.86 ± 0.21	0.20 ± 0.02*	0.38 ± 0.05	1.92 ± 0.13	0.24 ± 0.04	0.35 ± 0.02
	P188 D7	Control	1.86 ± 0.27	0.19 ± 0.03	0.42 ± 0.11	1.89 ± 0.33	0.22 ± 0.02	0.39 ± 0.09
		Treated	1.85 ± 0.19	0.20 ± 0.02	0.38 ± 0.04	1.83 ± 0.17	0.23 ± 0.06	0.37 ± 0.04
6 mo.	Recon	Control	1.57 ± 0.25	0.26 ± 0.04	0.44 ± 0.07	1.72 ± 0.24	0.24 ± 0.02	0.39 ± 0.03
		Treated	1.86 ± 0.43	0.25 ± 0.08	0.36 ± 0.07	1.62 ± 0.47	0.23 ± 0.05	0.45 ± 0.10
	P188 D0	Control	1.60 ± 0.12	0.19 ± 0.02	0.45 ± 0.08	1.79 ± 0.42	0.19 ± 0.01	0.40 ± 0.09
		Treated	1.85 ± 0.18	0.19 ± 0.03	0.36 ± 0.03	1.65 ± 0.26	0.19 ± 0.02	0.42 ± 0.08
	P188 D1	Control	1.87 ± 0.14	0.18 ± 0.03	0.39 ± 0.04	1.92 ± 0.22	0.21 ± 0.03	0.35 ± 0.05
		Treated	1.90 ± 0.3	0.19 ± 0.02	0.37 ± 0.07	1.93 ± 0.24	0.18 ± 0.01	0.37 ± 0.05
	P188 D7	Control	1.82 ± 0.19	0.20 ± 0.03	0.40 ± 0.02	1.88 ± 0.20	0.23 ± 0.01	0.35 ± 0.03
		Treated	1.81 ± 0.28	0.21 ± 0.03	0.40 ± 0.07	1.80 ± 0.21	0.19 ± 0.03	0.38 ± 0.06

The only morphometry change documented in the tibias was a 19% increase in Tb.Th in the medial compartment in the P188 D1 group at 6-months. There were no changes in the lateral compartment in the tibias (Table 5).

Table 5. Measured trabecular bone parameters for each compartment of the tibia. Values reported as average ± standard deviation. * denotes significant difference between treated (right) limb to respective control (left) limbs.

			Lateral			Medial		
			Tb.N (mm^{-1})	Tb.Th (mm)	Tb.Sp (mm^{-1})	Tb.N (mm^{-1})	Tb.Th (mm)	Tb.Sp (mm^{-1})
1 mo.	Recon	Control	1.75 ± 0.35	0.26 ± 0.04	0.40 ± 0.08	1.35 ± 0.19	0.33 ± 0.06	0.45 ± 0.1
		Treated	1.62 ± 0.27	0.26 ± 0.04	0.39 ± 0.06	1.77 ± 0.51	0.27 ± 0.06	0.40 ± 0.13
	P188 D0	Control	1.77 ± 0.56	0.22 ± 0.05	0.41 ± 0.13	1.74 ± 0.2	0.26 ± 0.05	0.39 ± 0.08
		Treated	1.81 ± 0.31	0.22 ± 0.03	0.38 ± 0.08	1.67 ± 0.41	0.22 ± 0.05	0.43 ± 0.13
	P188 D1	Control	1.96 ± 0.37	0.24 ± 0.04	0.33 ± 0.07	1.76 ± 0.43	0.27 ± 0.05	0.42 ± 0.12
		Treated	1.81 ± 0.48	0.24 ± 0.06	0.39 ± 0.1	1.86 ± 0.29	0.28 ± 0.07	0.35 ± 0.08
	P188 D7	Control	1.99 ± 0.21	0.24 ± 0.03	0.33 ± 0.05	1.81 ± 0.22	0.22 ± 0.04	0.39 ± 0.04
		Treated	2.14 ± 0.37	0.24 ± 0.04	0.32 ± 0.08	1.97 ± 0.21	0.26 ± 0.04	0.33 ± 0.06
3 mo.	Recon	Control	1.71 ± 0.44	0.28 ± 0.05	0.40 ± 0.09	1.62 ± 0.23	0.29 ± 0.03	0.39 ± 0.05
		Treated	1.49 ± 0.52	0.24 ± 0.05	0.43 ± 0.13	1.42 ± 0.43	0.25 ± 0.07	0.43 ± 0.15
	P188 D0	Control	1.98 ± 0.32	0.25 ± 0.03	0.35 ± 0.05	1.76 ± 0.45	0.27 ± 0.03	0.40 ± 0.09
		Treated	1.65 ± 0.41	0.18 ± 0.02	0.41 ± 0.09	1.71 ± 0.35	0.26 ± 0.09	0.40 ± 0.14
	P188 D1	Control	1.80 ± 0.27	0.26 ± 0.02	0.38 ± 0.06	1.61 ± 0.21	0.29 ± 0.07	0.43 ± 0.05
		Treated	1.71 ± 0.46	0.23 ± 0.02	0.40 ± 0.07	1.75 ± 0.16	0.27 ± 0.11	0.35 ± 0.08
	P188 D7	Control	1.85 ± 0.26	0.25 ± 0.02	0.36 ± 0.12	1.8 ± 0.14	0.28 ± 0.02	0.37 ± 0.05
		Treated	1.76 ± 0.49	0.20 ± 0.03	0.41 ± 0.12	1.7 ± 0.39	0.26 ± 0.05	0.37 ± 0.09
6 mo.	Recon	Control	1.77 ± 0.4	0.28 ± 0.05	0.39 ± 0.09	1.35 ± 0.48	0.33 ± 0.09	0.51 ± 0.18
		Treated	1.48 ± 0.41	0.27 ± 0.06	0.46 ± 0.14	1.83 ± 0.33	0.24 ± 0.05	0.36 ± 0.11
	P188 D0	Control	1.5 ± 0.37	0.27 ± 0.09	0.47 ± 0.16	1.72 ± 0.54	0.23 ± 0.03	0.39 ± 0.09
		Treated	1.67 ± 0.18	0.22 ± 0.03	0.43 ± 0.04	1.68 ± 0.26	0.24 ± 0.05	0.41 ± 0.04
	P188 D1	Control	2.18 ± 0.21	0.28 ± 0.04	0.30 ± 0.02	1.97 ± 0.26	0.29 ± 0.05	0.34 ± 0.09
		Treated	1.93 ± 0.38	0.21 ± 0.05	0.33 ± 0.04	1.9 ± 0.35	0.34 ± 0.14*	0.33 ± 0.09
	P188 D7	Control	2.05 ± 0.17	0.23 ± 0.04	0.34 ± 0.05	1.99 ± 0.25	0.29 ± 0.06	0.35 ± 0.07
		Treated	1.79 ± 0.20	0.21 ± 0.04	0.40 ± 0.05	1.91 ± 0.28	0.33 ± 0.09	0.32 ± 0.10

Cortical Bone

There were no documented changes in cortical BMD in either the lateral (Figure 23A) or medial (Figure 23B) femoral condyle. Similarly, there were no documented changes in cortical BMD in either the lateral (Figure 23C) or medial (Figure 23D) compartments of the tibia in any of the treatment groups at any time.

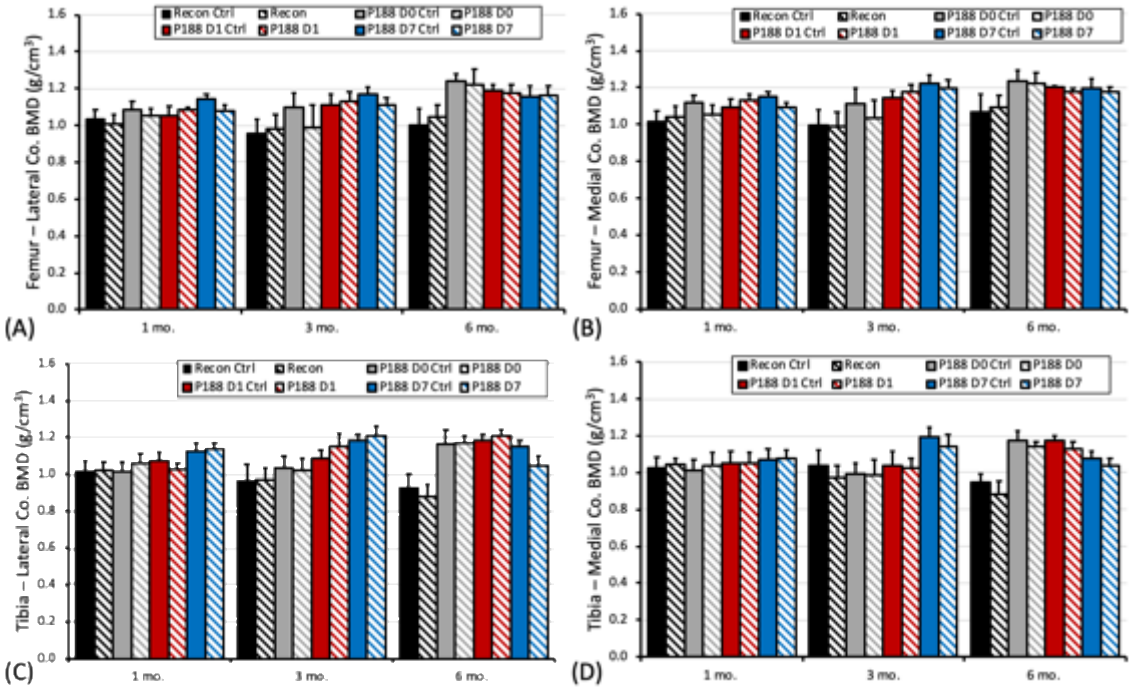

Table 23. Bone mineral density (BMD) measurements for the cortical bone of (A) lateral and (B) femoral condyles as well as the (C) lateral and (D) medial compartments of the tibia. Values reported as average ± standard error. * denotes significant difference between treated (right) limb to respective control (left) limbs.

Analyzing cortical bone porosity and thickness of the femurs found an increase in both parameters in the lateral condyle of the Recon group at 1-month. At 3-months, there was an increase in porosity in the P188 D0 group and a decrease in thickness in the P188 D1 group (Table 6). There was an increase in cortical thickness in the P188 D7 group at 6-months. In the medial condyle, only an increase in cortical thickness was found in the Recon group at 1-month.

Table 6. Measured cortical bone parameters for each condyle of the femur. Values reported as average ± standard deviation. * denotes significant difference between treated (right) limb to respective control (left) limbs.

			Lateral		Medial	
			Co.Po (%)	Co.Th (mm)	Co.Po (%)	Co.Th (mm)
1 mo.	Recon	Control	5.93 ± 2.04	0.57 ± 0.07	6.7 ± 3.89	0.60 ± 0.12
		Treated	8.59 ± 4.5*	0.67 ± 0.13*	7.95 ± 2.42	0.59 ± 0.04
	P188 D0	Control	3.53 ± 1.63	0.59 ± 0.05	2.64 ± 1.19	0.56 ± 0.08
		Treated	3.36 ± 1.98	0.61 ± 0.09	2.93 ± 2.11	0.61 ± 0.10
	P188 D1	Control	2.13 ± 1.25	0.6 ± 0.09	2.08 ± 1.71	0.66 ± 0.02
		Treated	4.36 ± 3.48	0.51 ± 0.09	1.51 ± 1.05	0.57 ± 0.10
	P188 D7	Control	2.58 ± 1.32	0.71 ± 0.06	1.8 ± 1.19	0.71 ± 0.10
		Treated	5.19 ± 3.2	0.67 ± 0.11	3.4 ± 2.14	0.73 ± 0.09
3 mo.	Recon	Control	10.29 ± 3.22	0.51 ± 0.06	7.60 ± 2.02	0.58 ± 0.13
		Treated	8.23 ± 2.39	0.62 ± 0.10	7.31 ± 1.76	0.68 ± 0.12*
	P188 D0	Control	2.05 ± 1.00	0.60 ± 0.05	2.84 ± 2.26	0.62 ± 0.12
		Treated	6.17 ± 5.81*	0.52 ± 0.15	3.13 ± 1.19	0.58 ± 0.05
	P188 D1	Control	3.81 ± 0.71	0.71 ± 0.13	4.74 ± 1.28	0.76 ± 0.09
		Treated	3.25 ± 0.98	0.53 ± 0.06*	3.40 ± 1.45	0.79 ± 0.16
	P188 D7	Control	4.82 ± 3.52	0.71 ± 0.08	3.33 ± 1.05	0.74 ± 0.15
		Treated	4.07 ± 2.07	0.59 ± 0.05	4.63 ± 0.90	0.75 ± 0.08
6 mo.	Recon	Control	8.97 ± 2.31	0.57 ± 0.13	7.96 ± 1.68	0.62 ± 0.11
		Treated	7.36 ± 1.65	0.57 ± 0.08	7.43 ± 4.92	0.61 ± 0.09
	P188 D0	Control	3.55 ± 2.62	0.69 ± 0.12	4.27 ± 2.68	0.70 ± 0.07
		Treated	5.29 ± 3.19	0.60 ± 0.10	4.40 ± 2.14	0.65 ± 0.04
	P188 D1	Control	3.92 ± 1.58	0.68 ± 0.10	3.11 ± 0.31	0.74 ± 0.09
		Treated	2.04 ± 1.08	0.63 ± 0.12	2.04 ± 0.97	0.63 ± 0.12
	P188 D7	Control	3.46 ± 2.19	0.64 ± 0.09	4.99 ± 1.33	0.66 ± 0.07
		Treated	5.82 ± 5.59	0.46 ± 0.10*	4.07 ± 3.84	0.68 ± 0.09

In the tibias, there was only a documented decrease in cortical bone thickness in the lateral plateau of the Recon group at 3-months. There were no documented changes in cortical porosity in either compartment of the tibia in any of the treatment groups (Table 7).

Table 7. Measured cortical bone parameters for each compartment of the tibia. Values reported as average ± standard deviation. * denotes significant difference between treated (right) limb to respective control (left) limbs.

			Lateral		Medial	
			Co.Po (%)	Co.Th (mm)	Co.Po (%)	Co.Th (mm)
1 mo.	Recon	Control	8.63 ± 4.5	0.64 ± 0.08	6.66 ± 1.89	0.74 ± 0.09
		Treated	7.28 ± 3.62	0.65 ± 0.07	6.32 ± 2.91	0.70 ± 0.04
	P188 D0	Control	5.69 ± 3.14	0.66 ± 0.12	5.51 ± 3.22	0.79 ± 0.18
		Treated	3.96 ± 1.15	0.68 ± 0.08	4.21 ± 2.24	0.75 ± 0.09
	P188 D1	Control	1.52 ± 1.39	0.67 ± 0.08	2.20 ± 1.30	0.71 ± 0.08
		Treated	3.37 ± 2.09	0.69 ± 0.11	3.71 ± 1.91	0.75 ± 0.09
	P188 D7	Control	3.33 ± 1.88	0.63 ± 0.14	5.72 ± 3.11	0.75 ± 0.13
		Treated	2.19 ± 0.96	0.63 ± 0.05	3.73 ± 1.32	0.68 ± 0.07
3 mo.	Recon	Control	7.90 ± 2.64	0.58 ± 0.12	8.28 ± 3.04	0.65 ± 0.09
		Treated	8.38 ± 3.69	0.46 ± 0.03*	8.32 ± 3.06	0.67 ± 0.13
	P188 D0	Control	11.52 ± 1.91	0.62 ± 0.06	10.2 ± 5.56	0.70 ± 0.1
		Treated	5.62 ± 4.98	0.60 ± 0.15	3.51 ± 2.56	0.75 ± 0.09
	P188 D1	Control	6.81 ± 2.16	0.69 ± 0.08	3.33 ± 1.99	0.77 ± 0.06
		Treated	3.12 ± 1.68	0.63 ± 0.07	3.51 ± 1.17	0.78 ± 0.1
	P188 D7	Control	4.60 ± 0.98	0.70 ± 0.09	6.65 ± 0.87	0.72 ± 0.07
		Treated	3.27 ± 1.72	0.57 ± 0.08	2.63 ± 0.85	0.65 ± 0.06
6 mo.	Recon	Control	8.60 ± 3.30	0.54 ± 0.04	9.36 ± 4.26	0.72 ± 0.13
		Treated	6.76 ± 1.57	0.57 ± 0.09	5.59 ± 0.84	0.7 ± 0.11
	P188 D0	Control	5.80 ± 3.19	0.70 ± 0.09	7.31 ± 6.62	0.81 ± 0.13
		Treated	4.07 ± 2.24	0.70 ± 0.13	3.96 ± 1.58	0.77 ± 0.09
	P188 D1	Control	3.61 ± 3.20	0.67 ± 0.02	4.37 ± 2.68	0.71 ± 0.04
		Treated	3.26 ± 2.01	0.60 ± 0.04	3.67 ± 1.78	0.76 ± 0.03
	P188 D7	Control	6.58 ± 0.97	0.64 ± 0.08	5.74 ± 0.64	0.71 ± 0.09
		Treated	4.74 ± 3.21	0.68 ± 0.08	3.33 ± 1.07	0.77 ± 0.11

Osteophyte Volume

No osteophytes were documented in either the femurs or tibias of the control limbs. However, osteophytes were present in all treated limbs, regardless of treatment group. There was a significant increase in osteophyte volume in both the femur and tibia at all-time points, with more significant volume being found on the tibias. (Figure 24) In the tibias, larger volumes of osteophytes were found in the multiple dose treatment groups (P188 D1 and P188 D7 group) at 3-months, when compared to the Recon only

group. In the femur, the only documented difference in osteophyte volume was found between the P188 D0 6-month group compared to the Recon group at the same time point. (Figure 24)

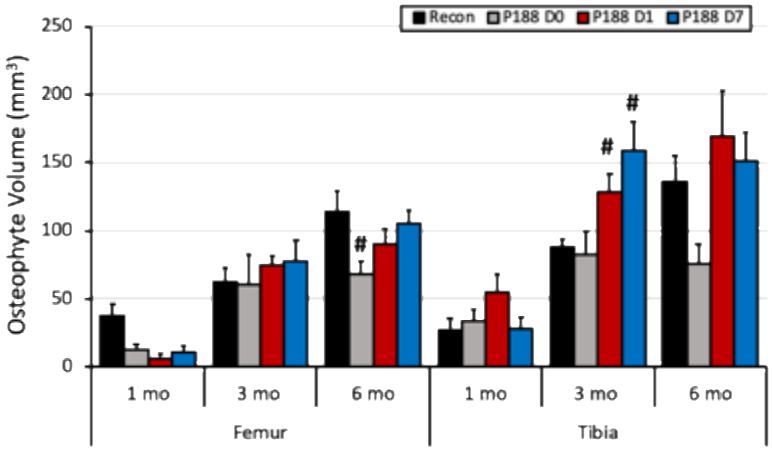

Figure 24. Osteophyte volume for femurs and tibias. Values reported as average ± standard error. # denotes significant difference with the Recon group.

Larger osteophyte volumes were more commonly observed in the compartment in which the bone tunnel was drilled during ACL reconstruction surgery; medial on the tibia and lateral on the femur (Figure 25).

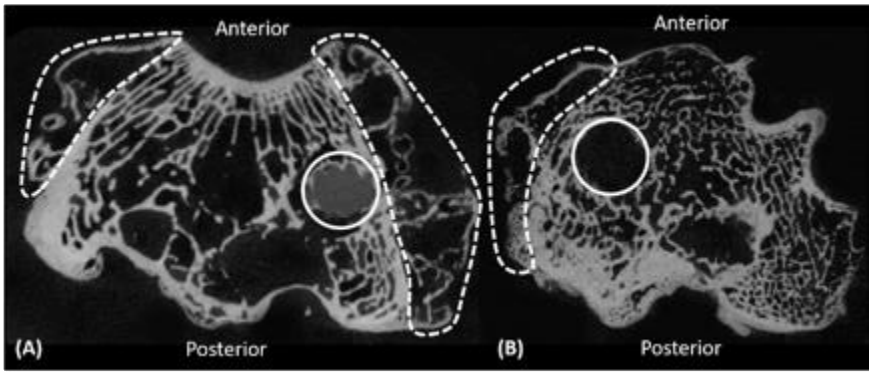

Figure 25. Representative images of a (A) tibia and (B) femur with osteophyte formation outside the normal joint margin. Areas enclosed with dotted lines represent osteophytic bone. Areas enclosed in the solid white circle indicate location of bone tunnels.

Discussion

This animal model was successful in simulating acute knee joint damage by causing rupture or damage to the ACL and menisci. The model showed consistent signs of PTOA including osteophyte formation. To the author's knowledge, this is the first study to document changes in subchondral bone in a combined P188 and surgical intervention *in-vivo* animal model following traumatic injury to the knee to study the onset and progression of PTOA. This new model documented changes in the subchondral bone as early as 1-month following the traumatic impact.

Focusing on the Recon group in the current study, more significant changes in subchondral bone quality and morphometry were documented in the tibias compared to the femurs. These changes were more commonly documented in the medial compartment at 6-months post impact. Using the same closed-joint impact animal model as in this study, without surgical intervention, a previous study showed significant changes in both compartments of subchondral bone for impacted limbs at 3-months (12 weeks).[128] Pauly et al. reported decreases in bone volume and mineral density as well as large osteophyte volumes, with larger volumes being documented in the tibias compared to the femurs. The Recon group of the current study showed similar trends in osteophyte volumes, however, the average value of 88 mm^3 documented for tibias in the impact-reconstructed limbs was lower than the reported average 120 mm^3 in the impact-only limbs. Osteophyte formation is thought to be caused by alterations in joint mechanics[16,67,123], with Hsia et al. documenting an increase in osteophyte volume associated with a decrease in joint laxity.[67] The data observed in the current study suggests that surgical intervention may

have been successful in returning some degree of normal knee kinematics, which in turn caused less formation of osteophytes and changes in subchondral bone health.

In the current study, besides osteophyte formation, few consistent changes in bone quality or morphometry in any of the treatment groups were noted. The changes that did occur in trabecular bone were usually offsetting resulting in no overall effect in the bone volume to tissue volume ratio. For example, even though there was a decrease in trabecular number in the 1-month P188 D1 group, there was a slight increase in trabecular thickness and decrease in trabecular separation. Therefore, no overall change in bone volume was found. Similar trends were observed in the other morphometry values of trabecular bone. The lack of consistent significant changes could be attributed to the bone tunnels that were drilled into both the femurs and tibias during reconstruction surgery of the ACL.

Previous studies assessing the effect of bone tunnels on bone health following ACL reconstruction surgery and the use of interference screws have shown that bone was able to remodel and return to normal architecture within months following surgery.[70,83,136,150] In a canine model, Rodeo et al. showed progressive increases in bone ingrowth and mineralization 12- and 26-weeks post-surgery.[136] In the current study, bone tunnels were present in the reconstructed limbs of all animals at 1-month, but the reconstructed limbs of animals in the 3- and 6-month time points were shown to have a small or no bone tunnels left. The tunnels were filled with new trabecular and cortical bone. Bone tunnels promoting bone growth and remodeling is further supported by the larger volumes of osteophytes being documented in the compartment in which the bone tunnels were drilled; that being the medial compartment on the tibia and the lateral

compartment on the femurs, as shown on Figure 25. This may suggest that the bone tunnels encouraged rapid bone remodeling in the reconstructed limbs, which aided in preventing significant changes in subchondral bone quality and morphometry, albeit at the expense of increased osteophytes.

As PTOA is considered to be a disease of the whole joint, it is important to note and highlight the differences observed in other tissues that may have affected the response of subchondral bone. Previous studies have found that areas of meniscal damage are usually correlated directly with areas of articular damage[73,152], which ultimately could affect the health of the underlying bone. As previously discussed in Chapter 3, when compared to their respective controls, more changes associated with PTOA were documented in the meniscus of the Recon group than in the P188 treated groups, especially at the later 6-month time point. Perhaps at the time points included in this study, the meniscus is performing its role within the joint and protecting the underlying articular cartilage, therefore few significant changes in subchondral bone health associated with the disease were observed. Ferretti et al., reported that patients who had tears in their meniscus and received a meniscectomy during reconstruction were more likely to develop the disease years following surgery, when compared to patients who received ACL reconstruction alone.[45] These previous findings, paired with the current study, strongly suggest that meniscal health following traumatic injury to the knee joint may play a much more significant role in overall knee joint health and the onset and progression of PTOA.

Some limitations of the current study include variations in locations of initial trauma. These locations may have been different in each animal, which could cause a

different response in bone resorption and remodeling of the subchondral bone. In order to determine the relationship between meniscal, articular cartilage, and subchondral bone health, future studies may want to include later time points to better assess the efficacy of surgical treatment, as well as combined P188 and surgical treatment, in limiting the disease.

CONCLUSIONS

This is the first study to assess changes in subchondral bone following combined P188 and surgical treatment. As osteophyte formation was the only changes associated with PTOA documented in all of the treatment groups, the current study suggests that reconstruction surgery alone may be able to limit changes in the tissue. Including a later time point may find the effectiveness of P188 treatment in preventing PTOA changes in subchondral bone, when compared to surgical treatment alone.

CHAPTER 5

DETERMINING THE PRESENCE OF BIOMARKERS ASSOCIATED WITH PTOA IN THE SYNOVIAL FLUID

INTRODUCTION

It has been established that surgical intervention following damage to the anterior cruciate ligament (ACL) and meniscus caused by a traumatic impact to the knee joint does not decrease the likelihood of a patient developing post-traumatic osteoarthritis (PTOA) years after the surgery.[46,50,115,131] Synovitis, inflammation of the synovium, is one of the early signs of PTOA and has been suggested to be a leading cause of pain in patients suffering from PTOA.[75,141,142] Synovitis is marked by hypervascularization of the synovium membrane, thickening of the lining cells, an increase in synovial fluid (SF) volume and secretion of biomarkers that cause further inflammation and degradation of the tissues within the joint.[15,75,142] As surgical intervention only addresses macroscopic damage to the tissues, it is believed that pharmaceutical treatment may be able to address the occult damage and aid in limiting changes in biomarker expression within the joint.

Poloxamer 188 (P188) has been shown to inhibit cell death in articular cartilage and meniscal explants following traumatic impact.[8,9,53,117,118,130] A single 8mg/mL dose of P188 has been shown to inhibit pathways associated with cell death, inflammation, and matrix degradation.[9] These findings suggest that P188 treatment may be able to help limit changes in the expression of biomarkers associated with PTOA and merits further *in-vivo* investigation. Thus, proteome analyses which can help determine a wide range of protein expression potentially affected by P188 treatment has not been performed. Additionally,

proteome analysis could help determine other key biomarkers and pathways the surfactant may be affecting.

Proteomic analysis of the SF from both human and animals has become a popular tool used to identify biomarkers linked with the pathology of PTOA.[10,66,72,92,95,96,135,156,158] Currently, the only studies evaluating changes in the proteome of lapine SF have either used an ACL transection model or injected monosodium iodacetate to induce PTOA.[92,95,96,156,158] Although these previous studies were successful in identifying biomarkers associated with PTOA, the clinical relevance of these findings are limited since these models were either surgically or chemically induced rather than resulting from a traumatic closed-joint injury. To the author's knowledge, changes in the SF proteome of a closed-joint impact and reconstruction model have not been reported.

The goals of the study were to assess the proteome of the SF in a closed-joint impact and surgical intervention model and to test the efficacy of combined surgical and intra-articular P188 treatment in preventing the expression of biomarkers associated with PTOA. It was hypothesized that biomarkers associated with the disease would be differentially expressed in the reconstruction only group and that combined P188 and surgical treatment would be more effective in mitigating changes in the expression of biomarkers associated with the disease in the SF.

METHODS

Animal Model

For more information regarding the Animal Model, treatments, and total number of samples used in the study, refer to the Methods section of Chapter 3.

Synovial Fluid Harvesting

Following euthanasia, the SF was immediately harvested from both knee joints by injecting 1.5cc of sterile 1x PBS using a 3cc syringe into the knee joint (Figure 26). While the syringe was in the knee capsule, the joint was articulated/flexed 10 times to ensure homogeneous fluid distribution. Fluid within the joint was then aspirated using a syringe, transferred to a sealed tube, and stores at -80°C for further analysis.

Figure 26 Synovial fluid being extracted from a rabbit knee joint using a syringe.

While samples from the P188 D0 treatment group and 3-month time point for all treatment groups were available, they were not included in the SF study due to unsatisfactory sample quality for proteomic analysis (i.e. varying volumes between treated and control limbs from each animal, blood contamination, etc.). Information regarding the treatment groups, time points, and animal sample size for each can be found in Table 8.

Table 8 Sample sizes included in the analysis of SF proteome for each treatment group and time point.

Group	1 mo.	6 mo.
Reconstruction (Recon)	3	3
Reconstruction + P188 Day 0 & 1 (P188 D1)	3	3
Reconstruction + P188 Day 0, 1, & 7 (P188 D7)	3	2

Sample Preparation

Samples went through a CaptureSelect MutliSpecies Albumin depletion column (#191085310, Thermo Scientific) per manufacturers specification to remove albumin, which is one of the most abundant proteins found in SF. Briefly, samples were thawed on ice and 200 uL of the depletion product were loaded onto a spin column and hydrated with 1x PBS three times and centrifuged at 3000 rpm for one minute. Once thawed, 200uL of SF sample were loaded into each spin column and were allowed to incubate at room temperature for 20 minutes, while occasionally vortexing. Flow through was collected by centrifuging the spin columns with sample at 3000 rpm for one minute and washed with 100 uL of 1x PBS twice.

Protein concentration for each sample were quantified via a bicinchoninic acid (BCA) protein assay with a standard curve reference of bovine serum albumin (BSA) from 0.125 – 2 mg/mL, and digested with 1 μg/mL hyaluronidase for 3 hours at 37°C with shaking at 750 rpm. Digested samples were then reduced with 5 mM DTT for 1.5 hours at room temperature and alkylated in darkness with 10 mM iodoacetamide for 45 minutes at room temperature. 100 μg of each sample was aliquoted for trypsin digestion overnight at a 1:20 protease:substrate ratio and subsequently desalted over Pierce C18 columns (#87851) per manufacturer's instructions. 100 ng of each sample was screened

by liquid chromatography-mass spectrometry (LC-MS) to verify digestion efficiency and peptide content.

Tandem Mass Target (TMT) Labeling

Desalted and screened samples were fully dried and resuspended in 50 mM triethylammonium bicarbonate (TEAB) and quantified by A_{280} measurements assuming 1 A.U. = 1 mg/mL. Per manufacturer's instructions, TMT reagents were equilibrated to room temperature and resuspended in 41 µL of anhydrous acetonitrile. Eighty µg of each sample were diluted to 100 µL total volume and reacted with a TMT reagent for 1 hour at RT. The reaction was quenched with 8 µL of 5% hydroxylamine for 15 minutes, dried completely, acidified, and desalted over Pierce C18 columns (#87851) with 5 total wash steps for complete removal of unreacted reagent. 100 ng of each sample were screened for labeling efficiency by LC/MS.

Sample Pooling and LC-MS Analysis

After verifying > 98% labeling efficiency for all samples, 3 µg of each sample was pooled within each plex of 6 and all plexes were diluted to equal total peptide concentrations. Samples were subjected to mass analysis using a Thermo Scientific Ultimate 3000 RSLCnano ultra-high-performance liquid chromatography (UPLC) system coupled to a high-resolution Thermo Scientific Q Exactive HF mass spectrometer. An aliquot of each peptide preparation in Solvent A (0.1% formic acid in H_2O) was injected onto a Waters BEH C18 analytical column (2 µm, 100 Å, 75 µm x 25 cm) and separated by reverse-phase chromatography over a 180-min gradient at 300 nL/min flow. Peptides were eluted directly into the QE-HF using positive mode electrospray ionization. MS scan acquisition parameters were set to 120,000 resolution, 1e6 AGC target, maximum

ion time (MIT) of 50 ms, and a mass range of 375-1400 m/z. Data dependent MS/MS scan acquisition parameters were set to 30,000 resolution, 1e5 AGC target, MIT 100 ms, loop count of 15, isolation window of 0.7 m/z, dynamic exclusion window of 30 s, a normalized collision energy of 33, fixed first mass of 100 m/z, with peptide match set to preferred and charge exclusion enabled for all unassigned, +1, and >+8 charged species. Sample screens for peptide content and labeling efficiency were analyzed with a 60-min UPLC gradient using the following MS acquisition parameters: MS scan resolution 60,000, MIT of 60 ms, mass range 300-1800 m/z; MS/MS scan resolution 15,000, MIT 40 ms, isolation window 2.0 m/z, normalized collision energy of 27.

Protein Identification and Quantification

Raw data files were uploaded into Proteome Discoverer v2.5 (Thermo Scientific) and searched using Sequest HT search engine against the Uniprot *Oryctolagus cuniculus* UP000001811 reference proteome database (accessed 20210608 and last updated 20210129) using the following parameters: trypsin enzyme specificity with 2 maximum missed cleavages, minimum and maximum peptide lengths of 6 and 144, respectively, static modifications of TMT6plex on peptide N-termini and Lys side chains, carbamidomethylation on Cys, and dynamic modifications of oxidation on Met, deamidation on Asn and Gln, protein N-terminal acetylation. Precursor and fragment mass tolerances were set to 10 ppm and 0.02 Da, respectively. All data were filtered to a strict 1% false discovery rate at the peptide spectrum matches, peptide, and protein levels. For TMT six plex-based reporter ion quantitation, the following parameters were used: quantitative value corrections set to “true,” a co-isolation threshold of 50, minimum

channel occupancy threshold of 32%, total peptide amount normalization "on," and protein ratio calculation was set to "Protein Abundance Based."

Statistics

To ensure high quality samples for TMT analyses, 1-month and 6-month samples were combined for each treatment group. Paired student t-tests were used to determine significant difference for protein expression levels between treated samples and respective controls. Samples with an Abundance Ratio Variability ≤ 20 and a p-value < 0.05 were deemed significant. For all statistical results, the ratio of protein expression in the treated (right) limbs over the protein expression in the control (left) limbs for each treatment group will be used.

RESULTS

In total, 714 proteins were identified between all of the samples included in the study. Comparing the control limbs of all treatment groups to each other found a total of 707 proteins, with 688 proteins being shared between the three different conditions (Figure 27A). Comparing the treated limbs of all treatment groups to each other found a total of 708 proteins, with 704 proteins being shared between the three different conditions (Figure 27B). Further analysis of the proteins that were exclusively expressed in one of the treatments or limbs found that these proteins were not associated with PTOA, inflammation or any other pathways of interest. Comparing the expressed ratios of treated limbs to control limbs for each condition found a total of 19 significant proteins (Figure 27C). Comparing the overlap between the ratios of the significantly expressed proteins in the three treatment groups found proteins that were present in more than one treatment group. More information regarding the significantly expressed proteins for each

treatment group, along with definition name, p-value, and ratio can be found in Tables x-x.

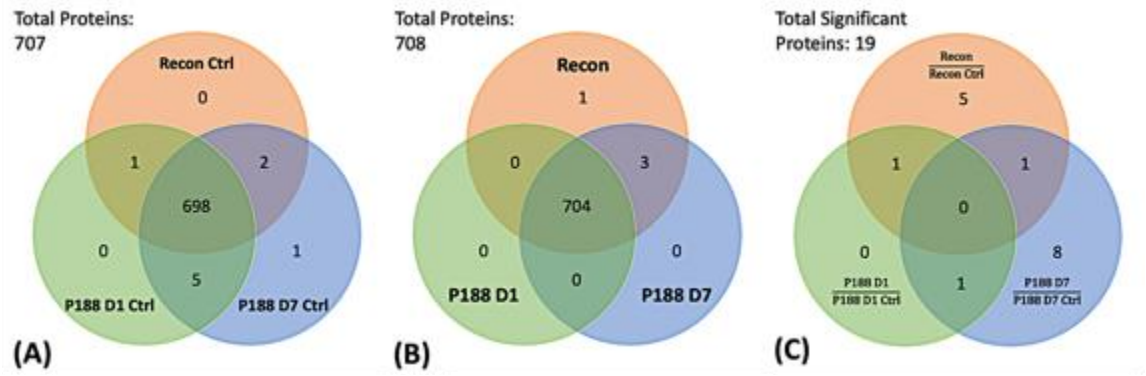

Figure 27. Total number of proteins and overlap for (A) control limbs of each treatment group, (B) the treated limbs of each treatment group, and (C) the total significant (ARV ≤ 20, p-value < 0.05) expressed proteins based on abundance ratio for each treatment group.

In the Recon group, out of 708 total proteins found in both treated and control limbs, there were seven significantly differentially expressed proteins (Figure 27C). Two proteins were expressed at lower levels (intercellular adhesion molecule 5, proteoglycan 4, and mimecan) and four proteins (periostin, coagulation factor V, tenascin C, and cystatin F) were expressed in higher levels in the treated limbs compared to controls (Table 9). A ratio < 1 means that the protein was under expressed in the treated limbs compared to control limbs and a ratio > 1 means that the protein was over expressed in the treated limbs compared to control limbs.

Table 9. Protein content ratios of the reconstruction limb and respective control limb (Recon group) for significantly differentially expressed proteins.

Protein ID	Definition name	P-value	Ratio
Q28730	Intercellular adhesion molecule 5	0.007144	0.322
G1TFQ7	Proteoglycan 4	0.000823	0.371
Q8MJF1	Mimecan	0.005963	0.453
A0A5F9CD23	Periostin	1.18E-06	2.121
A0A5F9CYY5	Coagulation factor V	0.000519	2.441
A0A5F9DIW0	Tenascin C	0.003623	2.493
A0A5F9DM57	Cystatin F	0.003817	2.73

In the P188 D1 group, out of a total of 707 proteins found in both treated and control limbs, there were two significantly differentially expressed proteins (Figure 27C). Mimecan was expressed at lower levels and proteasome subunit alpha type was expressed at higher levels in the treated limbs compared to controls (Table 10).

Table 10. Protein content ratios of the reconstruction and P188 Day 0 & 1 limb and respective control limb (P188 D1 group) for significantly differentially expressed proteins

Protein ID	Definition name	P-value	Ratio
Q8MJF1	Mimecan	0.00577	0.371
G1T2L1	Proteasome subunit alpha type	0.001559	2.408

In the P188 D7 group, out of a total of 708 proteins found in both treated and control limbs, there were ten significantly differentially expressed proteins (Figure 27C). Only one protein was expressed at lower levels and nine proteins were expressed at higher levels in the treated limbs compared to controls (Table 11). One of the higher expressed proteins was an uncharacterized protein for which further information regarding its definition name and function could not be found.

Table 11. Protein content ratios of the reconstruction and P188 Day 0, 1, & 7 limb and respective control limb (P188 D7 group) for significantly differentially expressed proteins.

Protein ID	Definition name	P-value	Ratio
G1SXM9	Lymphatic vessel endothelial hyaluronan receptor 1	0.002463	0.415
A0A5F9C5Y4	Phosphoacetylglucosamine mutase	0.005568	2.002
A0A5S8HX12	Translationally-controlled tumor protein	0.022714	2.107
A0A5F9C869	G2/M-phase specific E3 ubiquitin protein ligase	0.007858	2.228
P07452	Carbonic anhydrase 1 (Fragment)	0.008052	2.316
A0A5F9D6A8	Uncharacterized protein	0.007858	2.547
G1T2L1	Proteasome subunit alpha type	0.008028	2.687
G1T5H0	HtrA serine peptidase 1	0.029372	2.728
A0A5F9DIW0	Tenascin C	1.97E-05	2.746
A0A5F9DSX4	Collagen type V alpha 2 chain	0.004731	4.422

DISCUSSION

The present study is the first to perform proteomic analysis of SF in a combined P188 and surgical intervention *in-vivo* lapine model following traumatic injury to the knee to study the onset and progression of PTOA. The results of the study found that although the proteomes of the SF from the three treatment groups were mostly similar, there were a few significantly expressed proteins between the three treatment groups that are associated with PTOA.

More proteins whose change that are strongly associated with PTOA were found in the Recon only group, compared to the P188 treatment groups. In the current study, it was found that proteoglycan 4 (PRG4) was expressed at lower levels and that periostin (Postn) and tensacin C (TNC) were expressed at higher levels in the treated limbs compare to control limbs. PRG4 provides lubrication within the knee joint and is commonly found in the SF and the surfaces of articular cartilage and menisci.[76,77,133] Animal studies have reported that lower levels of the protein are associated with cartilage degeneration and as an early sign of PTOA.[37,169] An increase in Postn expression has been found to be induced following knee joint trauma and has been shown to be increased in mouse and human cartilage samples during the progression of osteoarthritis (OA).[7,26] In an ACL transection knockout mouse model, Attur et al reported that a deficiency in Postn provided a protective effect against PTOA[6], further highlighting the relationship between the protein and PTOA. Similarly, higher levels of TNC have been documented in multiple studies investigating the relationship between the protein and PTOA suggesting that the protein is a useful marker of disease progression.[60,61,116,125] In a canine model, Chockalingam et al. found an immediate increase in the expression of

TNC, which decreased over time, but was still expressed at higher levels compared to controls 12-months following joint trauma.[27] The changes in expression levels of these proteins suggest that reconstruction surgery alone is not able to fully mitigate the disease.

P188 treatment seemed to have helped prevent the expression of most of the proteins previously discussed. In the P188 D7 group, had a few proteins that have been shown to be associated with PTOA. TNC was the only significantly expressed protein at higher levels in the P188 D7 groups, similar to the Recon only group, but the other proteins, PRG4 and Postn, were not differentially regulated in either P188 treatment groups. In the P188 D7 group, both HtrA and carbonic hydrase 1 were found to be expressed at higher levels in the treated limbs compared to control limbs. Hu et al. reported a 7-fold increase in levels of HtrA, whose genetic code is conserved among mammals, in cartilage explants from OA patients, compared to non-OA controls.[68] Higher expression of carbonic hydrase 1, which promotes the formation of calcium carbonate in bone, were found in synovial tissues of patients suffering of end stage OA, compared to patients suffering of rheumatoid arthritis (RA).[23] Although there is a distinction between PTOA/OA and RA, it is interesting to note that a protein that has been shown to be overly expressed in the latter was found in the P188 D7 group, the translationally controlled tumor protein (TCTP). Kim et al. reported that TCTP triggers a histamine response and levels of the protein are correlated with RA disease progression along with inflammation.[81] While P188 treatment may not have been able to fully prevent the onset of PTOA, the results suggest that P188 may limit the number of biomarkers associated with the disease.

Previous studies have reported an increase in mimecan (MIME), a small proteoglycan which supports the collagen matrix, expression in hip cartilage from OA patients.[66] However, the current study found MIME to be expressed at lower levels in both the Recon and P188 D1 groups. The differences between the current and previous findings could be attributed to the time point in which the samples were obtained, as Hosseininia et al. used end-stage cartilage samples from patients vs. the current study that was within 6 months of an injury inducing impact.[66] Proteasome subunit alpha type was found to be significantly expressed in both the P188 D1 and P188 D7 groups. Unfortunately, due to the lack of clarification regarding the exact type of proteasome subunit alpha type, the current study was limited in investigating the role of this protein within the knee joint and disease pathology. Other proteins found, but that were not discussed due to a lack of previous detailed research describing the function of the proteins include: intercellular adhesion molecule 5, coagulation factor v, cystatin F, lymphatic vessel endothelial hyaluronan receptor 1, phosphoacetylglucosamine mutase, G2/M-phase specific E3 ubiquitin protein ligase, and collagen type V alpha 2 chain.

Limitations of the current study include limited sample sizes for each treatment group and time point. Similarly, varying sample sizes within each treatment group may have affected the results, especially for the P188 D7 group. Future studies should aim to account for possible unsatisfactory sample quality for proteomic analysis by increasing the sample size in each group. Another limitation is the exclusion of an impact only group, which would help divorce the effect of surgical intervention on the expression of biomarkers on the disease compared to those that may be present following a traumatic impact alone. As previously mentioned, this study combined samples across time points

to increase the sample size for each treatment and ensure high quality samples for TMT analyses. Previous studies have shown that both progression of the disease and protein expression are time dependent. Currently, there is another proteomic analysis being conducted with the samples used in this study that will include a variable for time point. This will help determine changes in the proteome across time, which could identify other proteins that play a key role in the onset and progression of PTOA.

CONCLUSIONS

This was the first study to analyze the proteome of SF in a closed joint impact and reconstruction model and a combined P188 and surgical treatment model. Biomarkers associated with PTOA were found to be elevated in the Recon group and not in the P188 treated groups, perhaps suggesting that reconstruction surgery alone may not be able to prevent the development of PTOA. Combined P188 and surgical treatment proved to be able to significantly limit the expression of these biomarkers, which could prove to be beneficial in future studies.

CHAPTER 6

CONCLUSIONS AND FUTURE WORK

The work presented in the preceding chapters provided an investigation into the use of combined single and multiple administrations of P188 and surgical reconstruction in an *in-vivo* closed-joint impact lapine model as potential treatment to help limit, delay, or mitigate the onset and progression of PTOA by assessing changes in multiple tissues within the knee joint. As it had been hypothesized that surgical intervention fails to address the occult damage to the tissues within the knee joint following mechanical trauma, P188 was chosen as previous studies had shown that the surfactant significantly prevented cell death following an injurious impact in *in-vitro* and *in-vivo* studies. Similarly, the surfactant has been shown to inhibit pathways associated with cell death, inflammation, and matrix degradation.

The results of the current study found that reconstruction surgery alone does not prevent the onset and progression of PTOA. Changes associated with the disease were found in all three of the analyzed tissues as early as 1-month following impact, with the severity of these changes increasing over time. Most of these changes were found in the meniscus, with an increase in tissue damage, decreases in the mechanical properties and loss of proteoglycans being reported. Proteomic analyses found that more proteins associated with the disease were expressed in the synovial fluid of the reconstructed only limbs as well, which could cause further degradation to other tissues within the joint. The only significant change found in the subchondral bone was the formation of osteophytes, which are one of the key markers used to diagnose the disease using non-invasive imaging modalities. The changes reported in the current study are corroborated by

findings in the clinical setting following surgical intervention and further highlight the need to find alternative or adjacent treatments to limit or prevent the disease.

Tying together the documented changes in the current study, it can be hypothesized that perhaps the decrease in the expression of Proteoglycan 4, which aids in lubrication within the joint, could be contributing to the early degeneration observed in the meniscus at the 1-month time point. A decrease in lubrication could be subjecting the tissue to more friction, which could be contributing to the increase in damage observed across all time points in the Recon group, as a decrease in Proteoglycan 4 was only observed in this treatment group, and not in any of the P188 treated groups analyzed. Similarly, higher expression of periostin and tenascin C have been observed in patients with more severe OA. These increases in the expression of both proteins in the Recon group could be contributing to the degradation documented in the mechanical properties and proteoglycan content of the meniscus, as these properties were much more negatively affected. These finding suggest that the menisci were effective in performing their role in protecting the underlying articular cartilage and subchondral bone, as few changes were documented in subchondral bone health.

A single or multiple administrations of P188 treatment, in conjunction with surgical intervention, proved to be able to limit the progression of PTOA, when compared to reconstruction surgery alone. In the meniscus, P188 treatment was able to prevent gross morphological changes in the lateral meniscus at the 1-month time point, but damage progressed in the tissue over time. All P188 treatment groups had less significant changes in both the mechanical properties and loss of proteoglycan content at later time points. Analyzing the proteome of the synovial fluid of the P188 D1 and P188

D7 groups found less significantly expressed proteins associated with PTOA, when compared to the reconstructed only group. Perhaps by inhibiting cell death post-impact, P188 treatment may have reduced the expression of the biomarkers associated with PTOA found in the Recon group, which could explain the less significant changes observed in these treatment groups. In the subchondral bone, there were few documented changes in architecture, or mineral composition, when compared to reconstruction only. The collaborating laboratory found that P188 treatment was able to prevent significant changes in the articular cartilage, suggesting that by maintaining the health of the tissue, the underlying bone was protected. The only consistent change found in subchondral bone linked with the onset and progression of the disease was the formation of osteophytes outside the normal joint margin, which could be associated with the higher expression of carbonic hydrase 1 found in the synovial fluid. At the 6-month time point, although not statistically significant, larger volumes of osteophytes were documented in the P188 D7 bones compared to the Recon group.

However, this study was not without large scale limitations. One limitation was the use of the animals left limb as the contralateral control instead of limbs from animals that received no treatment to any of their limbs. As it was noted, following both the traumatic impact and surgical intervention, the animals favored the untreated limb for a few days. These changes in gait could have resulted in long term changes in loading on the left limb of the animals. Additionally, cytokines from the treated limbs could have been secreted from the synovium into the blood stream, which could have affected the cytokines found in the control limb. Another limitation was the rate at which the impact was delivered, as knee injuries as a result from recreational activities or car crashes are

around 200 ms and the current study delivered the impact at 500 ms. The difference between the two rates could affect the amount of damage observed within the knee joint and perhaps the rate at which the diseases progressed over time. In the current study, the compressive modulus and GAG content of meniscal tissue were studied instead of collagen and tensile properties because it was expected that the traumatic impact and meniscectomy would cause the tissue to be heavily damaged. This would compromise the dog bone shapes that could be obtained from each sample. Currently, one of the most popular and reliable ways to determine collagen content within soft tissues is via immunohistochemistry. This methodology would be challenging in the current study due to the samples originating from rabbits, which would make it difficult to find antibodies that would be compatible with the samples. Despite these limitations, the findings of the study provided great insight into disease progression and alternative treatment options.

The findings of the current study suggest that, when compared to reconstructive surgery alone, combined P188 treatment and surgical intervention were able to limit the progression of the disease. Inflammation caused by surgical intervention may be attributed to some of the observed changes associated with PTOA in this model. Perhaps another administration of P188 immediately following the surgery may help reduce inflammation and limit the disease. Future studies may want to consider a targeted treatment of P188, as in the current study, it was unclear if the positive effects observed in the P188 treated limbs were due to direct or indirect treatment. Finding methods to track the surfactant as it is being diffused throughout the knee joint, such as radio or fluorescent labeling, would help determine which tissues P188 is directly helping and which ones are being indirectly affected by the treatment. Alternative meniscal

replacement options should be considered, as it has been well documented that meniscectomies lead to changes in joint loading and have a greater impact on whether or not a patient will require total knee replacement later in life. Combined treatments such as; surgical intervention to address the macroscopic damage and reduce joint laxity, P188 administration after injury and surgery to prevent cell death following each stressful event, and a total meniscal replacement to aid in load distribution and protect the underlying cartilage, may prove to be better treatment options to prevent the onset and progression of the disease.

REFERENCES

1. Akizuki, S., V. C. Mow, F. Muller, J. C. Pita, D. S. Howell, and D. H. Manicourt. Tensile properties of human knee joint cartilage: I. Influence of ionic conditions, weight bearing, and fibrillation on the tensile modulus. *Journal of Orthopaedic Research* 4:379–392, 1986.
2. Allen, Answorth, A., L. Caldwell Jr., George, and H. Fu, Freddie. Anatomy and biomechanics of the meniscus. *Operative Techniques in Orthopaedics* 5:2–9, 1995.
3. Amis, A. A., A. M. J. Bull, C. M. Gupte, I. Hijazi, A. Race, and J. R. Robinson. Biomechanics of the PCL and related structures: Posterolateral, posteromedial and meniscofemoral ligaments. *Knee Surgery, Sports Traumatology, Arthroscopy* 11:271–281, 2003.
4. Arnoczky, S. P. Anatomy of the Anterior Cruciate Ligament. *Clinical orthopaedics and related research* 172:19–25, 1983.
5. Aspden, R. M., Y. E. Yarker, and D. W. Hukins. Collagen orientations in the meniscus of the knee joint. *Journal of anatomy* 140 (Pt 3:371–80, 1985.
6. Attur, M., X. Duan, L. Cai, T. Han, W. Zhang, E. D. Tycksen, J. Samuels, R. H. Brophy, S. B. Abramson, and M. F. Rai. Periostin loss-of-function protects mice from post-traumatic and age-related osteoarthritis. *Arthritis Research and Therapy* 23:1–14, 2021.
7. Attur, M., Q. Yang, K. Shimada, Y. Tachida, H. Nagase, P. Mignatti, L. Statman, G. Palmer, T. Kirsch, F. Beier, and S. B. Abramson. Elevated expression of periostin in human osteoarthritic cartilage and its potential role in matrix degradation via matrix metalloproteinase-13. *The FASEB Journal • Research Communication FASEB J* 29:4107–4121, 2015.
8. Baars, D. C., S. A. Rundell, and R. C. Haut. Treatment with the non-ionic surfactant poloxamer P188 reduces DNA fragmentation in cells from bovine chondral explants exposed to injurious unconfined compression. *Biomechanics and Modeling in Mechanobiology* 5:133–139, 2006.
9. Bajaj, S., T. Shoemaker, A. A. Hakimiyan, L. Rappoport, C. P. Garrido, T. R. Oegema, M. A. Wimmer, and S. Chubinskaya. Protective effect of P188 in the Model of Acute Trauma to Human Ankle Cartilage: the Mechanism of Action. *Journal of orthopaedic trauma* 24:571–576, 2010.
10. Balakrishnan, L., M. Bhattacharjee, S. Ahmad, R. S. Nirujogi, S. Renuse, Y. Subbannayya, A. Marimuthu, S. M. Srikanth, R. Raju, M. Dhillon, N. Kaur, R. Jois, V. Vasudev, Y. L. Ramachandra, N. A. Sahasrabuddhe, T. S. K. Prasad, S. Mohan, H. Gowda, S. Shankar, and A. Pandey. Differential proteomic analysis of synovial fluid from rheumatoid arthritis and osteoarthritis patients. *Clinical Proteomics* 11:1–14, 2014.
11. Bansal, P. N., N. S. Joshi, V. Entezari, M. W. Grinstaff, and B. D. Snyder. Contrast Enhanced Computed Tomography can predict the glycosaminoglycan content and biomechanical properties of articular cartilage. *Osteoarthritis and Cartilage* 18:184–191, 2010.
12. Batiste, D. L., A. Kirkley, S. Laverty, L. M. F. Thain, A. R. Spouge, and D. W. Holdsworth. Ex vivo characterization of articular cartilage and bone lesions in a

rabbit ACL transection model of osteoarthritis using MRI and micro-CT. *Osteoarthritis and Cartilage* 12:986–996, 2004.
13. Batiste, D. L., B. Sc, A. K. M. D, S. L. Mvb, D. Acvs, L. M. F. T. M. D, A. R. S. M. D, J. S. Gati, M. Sc, P. J. Foster, D. Ph, D. W. Holdsworth, and D. Ph. High-resolution MRI and micro-CT in an ex vivo rabbit anterior cruciate ligament transection model of osteoarthritis. *Osteoarthritis and Cartilage* 12:614–626, 2004.
14. Bayar, A., S. Sarikaya, S. Keser, Ş. Özdolap, I. Tuncay, and A. Ege. Regional bone density changes in anterior cruciate ligament deficient knees: A DEXA study. *Knee* 15:373–377, 2008.
15. Bennett, M., and D. W. Gilroy. Lipid Mediators in Inflammation. *Microbiology Spectrum* 4:1–21, 2016.
16. Brandt, K. D. Osteophytes in osteoarthritis. Clinical aspects. *Osteoarthritis and Cartilage* 7:334–335, 1999.
17. Brown, T. D., R. C. Johnston, C. L. Saltzman, J. L. Marsh, and J. A. Buckwalter. Posttraumatic osteoarthritis: a first estimate of incidence, prevalence, and burden of disease. *Journal of orthopaedic trauma* 20:739–44, 2006.
18. Buckwalter, J. A., and H. J. Mankin. Instructional Course Lectures, The American Academy of Orthopaedic Surgeons - Articular Cartilage. Part I: Tissue Design and Chondrocyte-Matrix Interactions. *Journal of Bone & Joint Surgery* 79:600–611, 1997.
19. Bullough, P. G. The role of joint architecture in the etiology of arthritis. *Osteoarthritis and Cartilage* 12:2–9, 2004.
20. Burr, D. B. Anatomy and physiology of the mineralized tissues: Role in the pathogenesis of osteoarthrosis. *Osteoarthritis and Cartilage* 12:20–30, 2004.
21. Butler, D., F. Noyes, and E. Grood. Ligamentous restraints to anterior-posterior drawer in the human knee: A biomechanical study. *The Journal of Bone and Joint surgery* 62:259–270, 1980.
22. Chang, D. G., E. P. Iverson, R. M. Schinagl, M. Sonoda, D. Amiel, R. D. Coutts, and R. L. Sah. Quantitation and localization of cartilage degeneration following the induction of osteoarthritis in the rabbit knee. *Osteoarthritis and Cartilage* 5:357–372, 1997.
23. Chang, X., J. Han, Y. Zhao, X. Yan, S. Sun, and Y. Cui. Increased expression of carbonic anhydrase i in the synovium of patients with ankylosing spondylitis. *BMC Musculoskeletal Disorders* 11:, 2010.
24. Chen, C. T., N. Burton-Wurster, C. Borden, K. Hueffer, S. E. Bloom, and G. Lust. Chondrocyte necrosis and apoptosis in impact damaged articular cartilage. *Journal of Orthopaedic Research* 19:703–711, 2001.
25. Chia, H. N., and M. L. Hull. Compressive moduli of the human medial meniscus in the axial and radial directions at equilibrium and at a physiological strain rate. *Journal of Orthopaedic Research* 26:951–956, 2008.
26. Chinzei, N., R. H. Brophy, X. Duan, L. Cai, R. M. Nunley, L. J. Sandell, and M. F. Rai. Molecular influence of anterior cruciate ligament tear remnants on chondrocytes: a biologic connection between injury and osteoarthritis. *Osteoarthritis and Cartilage* 26:588–599, 2018.

27. Chockalingam, P. S., S. S. Glasson, and L. S. Lohmander. Tenascin-C levels in synovial fluid are elevated after injury to the human and canine joint and correlate with markers of inflammation and matrix degradation. *Osteoarthritis and Cartilage* 21:339–345, 2013.
28. Clark, C. R., and J. A. Ogden. Development of the menisci of the human knee joint. Morphological changes and their potential role in childhood meniscal injury. *The Journal of Bone and Joint surgery* 65:538–547, 1983.
29. Coatney, G. A., A. C. Abraham, K. M. Fischenich, K. D. Button, R. C. Haut, and T. L. Haut Donahue. Efficacy of P188 on lapine meniscus preservation following blunt trauma. *J Mech Behav Biomed Mater* 57:57–64, 2015.
30. Costouros, J. G., A. C. Dang, and H. T. Kim. Comparison of chondrocyte apoptosis in vivo and in vitro following acute osteochondral injury. *Journal of Orthopaedic Research* 22:678–683, 2004.
31. Crema, M. D., A. Guermazi, L. Li, M. H. Nogueira-Barbosa, M. D. Marra, F. W. Roemer, F. Eckstein, M. P. Hellio Le Graverand, B. T. Wyman, and D. J. Hunter. The association of prevalent medial meniscal pathology with cartilage loss in the medial tibiofemoral compartment over a 2-year period. *Osteoarthritis and Cartilage* 18:336–343, 2010.
32. Csintalan, R. P., M. C. S. Inacio, and T. T. Funahashi. Incidence Rate of Anterior Cruciate Ligament Reconstructions. *The Permanente Journal* 12:17–21, 2008.
33. DR, C., B. GS, W. M, S. RL, A. TP, and S. DJ. The mechanobiology of articular cartilage development and degeneration. *Clin Orthop Relat Res.* 427:69–77, 2004.
34. Duthon, V. B., C. Barea, S. Abrassart, J. H. Fasel, D. Fritschy, and J. Ménétrey. Anatomy of the anterior cruciate ligament. *Knee Surgery, Sports Traumatology, Arthroscopy* 14:204–213, 2006.
35. Eckstein, F., W. Wirth, L. S. Lohmander, M. I. Hudelmaier, and R. B. Frobell. Five-Year Followup of Knee Joint Cartilage Thickness Changes After Acute Rupture of the Anterior Cruciate Ligament. 67:152–161, 2015.
36. Eisenberg, S. R., and A. J. Grodzinsky. Swelling of articular cartilage and other connective tissues: Electromechanochemical forces. *Journal of Orthopaedic Research* 3:148–159, 1985.
37. Elsaid, K. A., G. D. Jay, M. L. Warman, D. K. Rhee, and C. O. Chichester. Association of articular cartilage degradation and loss of boundary-lubricating ability of synovial fluid following injury and inflammatory arthritis. *Arthritis and Rheumatism* 52:1746–1755, 2005.
38. Englund, M., A. Guermazi, F. W. Roemer, P. Aliabadi, M. Yang, C. E. Lewis, J. Torner, M. C. Nevitt, B. Sack, and D. T. Felson. Meniscal tear in knees without surgery and the development of radiographic osteoarthritis among middle-aged and elderly persons: The multicenter osteoarthritis study. *Arthritis and Rheumatism* 60:831–839, 2009.
39. Englund, M., and L. S. Lohmander. Risk factors for symptomatic knee osteoarthritis fifteen to twenty-two years after meniscectomy. *Arthritis and Rheumatism* 50:2811–2819, 2004.
40. Englund, M., and L. S. Lohmander. Risk factors for symptomatic knee osteoarthritis fifteen to twenty-two years after meniscectomy. *Arthritis and Rheumatism* 50:2811–2819, 2004.

41. Ewers, B. J., D. Dvoracek-Driksna, M. W. Orth, and R. C. Haut. The extent of matrix damage and chondrocyte death in mechanically traumatized articular cartilage explants depends on rate of loading. *Journal of Orthopaedic Research* 19:779–784, 2001.
42. Fairbank, T. J. Knee joint changes after meniscectomy. *The Journal of bone and joint surgery. American volume* 30 B:664–670, 1948.
43. Fauron, A. H., P. E. Vaughan, F. Wei, R. C. Haut, T. D. Haut, and L. M. Dejardin. Intracapsular Cranial Cruciate Ligament Reconstruction in a Lapine Model Using an Autogenous Semitendinosus Graft: Technique Description. , 2019.
44. Felson, D. T. An update on the pathogenesis and epidemiology of osteoarthritis. 42:1–9, 2004.
45. Ferretti, A., F. Conteduca, A. de Carli, M. Fontana, and P. P. Mariani. Osteoarthritis of the knee after ACL reconstruction. *International Orthopaedics* 15:367–371, 1991.
46. Fink, C., C. Hoser, W. Hackl, R. A. Navarro, and K. P. Benedetto. Long-term Outcome of Operative or Nonoperative Treatment of Anterior Cruciate Ligament Rupture ± Is Sports Activity a Determining Variable ? 304–309, 2001.
47. Fischenich, K. M., K. D. Button, G. A. Coatney, R. S. Fajardo, K. M. Leikert, R. C. Haut, and T. L. Haut Donahue. Chronic changes in the articular cartilage and meniscus following traumatic impact to the lapine knee. *Journal of Biomechanics* 48:246–253, 2015.
48. Fischenich, K. M., K. D. Button, C. Decamp, R. C. Haut, and T. L. H. Donahue. Comparison of two models of post-traumatic osteoarthritis; temporal degradation of articular cartilage and menisci. *Journal of Orthopaedic Research* 35:1–10, 2016.
49. Fischenich, K. M., G. a Coatney, J. H. Haverkamp, K. D. Button, C. DeCamp, R. C. Haut, and T. L. Haut Donahue. Evaluation of meniscal mechanics and proteoglycan content in a modified anterior cruciate ligament transection model. *Journal of biomechanical engineering* 136:1–8, 2014.
50. Fithian, D. C., E. W. Paxton, M. lou Stone, W. F. Luetzow, R. P. Csintalan, D. Phelan, D. M. Daniel, S. California, P. Medical, and E. Cajon. Prospective Trial of a Treatment Algorithm for the Management of the Anterior Cruciate Ligament – Injured Knee. *The American Journal of Sports Medicine* 33:335–346, 2005.
51. Fithian, D. C., E. W. Paxton, M. lou Stone, W. F. Luetzow, R. P. Csintalan, D. Phelan, D. M. Daniel, S. California, P. Medical, and E. Cajon. Prospective Trial of a Treatment Algorithm for the Management of the Anterior Cruciate Ligament – Injured Knee. 335–346.doi:10.1177/0363546504269590
52. Fithian, D., M. Kelly, and V. Mow. Material properties and structure-function relationships in the menisci. *Clin Orthop Relat Res.* 252:19–31, 1990.
53. Garrido, C. P., A. A. Hakimiyan, L. Rappoport, R. Theodore, M. A. Wimmer, and S. Chubinskaya. Degradation After Acute Trauma To Human Ankle. 17:1244–1251, 2010.
54. Gelber, A. C., M. C. Hochberg, L. A. Mead, N.-Y. Wang, F. M. Wigley, and M. J. Klag. Joint Injury in Young Adults and Risk for Subsequent Knee and Hip Osteoarthritis. *Annals of Internal Medicine* 133:321–328, 2000.

55. Goldring, M. B., and S. R. Goldring. Articular cartilage and subchondral bone in the pathogenesis of osteoarthritis. *Annals of the New York Academy of Sciences* 1192:230–237, 2010.
56. Goldring, M. B., and S. R. Goldring. Articular cartilage and subchondral bone in the pathogenesis of osteoarthritis. *Annals of the New York Academy of Sciences* 1192:230–237, 2010.
57. Goldring, M. B., and K. B. Marcu. Cartilage homeostasis in health and rheumatic diseases. *Arthritis Research and Therapy* 11:, 2009.
58. Gottlob, C., C. Baker, and L. Colvin. Cost effectiveness of anterior cruciate ligament reconstruction in young adults. *Clinical orthopaedics and related research* 367:272–82, 1999.
59. Gupta, T., B. Zielinska, J. McHenry, M. Kadmiel, and T. L. Haut Donahue. IL-1 and iNOS gene expression and NO synthesis in the superior region of meniscal explants are dependent on the magnitude of compressive strains. *Osteoarthritis and Cartilage* 16:1213–1219, 2008.
60. Hasegawa, M., H. Hirata, A. Sudo, K. Kato, D. Kawase, N. Kinoshita, T. Yoshida, and A. Uchida. Tenascin-C Concentration in Synovial Fluid Correlates with Radiographic Progression of Knee Osteoarthritis. *The Journal of Rheumatology* 31:2021–2026, 2004.
61. Hasegawa, M., T. Yoshida, and A. Sudo. Tenascin-C in Osteoarthritis and Rheumatoid Arthritisdoi:10.3389/fimmu.2020.577015
62. Hede, A., D. B. Jensen, P. Blyme, and S. Sonne-Holm. Epidemiology of meniscal lesions in the knee: 1,215 open operations in copenhagen 1982-84. *Acta Orthopaedica* 61:435–437, 1990.
63. Hellio Le Graverand, M. P., E. Vignon, I. G. Otterness, and D. A. Hart. Early changes in lapine menisci during osteoarthritis development part II: Molecular alterations. *Osteoarthritis and Cartilage* 9:65–72, 2001.
64. Hellio Le Graverand, M. P., E. Vignon, I. G. Otterness, and D. a Hart. Early changes in lapine menisci during osteoarthritis development: Part I: cellular and matrix alterations. *Osteoarthritis and cartilage / OARS, Osteoarthritis Research Society* 9:56–64, 2001.
65. Hellung-Larsen, P., F. Assaad, S. Pankratova, B. L. Saietz, and L. T. Skovgaard. Effects of Pluronic F-68 on Tetrahymena cells: Protection against chemical and physical stress and prolongation of survival under toxic conditions. *Journal of Biotechnology* 76:185–195, 2000.
66. Hosseininia, S., P. Önnerfjord, and L. E. Dahlberg. Targeted proteomics of hip articular cartilage in OA and fracture patients. *Journal of Orthopaedic Research* 37:131–135, 2019.
67. Hsia, A. W., M. J. Anderson, M. A. Heffner, E. P. Lagmay, R. Zavodovskaya, and B. A. Christiansen. Osteophyte formation after ACL rupture in mice is associated with joint restabilization and loss of range of motion. *Journal of Orthopaedic Research* 35:466–473, 2017.
68. Hu, S. I., M. Carozza, M. Klein, P. Nantermet, D. Luk, and R. M. Crowl. Human HtrA, an evolutionarily conserved serine protease identified as a differentially expressed gene product in osteoarthritic cartilage. *Journal of Biological Chemistry* 273:34406–34412, 1998.

69. Hufeland, M., M. Schünke, A. J. Grodzinsky, J. Imgenberg, and B. Kurz. Response of mature meniscal tissue to a single injurious compression and interleukin-1 in vitro. *Osteoarthritis and Cartilage* 21:209–216, 2013.
70. Hunt, P., O. Rehm, and A. Weiler. Soft tissue graft interference fit fixation: Observations on graft insertion site healing and tunnel remodeling 2 years after ACL reconstruction in sheep. *Knee Surgery, Sports Traumatology, Arthroscopy* 14:1245–1251, 2006.
71. Hunter, D. J., Y. Q. Zhang, J. B. Niu, X. Tu, S. Amin, M. Clancy, A. Guermazi, M. Grigorian, D. Gale, and D. T. Felson. The association of meniscal pathologic changes with cartilage loss in symptomatic knee osteoarthritis. *Arthritis and Rheumatism* 54:795–801, 2006.
72. Ikeda, D., H. Ageta, K. Tsuchida, and H. Yamada. ITRAQ-based proteomics reveals novel biomarkers of osteoarthritis. *Biomarkers* 18:565–572, 2013.
73. Intema, F., H. a W. Hazewinkel, D. Gouwens, J. W. J. Bijlsma, H. Weinans, F. P. J. G. Lafeber, and S. C. Mastbergen. In early OA, thinning of the subchondral plate is directly related to cartilage damage: results from a canine ACLT-meniscectomy model. *Osteoarthritis and cartilage / OARS, Osteoarthritis Research Society* 18:691–8, 2010.
74. Isaac, D. I., N. Golenberg, and R. C. Haut. Acute repair of chondrocytes in the rabbit tibiofemoral joint following blunt impact using P188 surfactant and a preliminary investigation of its long-term efficacy. *Journal of Orthopaedic Research* 28:553–558, 2010.
75. J, S., and F. Berenbaum. The role of synovitis in pathophysiology and clinical symptoms of osteoarthritis. *Nature Reviews Rheumatology* 6:625–35, 2010.
76. Jay, G., D. Britt, and C. Cha. Lubricin is a product of megakaryocyte stimulating factor gene expression by human synovial fibroblasts. *The Journal of Rheumatology* 27:594–600, 2000.
77. Jay, G. D., and K. A. Waller. The biology of Lubricin: Near frictionless joint motion. *Matrix Biology* 39:17–24, 2014.
78. Joshi, Meena, D., J.-K. Suh, T. Marui, and L.-Y. Woo, Savio. Interspecies variation of compressive biomechanical properties of the meniscus. *Journal of Biomedical Materials Rsearch* 29:823–828, 1995.
79. Katz, J. N., and S. D. Martin. Meniscus - Friend or foe: Epidemiologic observations and surgical implications. *Arthritis and Rheumatism* 60:633–635, 2009.
80. Khan, T., A. Alvand, D. Prieto-Alhambra, D. J. Culliford, A. Judge, W. F. Jackson, B. E. Scammell, N. K. Arden, and A. J. Price. ACL and meniscal injuries increase the risk of primary total knee replacement for osteoarthritis: a matched case–control study using the Clinical Practice Research Datalink (CPRD). *British Journal of Sports Medicine* bjsports-2017-097762, 2018.doi:10.1136/bjsports-2017-097762
81. Kim, M., Y. Choe, H. Lee, M. G. Jeon, J. H. Park, H. S. Noh, Y. H. Cheon, H. J. Park, J. Park, S. J. Shin, K. Lee, and S. il Lee. Blockade of translationally controlled tumor protein attenuated the aggressiveness of fibroblast-like synoviocytes and ameliorated collagen-induced arthritis. *Experimental and Molecular Medicine* 53:67–80, 2021.

82. Kisiday, J. D., E. J. Vanderploeg, C. W. McIlwraith, A. J. Grodzinsky, and D. D. Frisbie. Mechanical injury of explants from the articulating surface of the inner meniscus. *Archives of Biochemistry and Biophysics* 494:138–144, 2010.
83. Lajtai, G., G. Schmiedhuber, F. Unger, G. Aitzetmuüller, M. Klein, I. Noszian, and E. Orthner. Bone tunnel remodeling at the site of biodegradable interference screws used for anterior cruciate ligament reconstruction: 5-Year follow-up. *Arthroscopy* 17:597–602, 2001.
84. LaPrade, R. F., T. v. Ly, F. A. Wentorf, and L. Engebretsen. The Posterolateral Attachments of the Knee. A Qualitative and Quantitative Morphologic Analysis of the Fibular Collateral Ligament, Popliteus Tendon, Popliteofibular Ligament, and Lateral Gastrocnemius Tendon. *American Journal of Sports Medicine* 31:854–860, 2003.
85. Lee, R. C., J. Hannig, K. L. Matthews, A. Myerov, and C. T. Chen. Pharmaceutical therapies for sealing of permeabilized cell membranes in electrical injuries. *Annals of the New York Academy of Sciences* 888:266–273, 1999.
86. Lee, R. C., J. Hannig, K. L. Matthews, A. Myerov, and C. T. Chen. Pharmaceutical therapies for sealing of permeabilized cell membranes in electrical injuries. *Annals of the New York Academy of Sciences* 888:266–273, 1999.
87. Legendre, F., B. Patrick, K. Boumediene, and J.-P. Pujol. Role of interleukin 6 (IL-6)/IL-6R-induced signal tranducers and activators of transcription and mitogen-activated protein kinase/extracellular. *The Journal of Rheumotology* 32:1307–16, 2005.
88. Leist, M., and M. Jäättelä. Four deaths and a funeral: From caspases to alternative mechanisms. *Nature Reviews Molecular Cell Biology* 2:589–598, 2001.
89. Lenoch, F. Disturbance of nourishment of the articular cartilage and its relation to the development of osteoarthrosis. *Review of Czechoslovak Medicine* 16:113–17, 1970.
90. Levin, A., N. Burton-Wurster, C. T. Chen, and G. Lust. Intercellular signalling as a cause of cell death in cyclically impacted cartilage explants. *Osteoarthritis and Cartilage* 9:702–711, 2001.
91. Li, G., T. W. Rudy, C. Allen, M. Sakane, and S. L. Y. Woo. Effect of combined axial compressive and anterior tibial loads on In Situ forces in the anterior cruciate ligament: A porcine study. *Journal of Orthopaedic Research* 16:122–127, 1998.
92. Liu, W., J. He, R. Lin, J. Liang, and Q. Luo. Differential proteomics of the synovial membrane between bilateral and unilateral knee osteoarthritis in surgery-induced rabbit models. *Molecular Medicine Reports* 14:2243–2249, 2016.
93. Lohmander, L. S., P. M. Englund, L. L. Dahl, and E. M. Roos. The long-term consequence of anterior cruciate ligament and meniscus injuries: Osteoarthritis. *American Journal of Sports Medicine* 35:1756–1769, 2007.
94. Lohmander, L. S., a Ostenberg, M. Englund, and H. Roos. High prevalence of knee osteoarthritis, pain, and functional limitations in female soccer players twelve years after anterior cruciate ligament injury. *Arthritis and rheumatism* 50:3145–52, 2004.
95. Luo, Q., S. Ji, Z. Li, T. Huang, S. Fan, and Q. Xi. Effects of ultrasound therapy on the synovial fluid proteome in a rabbit surgery-induced model of knee osteoarthritis. *BioMedical Engineering Online* 18:1–15, 2019.

96. Luo, Q., X. Qin, Y. Qiu, L. Hou, and N. Yang. The change of synovial fluid proteome in rabbit surgery-induced model of knee osteoarthritis. *American Journal of Translational Research* 10:2087–2101, 2018.
97. Madry, H., C. N. van Dijk, and M. Mueller-Gerbl. The basic science of the subchondral bone. *Knee Surgery, Sports Traumatology, Arthroscopy* 18:419–433, 2010.
98. Majewski, M., H. Susanne, and S. Klaus. Epidemiology of athletic knee injuries: A 10-year study. *Knee* 13:184–188, 2006.
99. Mansour, J., F. Wentorf, and K. Degoede. In vivo kinematics of the rabbit knee in unstable models of osteoarthrosis. *Annals of Biomedical Engineering* 26:353–60, 1998.
100. Markatos, K., M. K. Kaseta, S. N. Lallos, D. S. Korres, and N. Efstathopoulos. The anatomy of the ACL and its importance in ACL reconstruction. *European Journal of Orthopaedic Surgery and Traumatology* 23:747–752, 2013.
101. Martin, R. B. Targeted bone remodeling involves BMU steering as well as activation. *Bone* 40:1574–1580, 2007.
102. McCann, L., E. Ingham, Z. Jin, and J. Fisher. Influence of the meniscus on friction and degradation of cartilage in the natural knee joint. *Osteoarthritis and Cartilage* 17:995–1000, 2009.
103. McDevitt, C., E. Gilbertson, and H. Muir. An experimental model of osteoarthritis; early morphological and biochemical changes. *The Journal of bone and joint surgery. British volume* 59:24–35, 1977.
104. McHenry, J. A., B. Zielinska, and T. L. Haut Donahue. Proteoglycan breakdown of meniscal explants following dynamic compression using a novel bioreactor. *Annals of Biomedical Engineering* 34:1758–1766, 2006.
105. van Meer, B. L., J. H. Waarsing, W. A. van Eijsden, D. E. Meuffels, E. R. A. van Arkel, J. A. N. Verhaar, S. M. A. Bierma-Zeinstra, and M. Reijman. Bone mineral density changes in the knee following anterior cruciate ligament rupture. *Osteoarthritis and Cartilage* 22:154–161, 2014.
106. Middleton, K. K., T. Hamilton, J. J. Irrgang, J. Karlsson, C. D. Harner, and F. H. Fu. Anatomic anterior cruciate ligament (ACL) reconstruction: A global perspective. Part 1. *Knee Surgery, Sports Traumatology, Arthroscopy* 22:1467–1482, 2014.
107. Mills, P. M., Y. Wang, F. M. Cicuttini, K. Stoffel, G. W. Stachowiak, P. Podsiadlo, and D. G. Lloyd. Tibio-femoral cartilage defects 3-5 years following arthroscopic partial medial meniscectomy. *Osteoarthritis and Cartilage* 16:1526–1531, 2008.
108. Mink, J., and D. AL. Occult cartilage and bone injuries of the knee: detection, classification, and assessment with MR imaging. *Radiology* 170:823–9, 1989.
109. Mow, V. C., S. P. Arnoczky, and D. W. Jackson. Knee Meniscus: Basic and Clinical Foundations. 1992.
110. Mow, V. C., S. C. Kuei, W. M. Lai, and C. G. Armstrong. Biphasic Creep and Stress Relaxation of Articular Cartilage in Compression: Theory and Experiments. *Journal of Biomechanical Engineering* 102:73–84, 1980.
111. Mow, V. C., and A. Ratcliffe. Structure and Function of Cartilage and Meniscus. Philadelphia: Lippincott-Raven, 1997, 113–177 pp.

112. Murray, M. M. Current Status and Potential of Primary ACL Repair. *Clinics in Sports Medicine* 28:51–61, 2009.
113. Myers, E. R., W. M. Lai, and V. C. Mow. A Continuum Theory and an Experiment for the Ion-Induced Swelling Behavior of Articular Cartilage. *Journal of biomechanical engineering* 106:151–158, 1984.
114. Myers, E. R., W. M. Lai, and V. C. Mow. A Continuum Theory and an Experiment for the Ion-Induced Swelling Behavior of Articular Cartilage. *Journal of biomechanical engineering* 106:151–158, 1984.
115. Myklebust, G., and R. Bahr. Return to play guidelines after anterior cruciate ligament surgery. *British Journal of Sports Medicine* 39:127–31, 2005.
116. Nakoshi, Y., M. Hasegawa, A. Sudo, T. Yoshida, and A. Uchida. Regulation of tenascin-C expression by tumor necrosis factor-α in cultured human osteoarthritis chondrocytes. *Journal of Rheumatology* 35:147–152, 2008.
117. Narez, G. E., F. Wei, L. Dejardin, R. C. Haut, and T. L. Haut Donahue. A single dose of P188 prevents cell death in meniscal explants following impact injury. *Journal of the Mechanical Behavior of Biomedical Materials* 117:1–7, 2021.
118. Natoli, R. M., and K. a Athanasiou. P188 reduces cell death and IGF-I reduces GAG release following single-impact loading of articular cartilage. *Journal of biomechanical engineering* 130:041012, 2008.
119. Nielsen, A. B., and J. Yde. Epidemiology of acute knee injuries: a prospective hospital investigation. *The Journal of trauma* 31:1644—1648, 1991.
120. Noyes, F., P. Torvik, W. Hyde, and J. Delucas. Biomechanics of Ligament Failure. *The Journal of Bone and Joint surgery* 56:1406–1418, 1974.
121. OARSI. Osteoarthritis: A Serious Disease, Submitted to the U. S. Food and Drug Administration. *Oarsi* 1–103, 2016.
122. Ollivierre, F., U. Gubler, C. A. Towle, C. Laurencin, and B. V. Treadwell. Expression of IL-1 genes in human and bovine chondrocytes: A mechanism for autocrine control of cartilage matrix degradation. *Biochemical and Biophysical Research Communications* 141:904–911, 1986.
123. Onur, T. S., R. Wu, S. Chu, W. Chang, H. T. Kim, and A. B. C. Dang. Joint instability and cartilage compression in a mouse model of posttraumatic osteoarthritis. *Journal of Orthopaedic Research* 32:318–323, 2014.
124. Papoutsakis, E. Media additives for protecting freely suspended animal cells against agitation and aeration damage. *Trends in Biotechnology* 9:316–24, 1991.
125. Patel, L., W. Sun, S. S. Glasson, E. A. Morris, C. R. Flannery, and P. S. Chockalingam. Tenascin-C induces inflammatory mediators and matrix degradation in osteoarthritic cartilage. *BMC Musculoskeletal Disorders* 12:, 2011.
126. Pauli, C., S. P. Grogan, S. Patil, S. Otsuki, A. Hasegawa, J. Koziol, M. K. Lotz, and D. D. D'Lima. Macroscopic And Histopathologic Analysis Of Human Knee Menisci In Aging And Osteoarthritis. *Osteoarthritis and Cartilage* 19:1132–1141, 2011.
127. Pauly, H. M., B. E. Larson, K. D. Button, C. DeCamp, R. C. Haut, and T. L. Haut Donahue. Micro-computed tomography comparison of trabecular bone changes in rabbits following surgical transection of anterior cruciate ligament and menisci or traumatic impact of tibiofemoral joint. , 2014.

128. Pauly, H. M., B. E. Larson, G. A. Coatney, K. D. Button, C. E. DeCamp, R. S. Fajardo, R. C. Haut, and T. L. Haut Donahue. Assessment of cortical and trabecular bone changes in two models of post-traumatic osteoarthritis. *Journal of Orthopaedic Research* 33:1835–1845, 2015.
129. Petersen, W., and B. Tillmann. Collagenous fibril texture of the human knee joint menisci. *Anatomy and Embryology* 197:317–324, 1998.
130. Phillips, D. M., and R. C. Haut. The use of a non-ionic surfactant (P188) to save chondrocytes from necrosis following impact loading of chondral explants. *Journal of Orthopaedic Research* 22:1135–1142, 2004.
131. von Porat, a, E. M. Roos, and H. Roos. High prevalence of osteoarthritis 14 years after an anterior cruciate ligament tear in male soccer players: a study of radiographic and patient relevant outcomes. *Annals of the Rheumatic Diseases* 63:269–273, 2004.
132. Proctor, C. S., M. B. Schmidt, R. R. Whipple, M. A. Kelly, and V. C. Mow. Material properties of the normal medial bovine meniscus. *Journal of Orthopaedic Research* 7:771–782, 1989.
133. Qadri, M., G. D. Jay, L. X. Zhang, H. Richendrfer, T. A. Schmidt, and K. A. Elsaid. Proteoglycan-4 regulates fibroblast to myofibroblast transition and expression of fibrotic genes in the synovium. *Arthritis Research and Therapy* 22:1–16, 2020.
134. Reuben, S. S., and J. Sklar. Pain Management in Patients Who Undergo Outpatient Arthroscopic Surgery of the Knee. *The Journal of Bone and Joint surgery* 82:1754–1766, 2000.
135. Ritter, S. Y., R. Subbaiah, G. Bebek, J. Crish, C. R. Scanzello, B. Krastins, D. Sarracino, M. F. Lopez, M. K. Crow, T. Aigner, M. B. Goldring, S. R. Goldring, D. M. Lee, R. Gobezie, and A. O. Aliprantis. Proteomic analysis of synovial fluid from the osteoarthritic knee: Comparison with transcriptome analyses of joint tissues. *Arthritis and Rheumatism* 65:981–992, 2013.
136. Rodeo, S. A., S. P. Arnoczky, P. A. Torzilli, C. Hidaka, and R. F. Waerren. Tendon-Healing in Bone Tunnel. *Journal of Bone & Joint Surgery* 75:1795–1803, 1993.
137. Ruifrok, A. C., and D. A. Johnston. Quantification of histochemical staining by color deconvolution. *Analytical and Quantitative Cytology and Histology* 23:291–299, 2001.
138. Rundell, S. A., D. C. Baars, D. M. Phillips, and R. C. Haut. The limitation of acute necrosis in retro-patellar cartilage after a severe blunt impact to the in vivo rabbit patello-femoral joint. *Journal of Orthopaedic Research* 23:1363–1369, 2005.
139. Samuels, J., S. Krasnokutsky, and S. B. Abramson. Osteoarthritis: A tale of three tissues. *Bulletin of the NYU Hospital for Joint Diseases* 66:244–250, 2008.
140. Sanchez-Adams, J., V. P. Willard, and K. A. Athanasiou. Regional variation in the mechanical role of knee meniscus glycosaminoglycans. *Journal of Applied Physiology* 111:1590–1596, 2011.
141. Saxne, T., M. Lindell, B. Månsson, I. Petersson, and D. Heinegård. Inflammation is a feature of the disease process in early knee joint osteoarthritis. *Rheumatology (Oxford)* 42:903–904, 2003.

142. Scanzello, C. R., and S. R. Goldring. The role of synovitis in osteoarthritis pathogenesis. *Bone* 51:249–257, 2012.
143. Schmidt, T. A., N. S. Gastelum, Q. T. Nguyen, B. L. Schumacher, and R. L. Sah. Boundary lubrication of articular cartilage: Role of synovial fluid constituents. *Arthritis and Rheumatism* 56:882–891, 2007.
144. Seedhom, B. B., D. Dowson, and V. Wright. Functions of the menisci: a preliminary study. *Annals of the Rheumatic Diseases* 33:111, 1974.
145. Sellam, J. & Berenbaum, F. Clinical features of osteoarthritis. In: Kelley's Textbook of Rheumatology, 8th edn vol. 1. 2008, pp. 1547–1560.
146. Sellam, J., and F. Berenbaum. The role of synovitis in pathophysiology and clinical symptoms of osteoarthritis. *Nature Reviews Rheumatology* 6:625–35, 2010.
147. Sellam, J., Herrero-Beaumont, G. &, and F. Berenbaum. Osteoarthritis: pathogenesis, clinical aspects and diagnosis. In: EULAR Compendium on Rheumatic Diseases. 2009, pp. 444–463.
148. Serbest, G., J. Horwitz, M. Jost, and K. Barbee. Mechanisms of cell death and neuroprotection by poloxamer 188 after mechanical trauma. *Federation of American Societies for Experimental Biology* 20:308–10, 2005.
149. Shin, S., B. Fermor, J. B. Weinberg, D. S. Pisetsky, and F. Guilak. Regulation of matrix turnover in meniscal explants: role of mechanical stress, interleukin-1, and nitric oxide. *Journal of Applied Physiology* 95:308–313, 2003.
150. Shinichi, Y., M. Nagano, M. Kurosaka, H. Muratsu, and K. Mizuno. Graft Healing in the Bone Tunnel in Anterior Cruciate Ligament Reconstruction. *Clinical orthopaedics and related research* 376:278–286, 2000.
151. Shirazi, R., and A. Shirazi-Adl. Analysis of partial meniscectomy and ACL reconstruction in knee joint biomechanics under a combined loading. *Clinical Biomechanics* 24:755–761, 2009.
152. Sniekers, Y. H., F. Intema, F. P. J. G. Lafeber, G. J. V. M. van Osch, J. P. T. M. van Leeuwen, H. Weinans, and S. C. Mastbergen. A role for subchondral bone changes in the process of osteoarthritis; a micro-CT study of two canine models. *BMC musculoskeletal disorders* 9:20, 2008.
153. Speer, K. P., C. E. Spritzer, F. H. I. Bassett, J. A. J. Feagin, and W. E. J. Garrett. Osseous injury associated with acute tears of the anterior cruciate ligament. , 1992.
154. Spindler, K., J. Schills, J. Bergfeld, J. Andrish, G. Weiker, T. Anderson, D. Piraino, B. Richmond, and S. Mendendorp. Prospective study of osseous, articular, and meniscal lesions in recent anterior cruciate ligament tears by magnetic resonance imaging and arthroscopy. *American Journal of Sports Medicine* 21:551–7, 1993.
155. Sturnieks, D. L., T. F. Besier, P. M. Mills, T. R. Ackland, K. F. Maguire, G. W. Stachowiak, P. Podsiadlo, and D. G. Lloyd. Knee joint biomechanics following arthroscopic partial meniscectomy. *Journal of Orthopaedic Research* 26:1075–1080, 2008.
156. Sulaiman, S. S., S. Lau, W. Tan, N. Rahmad, M. Md. Ajat, R. Radzi, and R. Mansor. Comparison of synovial fluid proteome profiles between chemically induced rabbit model and surgically induced rabbit model in mimicking early osteoarthritis. *Osteoarthritis and Cartilage* 28:S349, 2020.

157. Sweigart, M., C. Zhu, D. Burt, P. DeHoll, C. Agrawal, T. Clanton, and K. a Athanasiou. Intraspecies and interspecies comparison of the compressive properties of the medial meniscus. *Annals of Biomedical Engineering* 31:1569–79, 2004.
158. Tao, H., Y. Hu, Y. Qiao, Y. Xie, T. Chen, and S. Chen. Alternations of Metabolic Profiles in Synovial Fluids and the Correlation with T2 Relaxation Times of Cartilage and Meniscus - A Study on Anterior Cruciate Ligament- (ACL-) Injured Rabbit Knees at Early Stage. *BioMed Research International* 2019:1–9, 2019.
159. Teitelbaum, S. L. Osteoclasts: What do they do and how do they do it? *American Journal of Pathology* 170:427–435, 2007.
160. Thorlund, J. B., A. Holsgaard-Larsen, M. W. Creaby, G. M. Jørgensen, N. Nissen, M. Englund, and L. S. Lohmander. Changes in knee joint load indices from before to 12 months after arthroscopic partial meniscectomy: A prospective cohort study. *Osteoarthritis and Cartilage* 24:1153–1159, 2016.
161. Treppo, S., H. Koepp, E. C. Quan, A. A. Cole, K. E. Kuettner, and A. J. Grodzinsky. Comparison of biomechanical and biochemical properties of cartilage from human knee and ankle pairs. *Journal of Orthopaedic Research* 18:739–748, 2000.
162. Vignon, E., J. Bejui, P. Mathieu, J. Hartmann, G. Ville, J. Evreux, and J. Descotes. Histological cartilage changes in a rabbit model of osteoarthritis. *The Journal of Rheumatology* 14:104–6, 1987.
163. Walker, P. S., and M. J. Erkman. The role of the menisci in force transmission across the knee. 109:184–192, 1975.
164. Wei, F., L. Dejardin, A. Fauron, T. H. Donahue, and R. C. Haut. A novel lapine model of closed-joint knee injury with post-traumatic ACL reconstruction and meniscal debridement. , 2018.
165. Wei, F., T. Haut Donahue, R. C. Haut, M. D. Porcel Sanchez, and L. M. Dejardin. Reconstruction of the cranial cruciate ligament using a semitendinosus autograft in a lapine model. *Veterinary Surgery* 1–12, 2021.doi:10.1111/vsu.13643
166. Wojtys, E. M., A. M. Brower, and À. Bs. Anterior Cruciate Ligament Injuries in the Prepubescent and Adolescent Athlete: Clinical and Research Considerations. 45:509–512, 2010.
167. Wymenga, A. B., J. J. Kats, J. Kooloos, and B. Hillen. Surgical anatomy of the medial collateral ligament and the posteromedial capsule of the knee. *Knee Surgery, Sports Traumatology, Arthroscopy* 14:229–234, 2006.
168. Yoshioka, M., R. Coutts, D. Amiel, and S. Hacker. Characterization of a model of osteoarthritis in the rabbit knee. *Osteoarthritis and Cartilage* 4:87–98, 1996.
169. Young, A. A., S. McLennan, M. M. Smith, S. M. Smith, M. A. Cake, R. A. Read, J. Melrose, D. H. Sonnabend, C. R. Flannery, and C. B. Little. Proteoglycan 4 downregulation in a sheep meniscectomy model of early osteoarthritis. *Arthritis Research and Therapy* 8:4–9, 2006.
170. Zerahn, B., A. O. Munk, J. Helweg, and C. Hovgaard. Bone mineral density in the proximal tibia and calcaneus before and after arthroscopic reconstruction of the anterior cruciate ligament. *Arthroscopy - Journal of Arthroscopic and Related Surgery* 22:265–269, 2006.

APPENDICES

Appendix A Meniscus Live/Dead Protocol

Equipment/Supplies:

Item	Location
Specimens (Meniscus)	Incubator
Scalpel	Dissection Tools Drawer
Tweezers	
0.9% Saline Solution	
Drop cloth	
15 mLTest Tubes	Top of Incubator
Micron tube strips (2-4 depending on sample size)	On shelf above Cell Culture Supply drawer
Micron test tube holder	Next to micron test tube strips
Micro pipets (grey, orange, yellow)	On counter
0.6mL MicroCentrifuge Tube	Cell Culture Supplies Cabinet
4 Pipet tips	On counter
Calcein	In freezer in small cylindrical container (Freezer room)
Ethidium Homodimer-1	
Un-subbed slides	Glass Slides shelf
DI water	On counter
Sharps Container	Under dissection table
Portable Hard Drive	In portable hard drive drawer

Steps for preparation

1. Place 3 rows of micron tubes in the micron test tube holder
    a. One row for PBS to keep samples hydrated
    b. One row for Calcine/Ethidium mix
    c. One row for PBS washing step
2. Fill two rows (or one depending on number of samples) with PBS
3. Fill 15mL test tube with 4 mL of PBS
4. Fill 0.6mL microcentrifuge tube with 400uL of 10% formalin
    a. Use one tube per sample
5. Remove Calcein and Ethidium from freezer so they can start to thaw
    a. Be sure to keep them un exposed to the lights
6. Turn on Incubator (~ 37 degrees Celsius)
7. Set all pipettes to appropriate measures
    a. Grey top – 3 uL
    b. Orange top – 8 uL
    c. Yellow top – 150 uL

Steps for Slicing

1. Pour PBS from test tube into waste beaker
2. Take as thin of a slice (~0.5mm) from the cut face of the specimen
3. Place thin slice in micron vile

4. Place rest of sample in formalin microcentrifuge tube
5. Repeat for all specimens with enough testable tissue

Steps for Staining

1. Turn off lights
2. Add 3uL of Calcein (grey pipette) to 15mL test tube
1. Add 8uL of Ethidium (orange pipette) to 15mL test tube
2. Return Calcine and Ethidium vials to freezer
3. Vortex both test tube to mix stain into PBS
4. Pipette 150uL into empty micron test tube rows
5. Transfer meniscal slices from PBS micron test tube rows to fluorescence rows
6. Cap the rows
7. Slightly shake rows to mix
    a. Be sure not to mix up what specimen is what
    b. Make sure all meniscal slices are at bottom of test tube
8. Place in incubator for 25 mins
9. Remove from incubator
10. Move to meniscal slices to PBS micron test tube rows
11. Place in incubator for 5 mins for a "wash"
12. Remove from incubator
13. Turn off incubator
14. Remove slices from PBS and place on un-subbed slides
15. Cover specimens with DI water to stay hydrated

Steps for Imaging in Animal Cancer Center (ACC)

Make sure that slides are properly covered to prevent photo bleaching when transporting to ACC

1. Log hours
2. Log onto computer using regular engineering log in
3. Turn off light
4. Turn burner on
    a. Wait for green light
    b. If green light doesn't come on turn off let rest for 3 minutes and try again
5. Turn scope on
    a. Make sure shutter is off
6. Be sure in 2x
7. On Desktop open Q capture
8. Switch scope to camera
9. Will use green filter to image red (~600-900ms VERY variable)
10. Will use blue filter to image green (~1-2s but VERY variable)
11. Take photos of each image and save
    a. Name each image after the meniscal sample

Steps When Done Imaging

1. When all images have been taken close Q capture
2. Close shutter
3. Turn scope off
4. Turn burner off
5. Record hours
6. Log off computer
7. Place all slides in Sharps container

Appendix B Cryo-Embedding of Soft Tissue Protocol

Equipment/Supplies

Item	Amount	Location
Phosphate Buffered Saline (PBS)	NA	PBS Storage Tank
Chemistry Grade Crystalline Sucrose	Various	
Tissue Tek OCT	1 Tube	Shelf with embedding supplies
Tissue Tek Cryomolds	NA	Shelf with embedding supplies
Liquid Nitrogen	1 Dewar	
Styrofoam bowl	1	Tissue Tek Cabinet
Forceps/Tweezers	1 pair	Dissection Tools Drawer
Plastic Wrap	1 box	Shelf with embedding supplies
Weigh Boat	1	Drawer Under Scale
Beakers	3-4	Glassware Shelf

Prepared Solutions:

- 10% sucrose solution:
    1. Dissolve 10g crystalline sucrose in 100ml PBS.
- 20% sucrose solution:
    1. Dissolve 20g crystalline sucrose in 100ml PBS.
- 30% sucrose solution:
    1. Dissolve 30g crystalline sucrose in 100ml PBS.

Methods

1. Fill 100 mL glass beakers approximately half or ¾ full with *10% 20% and 30% sucrose solutions* respectively.
2. Place specimen into 10% beaker; the tissue should float.
3. Once the tissue drops to the bottom of the vial tissue has been infiltrated, move tissue to 20% beaker and repeat.
4. Once the tissue drops to the bottom of the vial, transfer tissue to 30% sucrose solution
5. Once the tissue drops to the bottom of the vial, remove tissue from vial and blot with Kimwipes.
6. Put small amount of OCT into a weight boat –
    - This will be used to apply a small amount of OCT to the cutting face of each specimen to aid in position detainment in cryo-mold during the freeze cycle.
7. Cut tissue if necessary to attain a flat cross section and orient appropriately in cryo-mold with the cut face lying flat on the bottom of the mold
8. Cover fill mold with OCT.
9. Pour liquid nitrogen into Styrofoam dish.

10. Carefully submerge tissue/mold in liquid nitrogen so as not to disrupt orientation of tissue in the mold.
11. Once the sample sinks to the bottom of the dish, remove and place on absorbent towel (slows down thawing of frozen specimen/OCT).
12. Allow sample to rest at room temperature for a minute to bring up to a temperature that is safe to handle and then remove from mold and wrap immediately cover with plastic wrap, label and store at -20°C.

Notes:

- Puck should "pop" out of sample. Be careful not to crack tissue/medium by forcing the puck to pop out.
- Options: Warm up with hand by holding/rubbing base of the mold to melt periphery of frozen OCT

Appendix C Cryo-Sectioning of Soft Tissue Protocol

Equipment/Supplies

Item	Amount	Location
Cryostat	1	Histology room
Tissue Tek OCT	1 Tube	On top of cryostat
Subbed Slides	NA	Drawer next to cryostat
Brush	1	Inside of cryostat
EtOH in Spray Bottle	1 Sprayer	Next to cryostat

Methods

1. Turn on the cryostat and let it reach -20˚C prior to using! This may take an hour or more depending on the outside temperature. Make sure to turn off the cryostat if it will not be in use for an extended period of time (more than 72hrs).
2. Inside the microtome, place the gold chuck (grooved platform) in one of the first four holes in the "fast freeze rail" (2 columns of 6 holes each located on the far left inside the microtome). These chucks can be left in the cryostat during cool-down time as well.
    - `The slots are NOT numbered – make sure to label the order of your samples if you are prepping more than one sample at a time.
3. Remove a blade from the blade container, or reuse one designated for your tissue, and grip it by the flat edge. Raise the clamp on the right hand side of the blade holder and slide the blade in along the left hand side of the blade holder. If it won't go in, push gently on the bottom edge of the blade holder (the side closest to you). Push the clamp back up to lock the blade in place.
    - Inspect the blade before putting it into the blade holder. Do not reuse the blade if there are any cosmetic defects, cracks, or chips taken from the blade.
4. Wearing gloves remove the chuck and hold the post in your hand, letting it warm up slightly. Spread embedding medium on the face of the chuck (over the grooved surface, making sure it goes down into the grooves), and put the chuck back in the fast freeze rail hole. NOTE: if the chuck is too cold when you put the medium on the grooved face, the medium will not go down into the grooves. You will have to pop off the frozen medium, wait for the chuck to warm up a bit more, and try again.
5. As soon as crystals start to appear on the outside edges of the embedding medium on the chuck face (this will happen quickly, and the medium will turn white near the chuck), push your embedded specimen into the center. The cutting surface (flat surface) should be exposed and parallel with the chuck surface.
6. Allow the entire chuck/specimen combination to freeze inside the cryostat. Keep window on cryostat closed during this period.
7. Insert the post of the chuck into the chuck holder. The small metal knob behind the chuck holder secures the chuck in the holder, and the black knob behind the blade/chuck allows the chuck to rotate once it has been loosened.
8. Adjust the vertical position of the sample with the handwheel so that it is centered vertically with respect to the blade.

9. Use the retract button on main screen of the cryostat to move chuck and holder away from blade. Make sure the notch needle on the displacement wheel is up when this is done.
10. Use the advance button on main screen of the cryostat to move chuck and holder toward the blade. Make sure the notch needle on the displacement wheel is when this is done.
11. Using the handwheel on the right hand side of the cryostat, raise and lower the embedded sample to trim through the frozen medium until you start to see the sample appear. Continue trimming until a good cross-section appears. Adjust the angle of the chuck if the sample appears to be cutting unevenly (i.e., if sections appear to be thicker on one side, if they appear angled, etc.). There is no blade guard, so MAKE SURE TO BE CAREFUL TO NOT CUT YOURSELF WITH THE BLADE when you do this.
12. Flip the "glass anti-curl plate" up so that any sections cut will slide into it underneath the glass; this will prevent sections from curling.
13. Start with 6um sections and increase to 8um if 6um does not yield good sections. Raise the glass plate periodically to clean out any "junk sections" with the brush kept inside the microtome
14. When your first good (even thickness, longitudinal appearance) section is cut, transfer it to a piece of slide glass by raising the anti-curl plate and pressing a piece of slide glass against the specimen.
15. Cut at least 2 more sections that you'll dispose of before the next section you plan to transfer to a slide (so that they'll be separated through the depth of the core). Do not place more than 3-4 sections per slide or the cover glass will not fit. Be careful of their placement when transferring to the slide glass – you won't be able to move them once they've been stuck to the slide, so make sure they're close enough together so that one coverglass will cover all 3. Obtain a total of 9 sections (2-3 per slide; 3-4 slides) per sample.
16. The remaining specimen can be refrozen by carefully melting the OCT medium from the underside the chuck with your fingers. DO NOT let the sample melt. Refold the sample in saran wrap and place in -20˚C non-frost free freezer.
17. Remove the blade from the cryostat; raise the blade clamp to unlock it and use forceps to gently push along the right hand side of the blade, pushing the blade out the left side of the holder. Place the used blade in the disposal side of the blade container.
18. Pull up the notch needle on the displacement wheel and push the "RETRACT" button to the left of the cryostat menu panel to retract the chuck and holder away from the blade holder.
19. Clean out any remaining junk by pushing it down to the side/bottom of the cryostat, but wipe out the junk while it is frozen before turning off the cryostat for an extended period of time.
20. Lay slides on a flat surface.

21. Using a spray bottle, spray 60˚C distilled water on slides to remove bubbles and promote the section adherence to the slide. Do not dip slides in water or saturate the slides. Cover slides with paper towels without touching the slides. Allow to dry overnight.

Troubleshooting:

1. If sectioning becomes inconsistent and slices appear shredded, one of these methods may alleviate the problem:
    a. Allow the sample to freeze longer in the chuck holder on the left side of the cryostat.
        i. Use the "Freeze" button on the cryostat menu to allow the temperature of the chuck tray to drop to -40˚C.
    b. Try the sample later!
    c. The sample may not have been embedded fully.
    d. The blade may not be cold enough! Allow the cryostat to drop in temperature.
    e. Try a thinner or thicker sectioning depth.
2. If you slice once or twice and nothing cuts, and on the third or fourth time you get a slice:
    a. The sample may not have been embedded fully.
    b. Try a thinner or thicker sectioning depth.

Appendix D Meniscus Safranin-O and Fast Green Stain Protocol

Prepared Solutions

- Weigerts Hematoxylin Working solution
    1. Mix equal parts of Part A and Part B
- Fast Green FCF Solution
    1. Dissolve 0.1g fast green FCFR in 1000mL DI water
- 1% Acetic Acid Solution
    1. Mix 10mL glacial acetic acid with 990mL DI water
- 0.1% Safranin O Solution
    1. Dissolve 30mL Safranin O (1%) in 300mL DI water

Set-Up:

Using staining tray in histology, set-up trays in the following order:

Hematoxylin	DI Water	DI Water	Fast Green	1% Acetic Acid	Saf-O	95% Ethanol	95% Ethanol	100% Ethanol	100% Ethanol	Xylene	Xylene

Methods

1. Place the slides in the slide holder.
2. Stain with Weigert's hematoxylin working solution for 10 minutes
3. Place slides in DI water using 2 changes for 2 minutes each
4. Stain with fast green (FCF) solution for 5 minutes
5. Rinse quickly with 1% acetic acid solution for no more than 10 – 15 seconds
6. Stain in 0.1% safranin O solution for 10 minutes
7. Dehydrate and clear with 95% ethanol, absolute ethanol and xylene, using 2 changes each, for 2 minutes each

Cleanup

Weigerts, Safranin O and Fast green are saved. Filter using funnel and filter paper back into their containers (Weigerts must be placed in used container as it comes separated and is mixed to activate). Acetic acid, ethanol and xylene washes are disposed of in respective labeled waste containers.

Tips

- Replace acetic acid wash every other round of staining. Replace first two ethanol washes after every round of staining.
- Trouble shooting
    - If slides still have stain on them, plunge slide holder up and down during the acetic acid wash and ethanol/xylene clearings
    - If samples are falling off, relax slides additional times before staining, review slicing methods – if slices are not smooth and uniform I have found they come off easier

Appendix E GAG Coverage Analysis Protocol

1. Open ImageJ
2. From the images folder, drag an image into ImageJ
3. Under the Process tab, click “Subtract Background”
4. Using the “Freehand Selection Tool” trace around the tissue
    a. Note: Leaving some white around the edges is ok
    b. Under the “Edit” tab click “Clear Outside”
        i. Rolling Ball Radius= 50 pixels
        ii. Check “Light background”
5. Under “File” click “Save As” then “Tiff” , save this image in its respective folder in Desktop> Images
    a. Label the image as _Trim
    b. Example: M20_LLA_Trim
6. If the Trim image is no longer open, open it and from the Image tab click “Color” then “Color Deconvolution”
    a. In the pop up menu, change H&E to “From ROI”, don’t check boxes, click “OK”
    b. In the “Color 1” pop up click “OK”
    c. Find the darkest red section on the tissue, draw a box around it without including any other colors, then right click to choose
    d. Again click OK and find the darkest blue section of the tissue, create box and right click
    e. Lastly create a box in the white background and right click
7. 3 images will pop up, delete Color 3, it’s not needed
    a. Save Color 2 Image as “FG” for Fast Green, then close window
        i. Example: M20_LLA_Trim_FG
    b. Save Color 1 as “SafO” for Safranin O, keep window open
        i. Example: M20_LLA_SafO
8. Have the Saf O image selected, then under the Image tab click “Adjust”, then “Threshold”
    a. Use the threshold tab to match the amount of red in the Saf O image to the Trim Image
    b. When accurate click apply
9. Under the Analyze tab click “Analyze Particles”
    a. In the Analyze Particles Tab, the Pixel size should be “0-infinity”, the circularity is 0.0 - 1.0, and show “Nothing”
        i. “Display Results”, “Clear Results” and “Summarize” should be checked off
    b. Click OK
10. Now select the Trim image, under the Image tab select “Type” then “8-bit”

    a. Now “Adjust” and “threshold” again, however this time you want to get as many red pixels on the WHOLE tissue as you can, without making the background color red as well
    b. Repeat step 9, and in the Analyze Particles tab check off “Pixel Units”
11. Record % Area Data in Excel sheet
12. Save analyzed Trim and SafO images as: M20_LLA_Trim_T and M20_LLA_SafO_R
13. Move completed sample files to _Processed

When a sample has two images:

1. Drag each image into ImageJ and complete steps 3 & 4 for each image
    a. Save images as M20_RMP_1_Trim etc.
2. While both images are still open go to Plugins>Stitching>deprecated>2D stitching
    a. For 1st reference image choose either “Sample_1_Trim” or “Sample_2_Trim”
    b. Choose the other image for 2nd register image
    c. Channel for 1st and 2nd should both be Red, Green, and Blue (RGB)
    d. Check use windowing and 5 peaks should be checked
    e. Check create merged image, method: linear blending, fusion alpha: 1.5, fusion image name can be whatever
    f. Check computer overlap, x:0 and y:0
    g. Click ok and remove any black area using clear outside function
3. Save image as M20_RMP_Combined
4. Proceed as normal, just note that images will be saved as Combined_FG instead of Trim_FG

Appendix F Promega TUNEL Protocol

NOTE: This SOP has been specifically tailored for **OCT embedded tissue sections**. This protocol will not work for paraffin embedded tissue sections or cell culture. See Promega protocol.

Material	Location
Promega TUNEL DeadEnd Kit	Small freezer in lab (bottom drawer)
Tissue Samples on slides	Small freezer in lab
1x PBS	Countertop
Propidium Iodide (PI) in PBS solution	15mL tube covered in foil in fridge
Proteinase K solution	Under fume hood
4% formaldehyde in 1x PBS	Under fume hood
2X SSC solution	Under fume hood
DI water	Counter top
Incubator	Counter top
Coplin jar	Histology supply cabinet (next to fume hood)
Cover slips	Histology supplies drawer
VectaShield	Black box in fridge
Pipettes	Counter top
Pipette tips	Counter top

Procedure	Time
1. Turn on Incubator to 37C and 0% CO2	
2. Wash slides in 1x PBS	5 min
3. Fix tissues in 4% formaldehyde in 1x PBS	15 min
4. Rinse in 1x PBS	5 min
5. Rinse in 1x PBS	5 min
6. Pipette 50uL of 20ug/mL of Proteinase K solution	2 min
7. Rinse in 1x PBS in Coplin jar	5 min
8. Fix tissues in 4% formaldehyde in 1x PBS	5 min
9. Rinse in 1x PBS	5 min
10. Tap off excess liquid	
11. Pipette 50uL Equilibration Buffer	10 min
MUST WORK WITH LIGHTS OFF FROM THIS STEP FORWARD	
12. Thaw Nucleotide Mix and rTdT on ice	
13. Create rTdT buffer solution:	
14. One rxn per slide	
15. Remove excess Equilibration Buffer	
16. Pipette 35uL of rTdT incubation buffer onto tissues	
17. Cover slide with glass cover slip and place incubator	1 hour
18. Carefully remove cover slip	
19. Pipette 50uL of 2X SSC to terminate rxn	15 min
20. Rinse in 1x PBS	5 min
21. Rinse in 1x PBS	5 min

22. Rinse in 1x PBS	5 min
23. Pipette 50uL of PI solution	10 min
24. Rinse in DI water	5 min
25. Rinse in DI water	5 min
26. Rinse in DI water	5 min
27. Add SMALL drop of VectaShield	
28. Image using Fluorescence Microscope	

Green fluorescence at 520±20nm (Apoptotic Cells)
Red fluorescence at >620nm (All cells)

Appendix G Cell Counting Protocol

1. Open FIJI ImageJ
2. Open both Live and Dead images of the same tissue
    a. Or Green and Red fluorescence for TUNEL, see note below
3. Stitch both images together
    a. Plugins → Stitching → Pairwise Stitching → OK on both pop up screens
4. Rotate image to make cropping easier
    a. Image → Transform → Rotate → Change angle and select preview box
5. Select the rectangle tool and enclose as much of the tissue as possible in the rectangle
6. Crop images
    a. Image → Crop
7. Save image as "FILE NAME_TRIM"
8. Filter image by color
    a. Image → Color → Split Channels
        i. For dead, keep red channel and save as "FILE NAME_TRIM_D"
        ii. For live, keep green channel and save as "FILE NAME_TRIM_L"
        iii. Delete blue channel image
9. Open original image "FILE NAME_TRIM" to use as reference for following steps
10. Convert both Images to 16 bit grayscale images
    a. Image → Type → 16-bit
11. Threshold Images to remove background noise
    a. Image → Adjust → Threshold
    b. There are two sliders:
        i. The bottom slider should be set to 255 (or max of the scale)
        ii. The top slider can be adjusted to remove as much background as possible while keeping most of the cells
    c. Hit "Apply", Image should now have white background with black dots (cells)
12. Identify cell size
    a. Using the "Circle" cursor, draw a circle around the smallest cell in the image
    b. Press "m" a new window should pop-up telling you the size (pixel^2) of the circle you drew, record for later use
13. Count cells
    a. Analyze → Analyze Particles
    b. In "Analyze Particles" window
        i. Change "Size (pixel^2)" to the size measured earlier to Infinity (ex. 55-Inifinity is what I most commonly use)
        ii. "Circularity" should be 0.00-1.00
        iii. "Outlines" to show all cells being counted
        iv. Check boxes "Clear Results". "Summarize", and "Add to Manager"
        v. Hit "OK"
14. Summary Window will pop-up, record the "Count" for the image
    a. Make sure the new image is counting the cells in your image
15. Repeat for other image (live or dead)

16. Cell Viability tracking
    a. In “Excel”
    b. Track sample name, # Dead, # Live, Total Cells (Live+Dead) and Percentage ((Live/Total)*100) in different columns

NOTE: For TUNEL

1. Green Image represents “Apoptotic Cells”
2. Red Image represents “All dead cells”
3. Percentage will track number of dead cells that died through apoptosis

Appendix H MTS Power Up and Warming Up Protocol

1) Turn on the monitor then the digital controller (Figure 1)
    a) The switch is on the back left of the FlexTest40

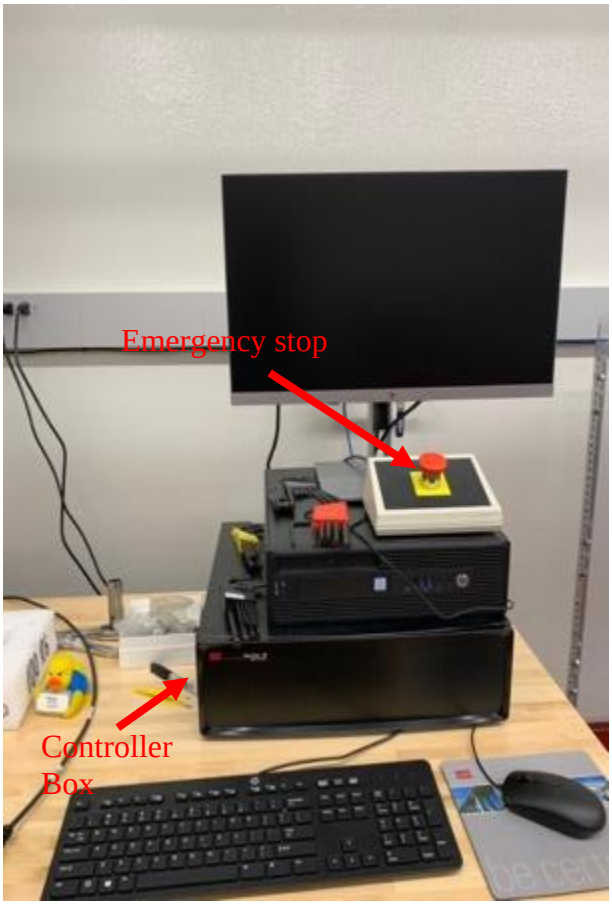

Figure 1. MTS Computer, Monitor and Controller Box set-up

2) Turn bottom right switch on front of MTS from “Turtle” mode to “Rabbit” mode (Figure 2)
    a) Switch should be glowing red now

Figure 2. Front switches of MTS. Left switch locks and unlocks crosshead. Middle switch moves crosshead up and down, when unlocked. Bottom right switch indicates turtle or rabbit mode. Large red button is emergency stop button.

3) Open “Station Manager” from Desktop
4) Open the normal configuration (10580179.cfg) and choose appropriate load cell from the menu on the bottom left of the pop-up window (Figure 3)

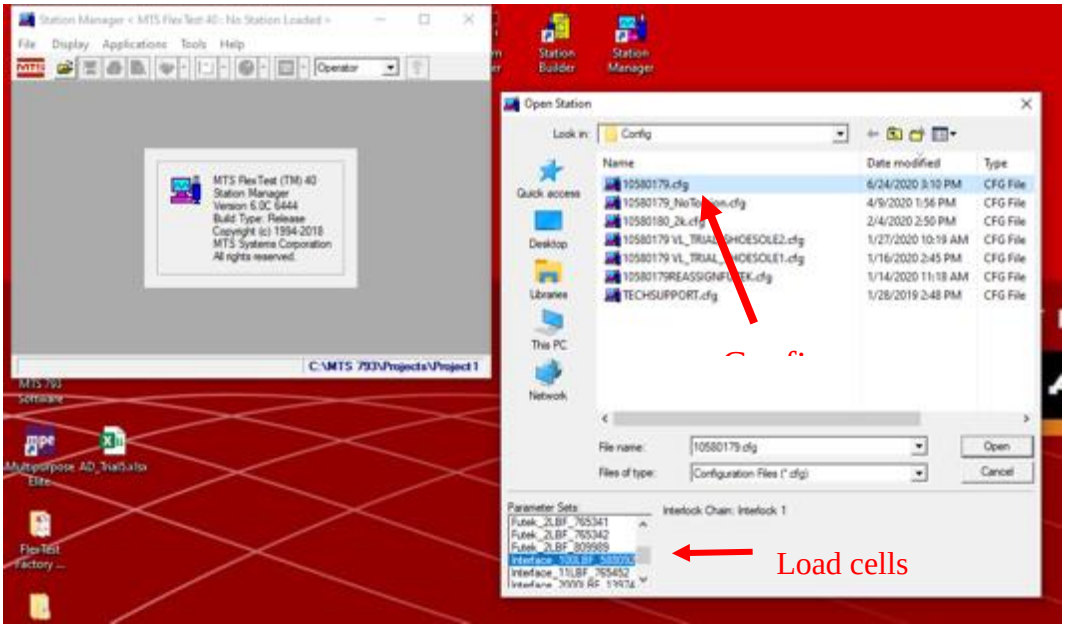

Figure 3. Selecting appropriate configuration and load cell for experiments

5) Interlock 1 will be red, make sure to reset (Figure 4)

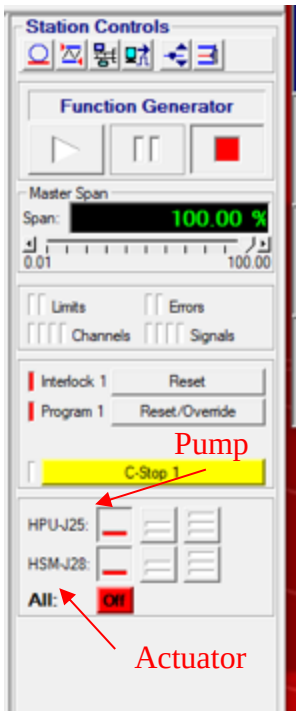

Figure 4. Left hand panel of Station Manager when opened.

6) Turn on the hydraulic pump (HPU-J25) by clicking the buttons with the levels
    a) It is important to go in order of Level 1, 2, and 3. Make sure the previous level glows yellow before moving on to the next level (Figure 4)
7) Repeat similar process as Step 6 for the actuator (HSM-J28) (Figure 4)
8) Move actuator to 0 using manual control, turn off manual control (Figure 5)
    a) Make sure to turn off manual control after using each time

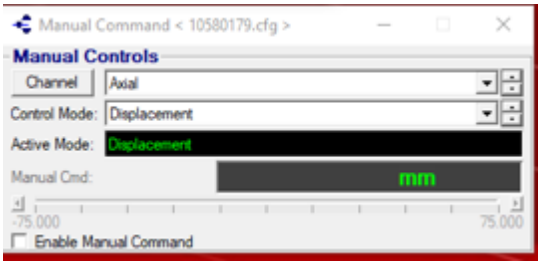

Figure 5. Manual Command window. When "Enabled" is on, user can manually move actuator up and down using "Axial Displacement" or spin using "Torsion"

9) To warm-up the machine, in Function Generator (top left) (Figure 6), create a warmup using an amplitude similar to that being used in the real test and at 1 Hz for 10 minutes
    a) Wave shape: Sine
    b) Compensator: None

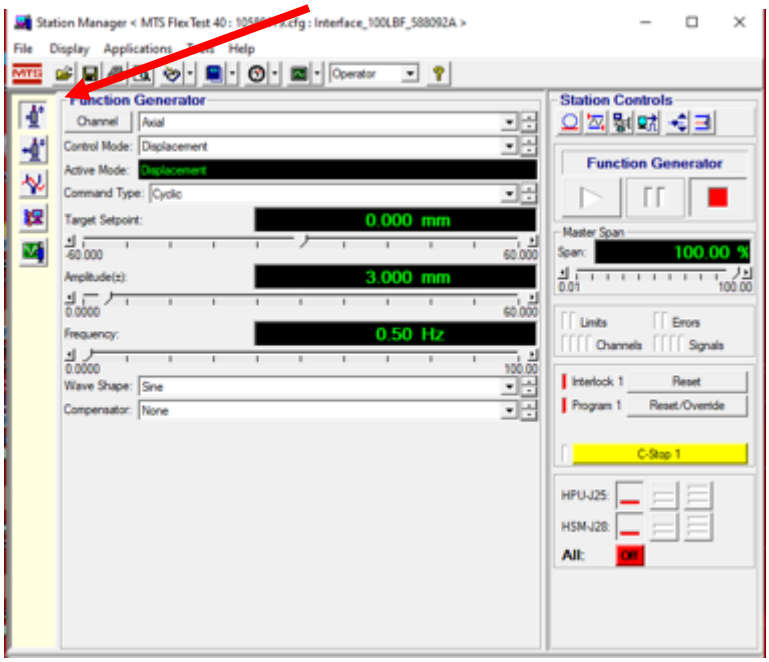

Figure 6. Function Generator screen to warm-up MTS

10) Press play button to start the warmup
11) Redo warmup using half the previous amplitude and frequency, again for 10 minutes
12) After roughly 20 minutes, warm-up is complete
13) Switch to MPT (Dog Bone Icon with Computer on Station Manager) and open the appropriate program for test being run

Appendix I Meniscus Indentation – Relaxation using MTS Protocol

Steps for Setting up Fixture on MTS

1. Attach X-Y plate adapter to lower load cell
2. Attach X-Y plate to X-Y plate adapter (smaller bolts 4)
3. Attach Camera Mount to Camera Mount Adapter Plate
4. Attach Camera Mount Adapter Plate to X-Y Plate (larger bolts 4)
5. Attach Water Bath Adapter Plate to Camera Mount
6. Attach Water Bath to Water Bath Adapter Plate

Figure 1. Lower Set Up for Indentation Testing

7. Attach 2 and 10 lb. Adapter Plate to the actuator
    a. Follow tightening instructions on coupler
8. Attach Adapter Block for 2lb. Load Cell

Set-up MTS Software and Warm-Up Machine

1. Refer to MTS Power-Up and MTS Warm-Up Protocols for these steps

Steps for Specimen Preparation

1) Lay out ½ Drop Cloth, Gauze, Test Tubes, Test Tube Rack, Disposable Pipets, Low Temp Freeze Vials, Tape, Marker, Camera on dissection table
2) Put roughly 3mL of 1x PBS in 12 15mL conical tubes
    a) Label the screw cap of each tube LLA, LLC, LLP, LMA, LMC, LMP, etc.

3) Remove specimens from packaging
4) Label Drop cloth with specimen name, limb, and hemijoint
5) Take photos of meniscal tissue as received laid by label
6) Using tweezers and scalpel remove excess synovial tissue
7) Take another photo of specimen
    a) Be sure to highlight any damage
    b) May need to take a photo of back few if damage is extensive
        i) Be sure to re-label if necessary
8) Section menisci
    a) Can do all sectioning at once or as you go – doing all at once is easier
    b) Will need anterior, central, and posterior regions for both lateral and medial
    c) Lateral posterior is a more ligamentous attachment so be sure to leave meniscal tissue when sectioning

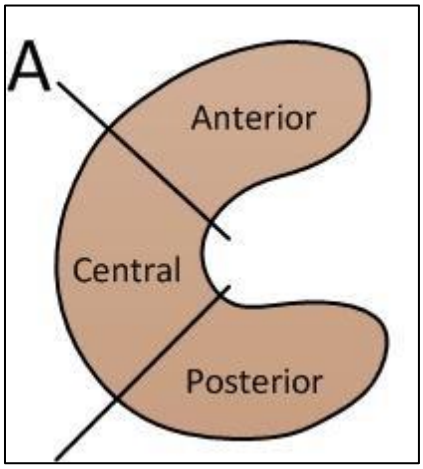

Figure 3. Meniscal Sectioning

9) Repeat for both joints
10) Place specimens in respective conical tube and put in ice until testing

Testing

1) Stop warm-up and switch to MPT
2) Be sure Procedure is set to "DOD_Indentation" can be found in Procedures → Gerardo
3) Attach 2lb. Load Cell
    a) Take note of how the load cell cable is attached to MTS
        i) When removing take special care
            (1) Hold square part of cable adjustments steady
            (2) Turn cylindrical part clockwise
4) Attach Load Cell to Indenter Adapter
5) Attach Indenter Tip (Just leave sitting beside if setting up a day early)
    a) NOTE: Do NOT run warm-up with indenter tip attached

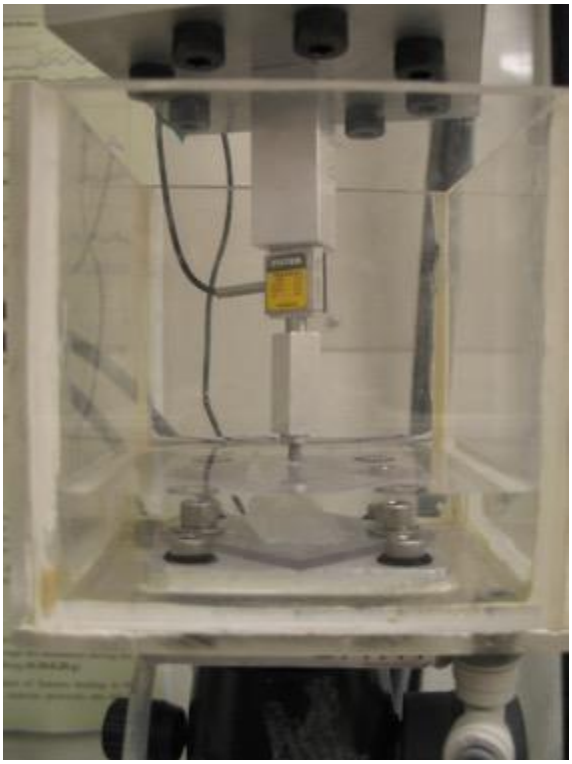

Figure 2. Upper Set Up for Indentation Testing (note this image was during testing and thus includes the wedge mount with specimen attached)

6) Clean wedge using razor blade to scrape off left over glue remnants
7) Place small amount of super glue on wedge mount
8) Place Specimen near top edge trying to get specimen face as "flat" as possible
9) Attach wedge to water bath
10) Fill water bath with PBS
    a) Be sure valve is closed
    b) Fill slightly over wedge but not far enough over that PBS will come in contact with nut on indenter when testing
11) Adjust crosshead so specimen will not bottom out if hydraulics are lost
12) Create new Specimen
    a) Label Ex. "BBGB4_LLA" , HIT ENTER
        (a) ****Very important to label this way when using my MATLab code to process
13) Lower indenter tip till just in water
14) Adjust X-Y plate to get specimen perpendicular to inventor tip and indenter tip is located over thickest part of specimen
15) Lower indenter tip till just above specimen
16) Zero out Axial Force 2
17) Apply 20mN force to specimen
18) Disable manual controls
19) Run ("Play")

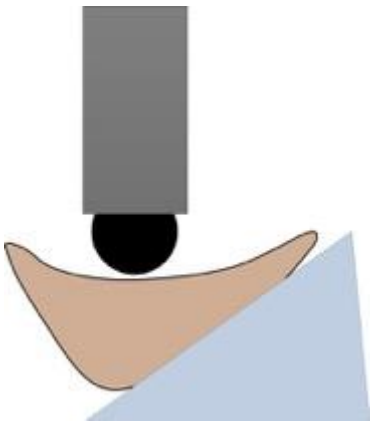

Figure 4. Indentation Alignment

Test Done – Specimen Removal

1. Create new Specimen
2. Manually enable controls
3. Raise up actuator
4. Remove wedge mount
5. Using razorblade carefully remove specimen
    a. Will need to remove all superglue
        i. If care is taken you can "pop" off specimen with razor bade
        ii. Alternatively once off wedge, can use scalpel to scrape off leftover superglue
6. Place specimen in corresponding PBS filled test tube
7. Repeat Testing for all samples

All Testing Done – Shut Down

1. Be sure when hydraulics are turned off and actuator drops to -50mm it would hit anything
    a. Adjust crosshead if necessary
2. Disable Hydraulics
    a. HSM1 & HPU Off
3. Close Station Manager
4. Turn off controller and record Pump Time
5. Create Folder in "Specimens" file found on desktop for animal(s) tested that day
    a. Label Ex. "BBGB4"
6. Move folder from "Specimens" into "TH Donahue" → "Gerardo"

Appendix J Bruker Skyscan 1276 µCT - Scanning Protocol

Note - This protocol is intended for Flemish giant rabbit femurs and tibias. Depending on sample being scanned, different voxel size may need to be used.

1) Log in to the computer, the password is **brukerct**

2) Open Skyscan 1276 software and click the radiation button
    a) The machine takes 15 minutes to warm-up

3) Insert parameters on the bottom left of the screen
    a) Al-Cu filter
    b) 2016x1344

4) Load Std Res file by opening Options, configurations, load, std

5) Turn off x-ray to open scanning bed and insert the first sample, create a folder with sample name

6) In Actions menu, press Scout + batch scan, can press cancel once past area of interest

7) Click on Grab button (TV icon) then double click on the sample on the scout screen to the left

8) Right-click in the main window, make sure min transmission is about 30%
    a) If not, can increase voltage and current in Scanning Modes page

9) Go up to roughly y=0 by double-clicking on scout screen and turn flat field off by double-clicking ff icon

10) Press Shift-Alt-Ctrl-S to unlock modes

11) Under the Options menu, select Scanning Modes
    a) Change exposure for correct parameters to bring average transmission to 60%

12) Turn flat field back on and update the flat field in the options menu

13) Redo Scout and Batch scan, can cancel once past sample
    a) If the scout scan appears very white, it is because the hi-res setting was loaded
        i) Go to the options menu, click on load and select std res file
        ii) Check to make sure parameters and transmissions are correct

14) Control-click and drag from just above bone to just below the bone

15) Add to oversized batch, insert correct name and file location

a) Select X-ray off after scanning and 360 Scanning

16) Start Scan

17) Once complete, delete the previous scan from batch and oversize scanning window

18) Remove sample from scanning bed and mark as scanned

19) Repeat, there is no need to change any parameters unless rebooting software or someone changed them between uses.

Appendix K Bruker NRecon - Reconstruction Protocol

1) Open NRecon software, click action and open desired dataset

2) Click and open an image with a number in the name (Just not one of the first 5 or so)

3) Drag outer limits (red lines on the screen) to just above and below the sample, drag center line to the primary area of interest

4) On settings tab to the right, change misalignment compensation to 0

5) On start tab, click fine-tuning
   a) Post alignment
   b) 5 Trials
   c) 1.0 Step

6) Fine-tune, then find the clearest image
   a) Scroll through the five new trials (-2, -1, 0, 1, 2), the clearest of the five will be your new reference image

7) In output tab, change min to 0 and max to .027
   a) This number is for Flemish Giant rabbit bones for the DOD study, for different studies, it is crucial to use the same numbers for your scale

8) Fine-tune again with same parameters, again finding the clearest image and add it to batch on the start tab

9) If running multiple samples in one large batch, select “Add to Batch” and then open a new sample to reconstruct and repeat steps 1 - 8
   a) If not running in a batch, select “Start”

10) Once all desired samples are added, start the batch

Appendix L Bruker CTAn – Trabecular Bone Analysis Protocol

Note – this protocol is intended for the Flemish Giant rabbit femurs and tibias in the DOD project (2017-2021). Steps may need to be changed to suit different study needs.

1) In original sample folder (outside of the Reconstruction folder) create five new folders
   a) VOI
   b) Lateral_Uncovered
   c) Lateral_Covered
   d) Medial_Uncovered
   e) Medial_Covered
   f) These folders will be used later to save images/data

2) Open reconstructed file in DataViewer Software

3) In DataViewer, select "Allow Projections in 3D Viewing"

4) Holding SHIFT, reorient bone so that is it parallel
   a) Let the software re-orient, takes a few seconds

5) Select the Volume of Interest (VOI)
   a) Actions → Draw/Save Multiple Volume of Interest(VOI)

6) Blue boxes will show up in all three different views
   a) Resize the highlighted box to fit the VOI
   b) Top: Small space above tallest point of bone
   c) Bottom: Small space below the growth plate (physeal scar)

7) Move scale bar through depth of tissue to ensure area between top of bone and growth plate are within the box

8) In DataViewer Software, save the VOI into the "VOI" folder created in Step 1
   a) Make sure to save top down view (might be coronal or transverse depending on scan orientation)

9) Open the newly saved VOI in CTAn

10) Scroll through the "Raw Images" and find the Image that shows the full tibia with cortical bone

11) Set this as your top image
   a) Right click on the Z-Position → "Set the Top of Selection"
   b) RECORD this number on the Google Doc titled "CTAn Bone Tracking"

12) Find and set the bottom image

a) We will be imaging 90 slices from the top to bottom (~2mm depth)
b) Add or Subtract 90 from the Top Image Z-position
    i) Add if orientated tibial plateau down
    ii) Subtract if orientated tibial plateau up

13) Select "Regions of Interest Preview" tab

14) Create box to determine center of ROI*

Femur	**Tibia**
Lateral Uncovered:	*Lateral Uncovered:*
Width - 340, Height - 321	Width - 162, Height - 240
Lateral Covered:	*Lateral Covered:*
Width - 212, Height - 218	Width - 181, Height - 77
Medial Uncovered:	*Medial Uncovered:*
Width - 215, Height - 358	Width - 205, Height - 310
Medial Covered:	*Medial Covered:*
Width - 187, Height - 223	Width - 201, Height - 121

*All values converted to Pixels, if interested in mm, multiply pixel size by voxel size (0.020mm or 20um)

Femur

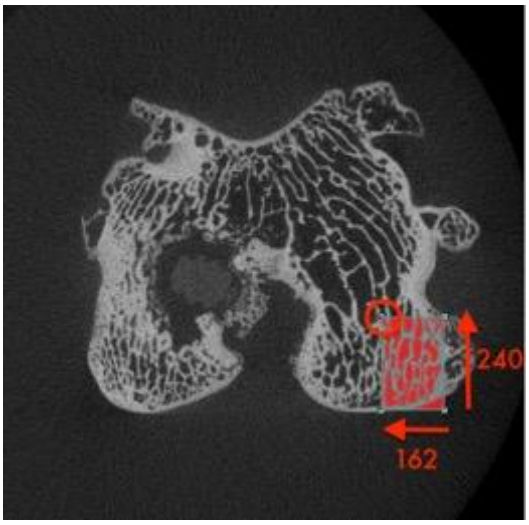

Tibia

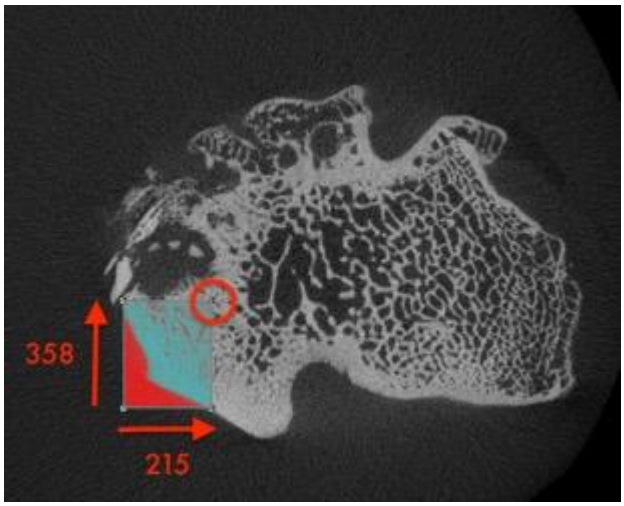

15) Align the edges of the box with cortical bone image
    a) See picture to determine placement

16) Determine coordinate of corner
    a) RECORD x and y values in "CTAn Bone Tracking"
    b) Select "Measure angle, distance or path" → "Coordinate" → Click on corner of interest on the ROI box → Write down
    c) CTAn Bone Tracking will automatically convert mm (given) to pixel

i) If interested, 1mm = 50 pixels, so multiply coordinate number by 50

17) Repeat steps 14-16 for the remaining three ROIs
    a) Change dimensions of box for next ROI

18) Once all coordinates have been determined, create a circle shaped ROI
    a) Width - 80, Height - 80
    b) 80 pixels corresponds to 1.6mm diameter, the same size as the indenter tip used to determine the mechanical properties of articular cartilage at MSU

19) Using known coordinates for the locations of interest, change the center of the circle ROI to one of the four locations

20) Once the circle ROI is on the right location, select "Save new Dataset from ROI" in its appropriate folder created in Step 1
    a) Save Images from ROI window → Location → Browse → Select appropriate folder

21) "Binary Selection Preview" tab
    a) This will create the data into black and white images in order to analyze

22) Threshold the data
    a) Histogram tab → select "Automatic Thresholding"

23) Start Analyzing - "Morphometry preview" tab
    a) Analysis tab → "3D" analysis
    b) Save data
    c) 3D analysis tab
        i) Check:
            (1) Basic Values
            (2) Additional Values
            (3) Structure Model Index
            (4) Trabecular Thickness
            (5) Trabecular Separation
    d) Continue
    e) Save the text file in appropriate folder

24) Repeat Steps 19-23 for remaining three locations

Appendix M Bruker CTAn – Cortical Bone Analysis Protocol

Note – this protocol is intended for the Flemish Giant rabbit femurs and tibias in the DOD project (2017-2021). Steps may need to be changed to suit different study needs.

1) Create a “Lateral Cortical” and “Medial Cortical” folder within the main folder of the bone being analyzed

2) Open cortical VOI of desired bone in CTAn

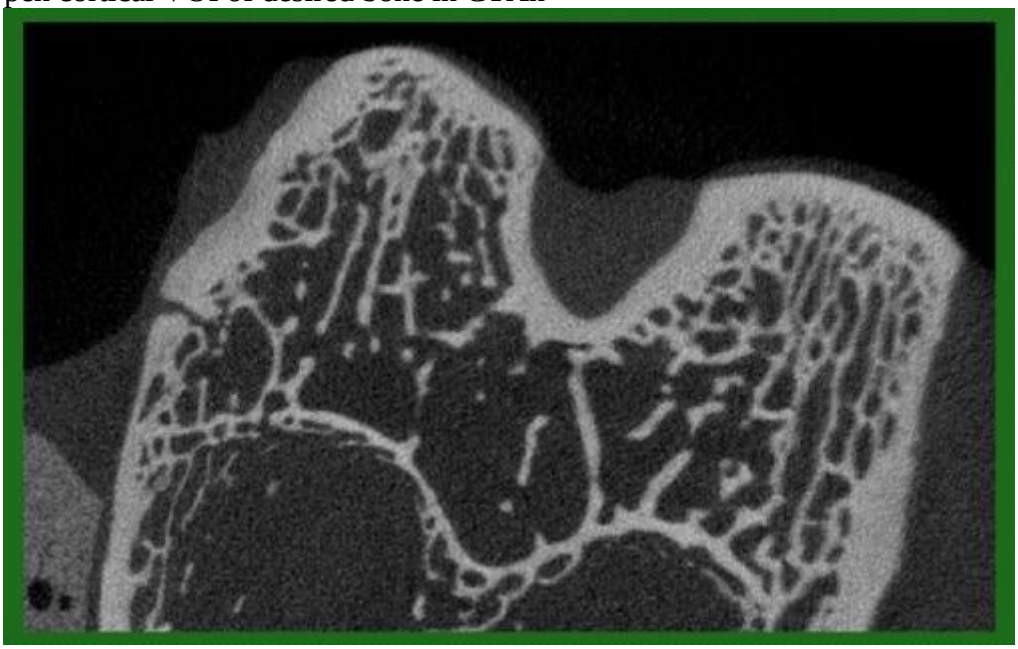

3) Choose a 50 slice chunk in the middle of the bone and set upper and lower bounds

4) On the same slice, take 5 thickness measurements from the middle of both lateral and medial condyles. Enter into the spreadsheet.

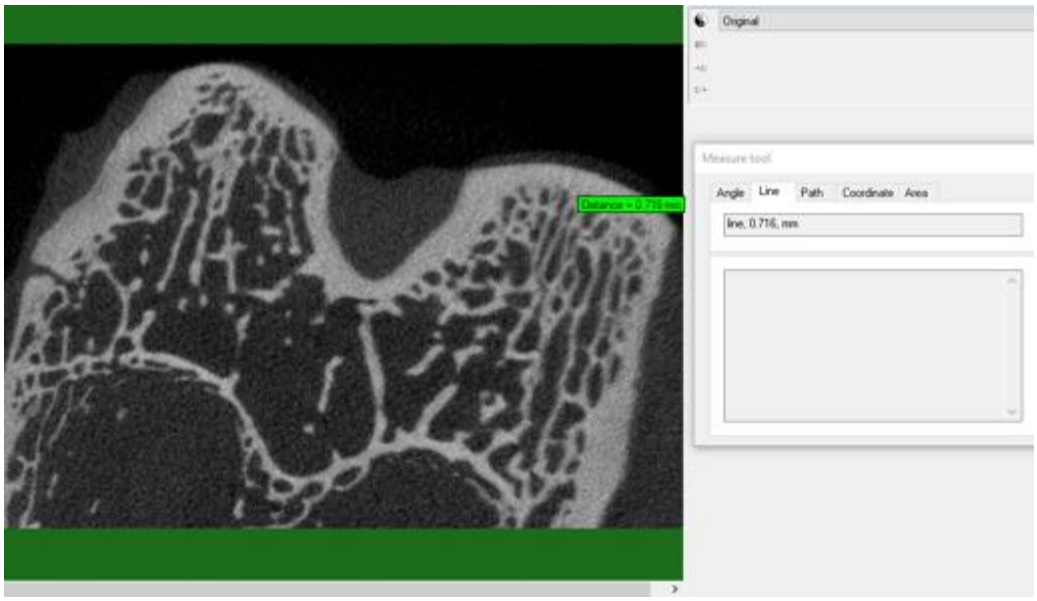

5) At the top of the selected VOI, create a rectangular ROI on the cortical bone of either condyle. Edit ROI every 10 slices through entire VOI

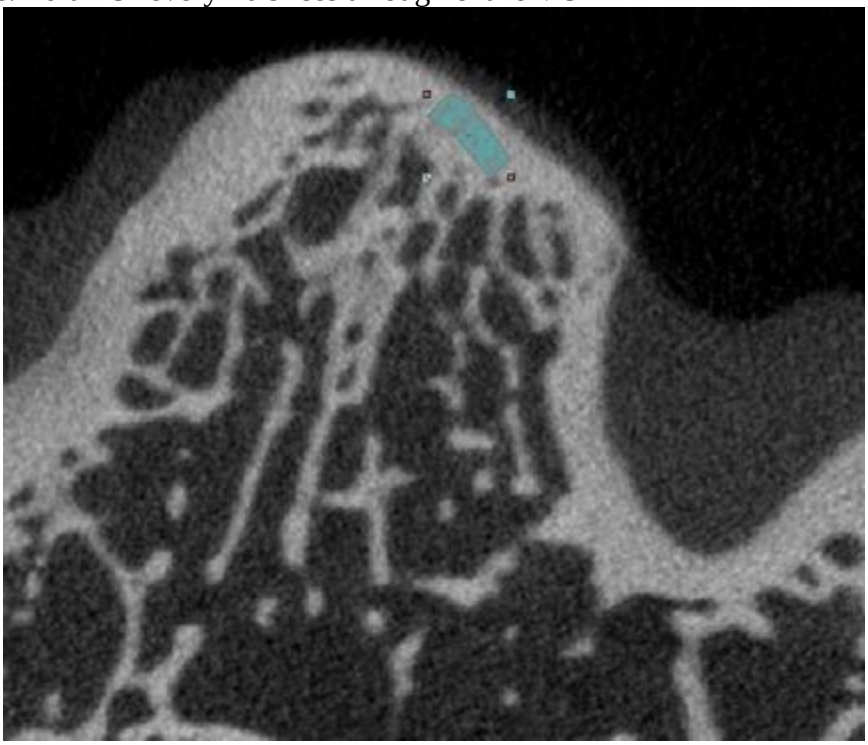

6) In binary selection, match up as best as possible with the raw image. Save histogram with vBMD in the appropriate folder

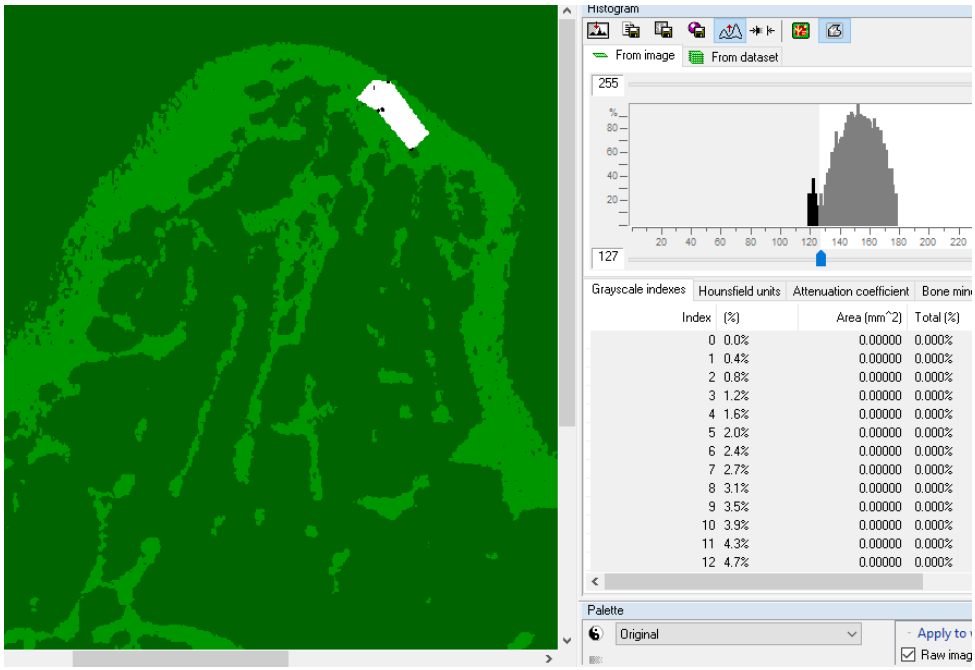

7) Run the 3D analysis, making sure porosity is selected from the additional values. Save resulting file in the appropriate folder

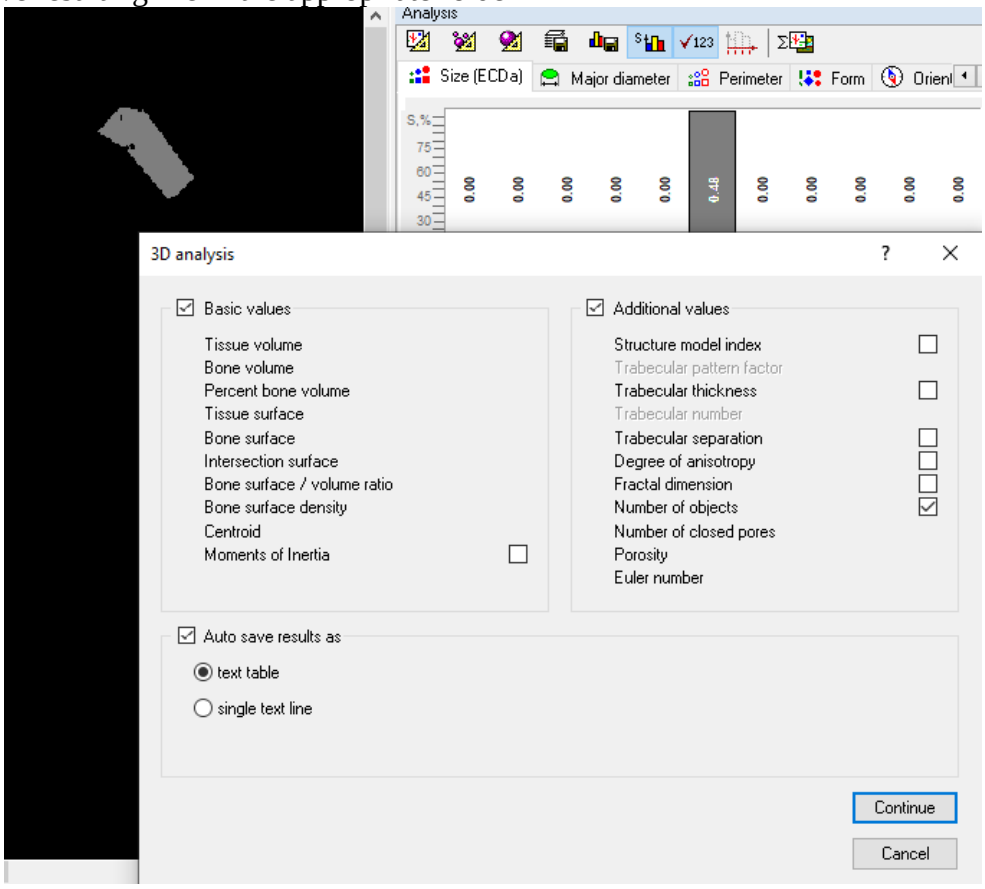

8) Repeat steps 5-7 for the remaining condyle.

Appendix N Bruker CTAn – Osteophyte Bone Volume Analysis Protocol

Note – this protocol is intended for the Flemish Giant rabbit femurs and tibias in the DOD project (2017-2021). Steps may need to be changed to suit different study needs.

Useful Controls:

Command	**Action**
Shift + Right-Click	Adds area to ROI
Shift + Left-Click	Creates new ROI, will delete any existing ROI on the slice
Cntrl + Right-Click	Deletes any selected area from ROI

1) Open Trabecular VOI folder of desired bone in CTAn

2) Starting from the top of the scan (condyles), go down 10 mm or 500 slices and set top and bottom of VOI

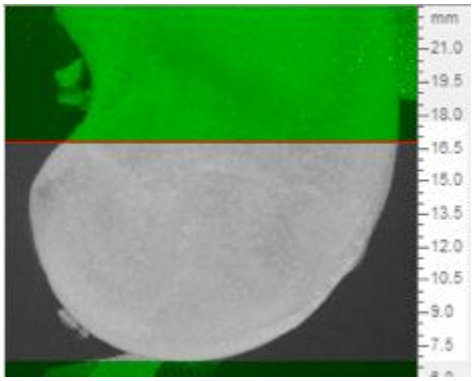

3) Go down to the bottom of the selection (shaft) and begin highlighting all bone and osteophyte while leaving out any of the greyish potting material.

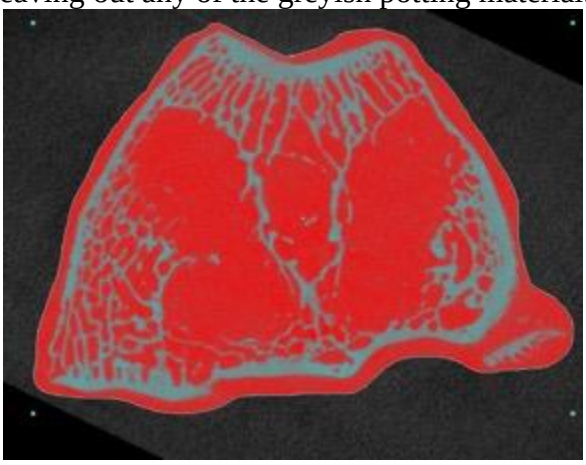

4) Edit this VOI every 50 slices

5) Once done, save this VOI in the “osteophyte” folder and open VOI in CTAn

6) Create another VOI but this time only highlight the actual bone and none of the osteophyte tissue

7) Edit this VOI every 10 slices

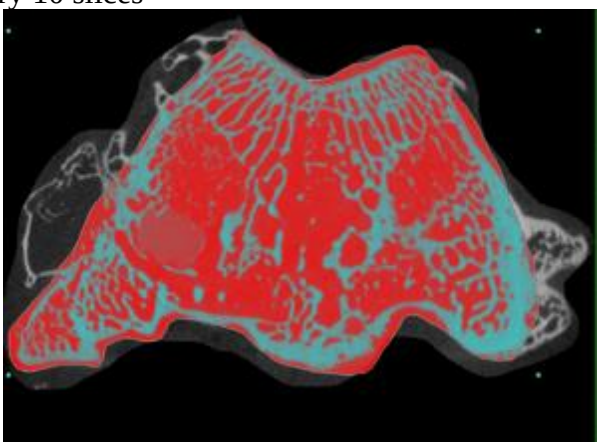

8) Once done, select the subtractive VOI bottom

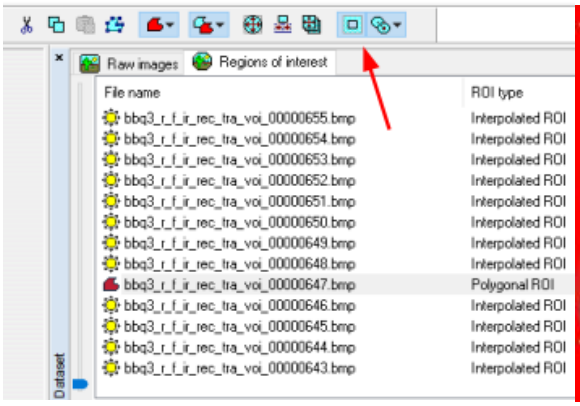

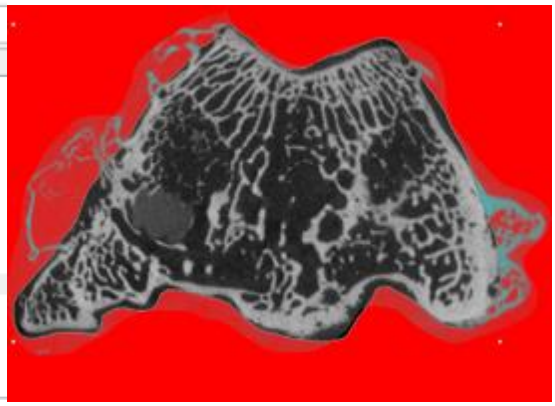

9) Select binary projection and match up as much as possible with the raw image

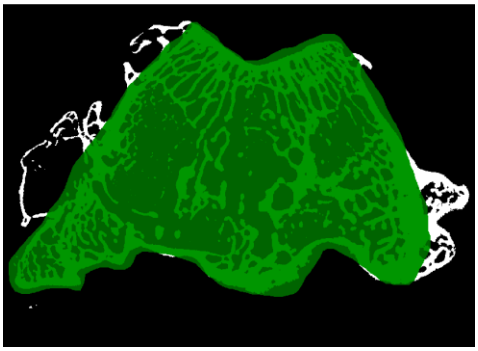

10) Click on 3D analysis, and unselect all but basic values

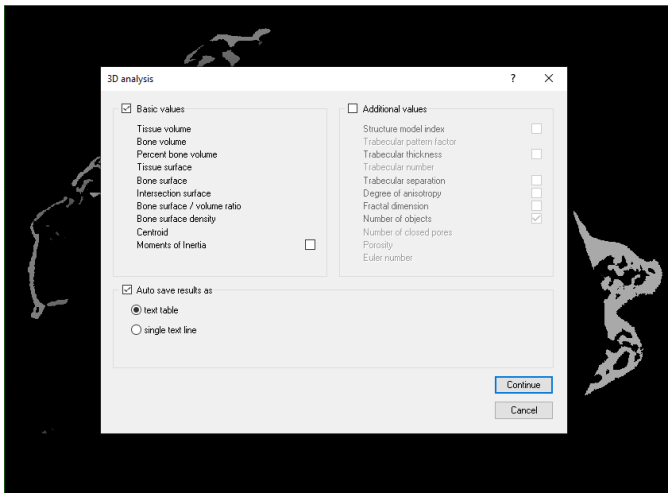

11) Take Bone Volume value and input it into the spreadsheet

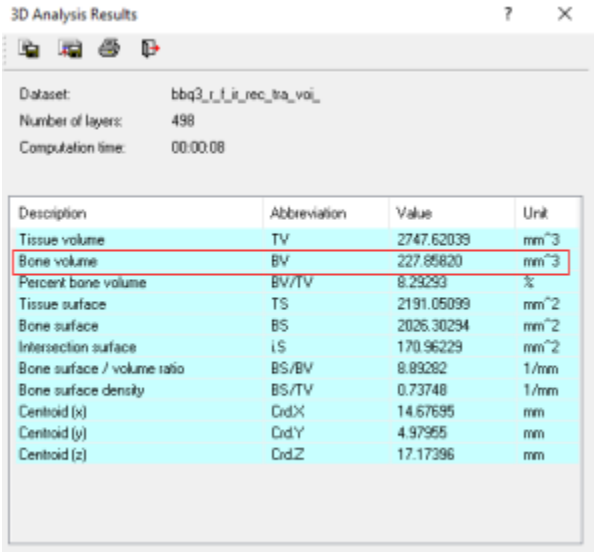

Appendix O CaptureSelect Multispecies Albumin Depletion Protocol

1. Thaw synovial fluid sample on ice (~30 minutes)
2. While sample thaws, prep depletion spin column
3. Load 200uL of CaptureSelect Multispecies Albumin depletion product into spin column
4. Wash and hydrate the resin by loading 500uL of 1x PBS
5. Remove the twist off tip at the bottom of spin column and place in an empty 2mL capture tube
6. Centrifuge at 3000 rpm (700 xg) for 1 minute
7. Discard flow through PBS
8. Repeat steps 4-7 two more times
9. Once sample is thawed, load 200uL of sample into the depletion spin column
10. Move depletion spin column into a new 2mL conical tube
11. Incubate for 20 minutes and vortex every few minutes
12. Collect flow through by centrifuging spin column at 3000 rpm for 1 minute
13. Rinse spin column with 100 uL of 1x PBS, centrifuge at 3000 rpm for 1 minute and collect flow through in the same tube
14. Repeat step 13 two more times
15. Sample is ready for further steps

Appendix P Preliminary Synovial Fluid Work

First Run – High Select MARS-14 Mini Spin Columns

The first attempt of performing proteomic analysis of the synovial fluid used the High Select Top 14 Abundant Protein Depletion Mini Columns from Thermo Fisher (A36369). Unfortunately, these samples were run prepared with chemicals and laboratory equipment (i.e. pipette tips, conical tubes, plastic ware) that were not graded to be used for mass spectrometry. This led to large plastic contamination.

The initial volume of 10uL of raw samples was too small to begin with, by the end of the sample preparation process, samples had very low protein concentrations. These low concentrations made the issue of plastic contamination much more severe and which greatly affected the proteins found using mass spec. Due to the COVID-19 pandemic, there was a six-month period in which no new trials for proteomic analysis were conducted (February 2020 to August 2020).

Synovial Fluid Sample Prep – Run 1 SOP

Determine Protein Concentration – BCA Assay

1. Prepare standards and working reagent for the Micro BCA Protein Assay Kit prior to starting the rest of protocol
2. Thaw samples to room temp
3. Transfer SF to 1.5mL tube and centrifuge at 2000 rpm for 10 min and keep supernatant
4. While samples are in the centrifuge, load 150 uL (in duplicate) of each standard into a 96 well plate
5. Remove samples from centrifuge and move supernatant to a new -80 tube
6. Load 150uL of sample (in duplicate) into 96 well plate – record which well each sample is loaded onto
7. Put samples in fridge until Step 2 (page 2)
8. Add 150uL of working reagent to each well and mix plate on shaker plate for 30 seconds
9. Cover plate with parafilm and incubate at 37C for 2 hours
10. While plate incubates, prepare plate reader (located in microscopy room) by loading the Micro BCA Assay Protocol

11. In SpectraMax Software, label plate with appropriate labels for wells containing sample
12. Following incubation, cool plate to room temperature
13. Measure the absorbance of the plate at 562nm
14. Subtract the average 562nm absorbance reading from the Blank standard replicates from the 562nm reading of all other individual standard and unknown sample replicates
15. Prepare a standard curve by plotting the average corrected reading for each BSA standard vs its concentration in ug/mL.
16. Use the standard curve to determine the protein concentration of each unknown sample.

Mini Spin Column Methods

1. Thaw samples to room temp.
2. Centrifuge SF sample at 2000 rpm for 10 min and keep supernatant.
3. Run SF through MARS-14 mini spin column to deplete top 14 abundant proteins
    a. Equilibrate the depletion spin column to room temperature.
    b. Remove the column screw cap and add 10µL of SF directly to the resin slurry in the column.
    c. Cap the column and invert the column several times until the resin is completely suspended in the solution.
    d. Incubate the mixture in the column with gentle end-over-end mixing for 60 minutes at room temperature.
    e. Make sure the sample mixes with the resin during the incubation period. Alternatively, vortex every 5 minutes.
    f. Twist off the bottom closure and loosen the cap.
    g. Place column into a 2mL collection tube and centrifuge at 1000 × g for 2 minutes.
    h. Discard the column containing the resin.

Methods for Alkylation and Reduction

1. Add 15µL of Digestion Buffer and 1.5µL of Reducing Buffer to a 0.5mL microcentrifuge tube.
2. Add ≤ 10.5µL of SF to the tube and adjust the final volume to 27µL with ultrapure water.
3. Incubate sample at 95°C for 5 minutes and allow to cool.
4. Prepare alkylation buffer.
5. Add 9mg of Iodoacetamide (IAA) to a foil wrapped tube.
6. Add 500µL of ultrapure water to the IAA. (conc ~100mM)
7. Add 3µL of Alkylation Buffer to the tube and incubate in the dark at room temperature for 20 minutes.

Methods for In-Solution Trypsin Digestion

1. Prepare activated trypsin.
2. Create Trypsin Stock.

    a. Add 20µL of Trypsin Storage Solution to the vial containing lyophilized Trypsin Protease.
    b. Divide solution into four separate tubes with ~5µL each.
    c. Store at -20°C.
3. Thaw a Trypsin Stock aliquot on ice.
4. Dilute stock 10-fold by adding 45µL of ultrapure water for a final concentration of ~100ng/µL). Store this solution at -20°C for up to two months.
5. Add 1µL of Activated Trypsin to the reaction tube and incubate at 37°C for 3 hours.
6. Add an additional 1µL of Activated Trypsin to the reaction tube and incubate at 37°C for 2 hours.

Methods for Guanidination

1. The digested sample may be divided at this time to provide a no guanidination control, or the entire digest may be guanidinated.
2. To divide digest, place 16µL of the digest to a new tube and label as no guanidination control.
3. To the remaining digest add 16µL of ultrapure water.
4. Add 10µL of Ammonium Hydroxide to the digest and vortex to mix well.
5. Create Guanidination Reagent.
    a. Dissolve 50mg of *O*-Methlyisourea hemisulfate in 51µL of ultrapure water.
    b. Final volume will be ~80µL.
    c. Store excess at -20°C.
6. Add 6µL of Guanidination Reagent and vortex to mix well.
7. Incubate sample at 65°C for 12 minutes.
8. Add 3µL of Trifluoroacetic acid to stop reaction, or proceed directly to sample preparation appropriate for downstream analysis.
9. The stopped rxn may be stored at -20°C for an extended period.

Methods for Cleaning Samples

1. Prepare conditioning/washing solution by adding 2µL of TFA to 2mL of ultrapure water
2. Prepare the elution solution by combining 2µL of TFA, 1mL of water, and 1mL acetonitrile in a tube
3. Prepare TMT washing solution by adding 50µL of methanol and 1µL of TFA to 950µL of ultrapure water and mix
4. Remove white tip from the bottom column and discard
5. Place column in 2mL microcentrifuge tube and centrifuge at 5,000g for 1 min and discard liquid
6. Remove top screw cap and add 300µL ACN and replace cap
7. Centrifuge at 5,000g for 1 min in 2mL microcentrifuge tube
8. Discard ACN and repeat wash step
9. Wash spin column twice with 0.1% TFA in water as described in steps 6-8
10. Dissolve 5µg of sample in 300µL of 0.1% TFA in water

11. Place in 2mL microcentrifuge tube and load 300µL of the sample in solution.
12. Replace cap, centrifuge at 3,000g for 1 min, and discard flow through
13. Load 300µL 0.1% TFA in water into column and centrifuge at 3,000g for 1 min
14. Discard eluate and repeat this step 2 more times
15. Wash column with 300µL of TMT washing solution twice as described in step 13
16. Place column in new 2mL microcentrifuge tube, load 300µL of elution solution, and centrifuge at 3,000g for 1 min
17. Add another 300µL of elution solution and centrifuge at 3,000g for 1 min
18. Evaporate the liquid contents of each sample tube to dryness using vacuum centrifugation

Second Run – High Select MARS-14 Midi Spin Columns

The second attempt of performing proteomic analysis of the synovial fluid used the High Select Top 14 Abundant Protein Depletion Midi Spin Columns from Thermo Fisher (A36371). For this trial, mass spectrometry grade reagents, chemicals, and plastic ware were used to decrease the number of plastic contaminants in the samples. Midi spin columns were used for this step, in order to increase the initial amount of raw sample used from 10uL to 100uL. Following the advice from the UMass Mass Spec CORE Facility, two extra washing steps were included in the desalting column prep prior to samples being loaded to ensure any plastic contaminants from these tubes were not also affecting our outcomes.

During this trial, there were low amounts of plastic contaminants found in the samples. However, large amounts of proteins that were supposed to be depleted by the spin column were still present. This indicated that the spin column was not ideal to be used for rabbit samples.

Synovial Fluid Sample Prep – Run 2

All steps from Run 1 were similar, except for the use of the Midi Spin Column instead of the Mini Spin Columns and the Guanidinatio step was skipped.

Methods for Depletion – Midi Spin Column

1. Thaw samples to room temp.
2. Centrifuge SF sample at 2000 rpm for 10 min and keep supernatant.
3. Run SF through MARS-14 midi spin column to deplete top 14 abundant proteins
    a. Equilibrate the depletion spin column to room temperature.
    b. Remove the column screw cap and add 100µL of SF directly to the resin slurry in the column.
    c. Cap the column and invert the column several times until the resin is completely suspended in the solution.

d. Incubate the mixture in the column with gentle end-over-end mixing for 60 minutes at room temperature.
e. Make sure the sample mixes with the resin during the incubation period. Alternatively, vortex every 5 minutes.
f. Twist off the bottom closure and loosen the cap.
g. Place column into a 15mL collection tube and centrifuge at 1000 × g for 2 minutes.
h. Discard the column containing the resin.

Methods for Cleaning Samples

1. Prepare conditioning/washing solution by adding 2µL of TFA to 2mL of ultrapure water
2. Prepare the elution solution by combining 2µL of TFA, 1mL of water, and 1mL acetonitrile in a tube
3. Prepare TMT washing solution by adding 50µL of methanol and 1µL of TFA to 950µL of ultrapure water and mix
4. Remove white tip from the bottom column and discard
5. Place column in 2mL microcentrifuge tube and centrifuge at 5,000g for 1 min and discard liquid
6. Remove top screw cap and add 300µL ACN and replace cap
7. Centrifuge at 5,000g for 1 min in 2mL microcentrifuge tube
8. Discard ACN and repeat wash step
9. Wash spin column twice with 0.1% TFA in water as described in steps 6-8
10. Dissolve 5µg of sample in 300µL of 0.1% TFA in water
11. Place in 2mL microcentrifuge tube and load 300µL of the sample in solution.
12. Replace cap, centrifuge at 3,000g for 1 min, and discard flow through
13. Load 300µL 0.1% TFA in water into column and centrifuge at 3,000g for 1 min
14. Discard eluate and repeat this step 2 more times
15. Wash column with 300µL of TMT washing solution twice as described in step 13
16. Place column in new 2mL microcentrifuge tube, load 300µL of elution solution, and centrifuge at 3,000g for 1 min
17. Add another 300µL of elution solution and centrifuge at 3,000g for 1 min
18. Evaporate the liquid contents of each sample tube to dryness using vacuum centrifugation

Third Run – Albumin Depletion Product and Tandem Mass Target Labeling

For the third attempt, a MultiSpecies Albumin Depletion product (191085310) from Thermo Fisher was used along with Tandem Mass Target labeling. The manufacturer suggested this product as previous clients had used it to remove albumin from rabbit samples. Since the end goal was to quantify and receive a ratio of proteins expressed between the treated (right) and control (left) limbs, samples were labeled for Tandem Mass Target (TMT).

The outcomes of this trial showed that the albumin depletion product was successful in removing large amounts of the protein in the samples. Unfortunately, the desalting columns used for this run were not compatible with the TMT labels. This meant that only proteins without TMT labels were used for proteomic analyses making it impossible to determine which proteins came from which sample.

Synovial Fluid Sample Prep – Run 3 SOP

Determine Protein Concentration – BCA Assay

1. Prepare standards and working reagent for the Micro BCA Protein Assay Kit prior to starting the rest of protocol
2. Thaw samples to room temp
3. Transfer SF to 1.5mL tube and centrifuge at 2000 rpm for 10 min and keep supernatant
4. While samples are in the centrifuge, load 150 uL (in duplicate) of each standard into a 96 well plate
5. Remove samples from centrifuge and move supernatant to a new -80 tube
6. Load 150uL of sample (in duplicate) into 96 well plate – record which well each sample is loaded onto
7. Put samples in fridge until Step 2 (page 2)
8. Add 150uL of working reagent to each well and mix plate on shaker plate for 30 seconds
9. Cover plate with parafilm and incubate at 37C for 2 hours
10. While plate incubates, prepare plate reader (located in microscopy room) by loading the Micro BCA Assay Protocol

11. In SpectraMax Software, label plate with appropriate labels for wells containing sample
12. Following incubation, cool plate to room temperature
13. Measure the absorbance of the plate at 562nm
14. Subtract the average 562nm absorbance reading from the Blank standard replicates from the 562nm reading of all other individual standard and unknown sample replicates
15. Prepare a standard curve by plotting the average corrected reading for each BSA standard vs its concentration in ug/mL.
16. Use the standard curve to determine the protein concentration of each unknown sample.

CaptureSelect Multispecies Albumin Depletion Protocol

16. Load 100uL of CaptureSelect Multispecies Albumin depletion product into spin column
17. Wash and hydrate the resin by loading 500uL of 1x PBS
18. Remove the twist off tip at the bottom of spin column and place in an empty 2mL capture tube
19. Centrifuge at 3000 rpm (700 xg) for 1 minute
20. Discard flow through PBS
21. Repeat steps 4-7 two more times
22. Once sample is thawed, load 100uL of sample into the depletion spin column
23. Move depletion spin column into a new 2mL conical tube
24. Incubate for 20 minutes and vortex every few minutes
25. Collect flow through by centrifuging spin column at 3000 rpm for 1 minute
26. Rinse spin column with 100 uL of 1x PBS, centrifuge at 3000 rpm for 1 minute and collect flow through in the same tube
27. Repeat step 13 two more times
28. Sample is ready for further steps

Methods for Alkylation and Reduction

1. Create Reducing buffer by adding 500 uL of ultrapure water to a 7.7mg tube of DTT for a final concentration of 100mM
   - Store in glass vial at -20C
2. Create Alkylation buffer by adding 9mg of IAA to 500uL of ultrapure water for final concentration of 100mM
   - Store in glass vial at -20C
3. Transfer 50uL of sample into a new 0.5mL tube (make sure to write down protein concentration in notebook)
4. Add 15uL of Reducing buffer to each sample
5. Incubate samples at 95C on a heat block for 5 minutes and allow to cool
6. Add 11uL of Alkylation buffer to each sample and incubate in the dark at room temperature for 20 minutes

Methods for Trypsin Digestion

1. Add 150uL of SMART Digest buffer to the tube

2. Add 5uL of SMART Digest soluble trypsin
3. Incubate samples overnight (8 hours) at 30C

Methods for TMT Labelling

1. Equilibrate the TMT Label Reagents to room temperature
2. Add 41µL of anhydrous acetonitrile to each tube
3. Allow the reagent to dissolve for 5 minutes with occasional vortexing
4. Briefly centrifuge the tube to gather the solution
5. Transfer 100uL of reduced and alkylated protein digest to the TMT Reagent vial
    a. Make sure to record which sample went into which TMT label tube
6. Incubate the reaction for 1 hour at room temperature
7. Add 8µL of 5% hydroxylamine to the sample and incubate for 15 minutes to quench the reaction
8. Combine equal amounts of each sample to a new microcentrifuge tube

Fourth Run – Pierce C18 Spin Columns

For the fourth attempt, Pierce C18 Spin desalting columns (89873) were obtained from Thermo Fisher after consulting with the UMass Mass Spec CORE facility, the manufacturer, and the literature. These columns are compatible with the TMT labels being used for the study. The results of the study showed that samples still had low labelling efficiency. This meant that proteins from each individual sample were not labeled efficiently, so during protein identification and quantification, after all ten samples were mixed into one tube for proteomic analysis, it was impossible to determine which proteins came from which sample. Ratios between treated and control limbs could not be obtained. Possible errors for this could be due to earlier sample preparation.

After this trial, the UMass CORE Facility recommended that our group reach out to other Mass Spec CORE facilities who had more experience working with Synovial Fluid samples and could prepare the samples for us. After looking at potential options, we decided to work with the University of Connecticut Mass Spec CORE Facility.

Synovial Fluid Fourth Run SOP

All steps from the Third Run were used, but different desalting columns were used to clean the samples. Methods below:

Methods for Sample Clean-Up using C18 spin column

1. Create elution solution by adding 2uL of TFA, 1mL of ultra-pure water, and 1mL acetonitrile in a glass vial
2. Condition the disk by pipetting 250uL of methanol through the C18 cartridge
3. Centrifuge the disk at 1200rpm for 2 min in a 15mL conical tube
   - Make sure surface of disk remains wet
4. Remove residual methanol by pipetting 500 uL of DI water
5. Centrifuge the disk at 1200rpm for 2 min
   - Make sure surface of disk remains wet
6. Load sample and centrifuge at 2500rpm for 2 min
7. Load 500uL of DI water to remove unbinding proteins and centrifuge at 2500rpm for 2 min

8. Load 500uL of 5% ACN in DI water and centrifuge at 2500rpm for 2 min
9. Move disk onto a new 15mL conical tube – next step will collect sample from tube
10. Load 300uL of elution solution and centrifuge at 2500g for 2 min
11. Transfer sample into a new 2mL tube and label
12. Dehydrate samples using nitrogen gas in fume hood – takes roughly 1 hour
13. Place dehydrated samples in the UMass Mass Spec freezer located in the hallway on the fifth floor (near uCT room)

Fifth Run – Working with UConn Mass Spec CORE

Following the suggestion from the UMass Mass Spec CORE facility, our group began to work with the Mass Spec CORE facility at the University of Connecticut (UConn). For the fifth run, the UConn group was interested in determining the total amount of protein our samples contained by using the recommended raw sample volume, doubling it, and if using a hyaluronidase enzyme before or after the depletion column, would result in higher quality samples by removing more albumin.

For this trial, two samples from the same animal and limb were prepared at UMass using the MultiSpecies Albumin Depletion product using two different volumes (100uL and 200uL) of the sample to determine if more product would be able to remove more albumin from the samples. Two more vials of the same sample (100uL and 200uL) were shipped to them along with the depletion product for UConn to determine if adding the enzyme before or after the depletion column affected the total number of proteins.

The results from this trial run showed that doubling the initial volume of raw sample used provided us with the enough protein concentrations to confidently conduct the experiment. The results also showed that adding the hyaluronidase enzyme before or after the depletion product did not affect the outcome of protein concentrations. Therefore, moving forward, the following depletion product was used:

CaptureSelect Multispecies Albumin Depletion Protocol

1. Load 200uL of CaptureSelect Multispecies Albumin depletion product into spin column
2. Wash and hydrate the resin by loading 500uL of 1x PBS
3. Remove the twist off tip at the bottom of spin column and place in an empty 2mL capture tube
4. Centrifuge at 3000 rpm (700 xg) for 1 minute
5. Discard flow through PBS
6. Repeat steps 4-7 two more times

7. Once sample is thawed, load 200uL of sample into the depletion spin column
8. Move depletion spin column into a new 2mL conical tube
9. Incubate for 20 minutes and vortex every few minutes
10. Collect flow through by centrifuging spin column at 3000 rpm for 1 minute
11. Rinse spin column with 100 uL of 1x PBS, centrifuge at 3000 rpm for 1 minute and collect flow through in the same tube
12. Repeat step 13 two more times
13. Sample is ready for further steps

Sixth Run – Working with UConn Mass Spec CORE

Once it was established that each sample contained enough proteins to conduct the experiment, UConn began to move forward with the experiment. For the TMT analysis, 6-plex labels would be used to run 6 sets of 6 samples. For these labels, 1ug of each sample was needed to run the experiments in order to confidently say that the ratios obtained from the experiment between treated and control limbs were accurate.

For the first mix (Mix 1), it was determined that the values were close to 1ug, but not as close as the UConn group would feel comfortable making conclusions with. It was unclear if there were label discrepancies or if the readings from the A280 NanoDrop were inaccurate.

For the second mix (Mix 2), the group at UConn first determined the label efficiency was up to their standards and that the NanoDrop readings could be slightly off. The results gave protein values closer to 1 and made the UConn group more comfortable for our group to draw conclusions with. These samples were used in Chapter 5 of this dissertation.

They suggested a final mix (Mix 3), in which total proteins in the sample would quantified using a Colorimetric Peptide Concentration Assay, instead of the A280 NanoDrop. However, the protein values used in this study were not 1 or better than the values for Mix 2. This mix did account for the samples being from either the 1 month or 6-month time point, so comparison of changes in protein expression over time in each treatment group could be made.